JOURNAL OF FOOD PROCESS ENGINEERING

D.R. HELDMAN
and
R.P. SINGH
COEDITORS

FOOD & NUTRITION PRESS, INC.

VOLUME 19, NUMBER 1 APRIL 1996

JOURNAL OF FOOD PROCESS ENGINEERING

All articles for publication and inquiries regarding publication should be sent to DR. D.R. HELDMAN, COEDITOR, *Journal of Food Process Engineering*, Food Science/Engineering Unit, University of Missouri-Columbia, 235 Agricultural/Engineering Bldg., Columbia, MO 65211 USA; or DR. R.P. SINGH, COEDITOR, *Journal of Food Process Engineering*, University of California, Davis, Department of Agricultural Engineering, Davis, CA 95616 USA.

All subscriptions and inquiries regarding subscriptions should be sent to Food & Nutrition Press, Inc., 6527 Main Street, P.O. Box 374, Trumbull, CT 06611 USA.

One volume of four issues will be published annually. The price for Volume 19 is $149.00, which includes postage to U.S., Canada, and Mexico. Subscriptions to other countries are $172.00 per year via surface mail, and $183.00 per year via airmail.

Subscriptions for individuals for their own personal use are $119.00 for Volume 19, which includes postage to U.S., Canada and Mexico. Personal subscriptions to other countries are $142.00 per year via surface mail, and $153.00 per year via airmail. Subscriptions for individuals should be sent directly to the publisher and marked for personal use.

The *Journal of Food Process Engineering* (ISSN:0145-8876) is published quarterly (March, June, September and December) by Food & Nutrition Press, Inc.—Office of Publication is 6527 Main Street, P.O. Box 374, Trumbull, Connecticut 06611 USA. Current issue is April 1996.

Second class postage paid at Bridgeport, CT 06602.

POSTMASTER: Send address changes to Food & Nutrition Press, Inc., 6527 Main Street, P.O. Box 374, Trumbull, Connecticut O6611 USA.

JOURNAL OF FOOD PROCESS ENGINEERING

JOURNAL OF FOOD PROCESS ENGINEERING

Journal of FOOD PROCESS ENGINEERING

VOLUME 19
NUMBER 1

Coeditors: D.R. HELDMAN
R.P. SINGH

FOOD & NUTRITION PRESS, INC.
TRUMBULL, CONNECTICUT 06611 USA

ISSN 0145-8876

Printed in the United States of America

CONTENTS

VARIABLE CONTROL OF A BATCH RETORT AND PROCESS SIMULATION FOR OPTIMIZATION STUDIES

J. FASTAG, H. KOIDE and S.S.H. RIZVI[1]

Institute of Food Science
Cornell University
Ithaca, NY 14853

Accepted for Publication November 17, 1994

ABSTRACT

A microcomputer was interfaced with a batch retort for digital PI control of the retort temperature. Six retort temperature profiles (three isothermal, sinusoidal, step, and ramp) were examined for processing pea puree to nearly the same lethality values in 211 × 400 cans. Thiamine content and steam consumption were measured. Thiamine retentions in non-isothermal processes were greater than in the isothermal processes, but there was no significant difference in the steam consumption.

Lethality and thiamine retention were also simulated using a finite difference model for the same heating profiles, with good agreement with experimental results. The simulation suggests that differences in thiamine retention due to differing heating regimes are significant only for large lethality values and smaller cans. For F_0 values smaller than 10 min, the simulation suggests that the sinusoidal heating regime will provide better thiamine retention. Limitations of the model and suggestions for future improvement are also discussed.

INTRODUCTION

Computer-aided methods have been applied to the thermal processing of foods to improve nutrient retention and to automate the process. Teixeira *et al.* (1969) developed a numerical model to predict lethality and nutrient retention using a FORTRAN program. Teixeira *et al.* (1975b) also investigated various retort temperature profiles to maximize thiamine retention by a trial and error method, using this computer program to simulate the process. They concluded that the effect of package dimension affects nutrient retention more than varying the retort temperature profiles. However, only the constant-temperature and

[1] Correspondence should be addressed to: Dr. Syed S.H. Rizvi, Institute of Food Science, Stocking Hall, Cornell University, Ithaca, NY 14853.

Journal of Food Process Engineering **19** (1996) 1–14.

stepwise heating regimes were carried out experimentally (Teixeira *et al.* 1975b). Datta *et al.* (1986) developed an on-line computer based retort control system for processing canned foods. The system ensured the desired level of sterilization and automatic correction for deviations of the retort temperature. Lappo and Povey (1986) developed a retort control and data acquisition system with a digital PID controller.

The merits of a computerized retort control system are generally summarized as: (1) minimization of process deviations, (2) on-line computation of the degree of thermal sterilization, (3) automatic documentation of the process, and (4) optimization of nutrient, texture, flavor, and color characteristics.

The objectives of this study were: (1) implementation of a computerized retort control system capable of fulfilling any predetermined heating/cooling strategy, (2) verification of the accuracy of control, (3) investigation of the effect of various retort time-temperature profiles on nutrient retention and energy efficiency, and (4) investigation of the effect of various retort time-temperature profiles and can sizes on nutrient retention, via simulation, for varying target lethality values.

MATERIALS AND METHODS

Original Retort

The retort used for this study was a Hydrolock Simulator (WSF Industries, Tonawanda, NY). It was developed for laboratory heat penetration studies and to closely simulate the operation of a commercial Hydrolock continuous pressure cooker.

Computer System

An IBM Personal Computer XT (IBM Corp., Boca Raton, FL), equipped with 512 Kbytes of RAM, a 10 Mbyte hard disk, a 360 Kbyte floppy disk drive, an Enhanced Graphic Adaptor video card (EGA), parallel and serial ports, an IBM Personal Computer Data Acquisition and Control Adapter (DACA), and a DT2801 data acquisition board (Data Translation Inc., Marlboro, MA) were used. The DACA and the DT2801 boards enable digital and analog I/O through screw terminal panels. These boards handle on-off valves, proportional valves, and digital thermometers. The system configuration is shown in Fig. 1 and 2.

Control Program

A retort control program was written in Turbo Pascal (Borland International, Scotts Valley, CA) with a few assembly-language routines (Koide 1989). The program requires the input of process conditions, such as desired lethality,

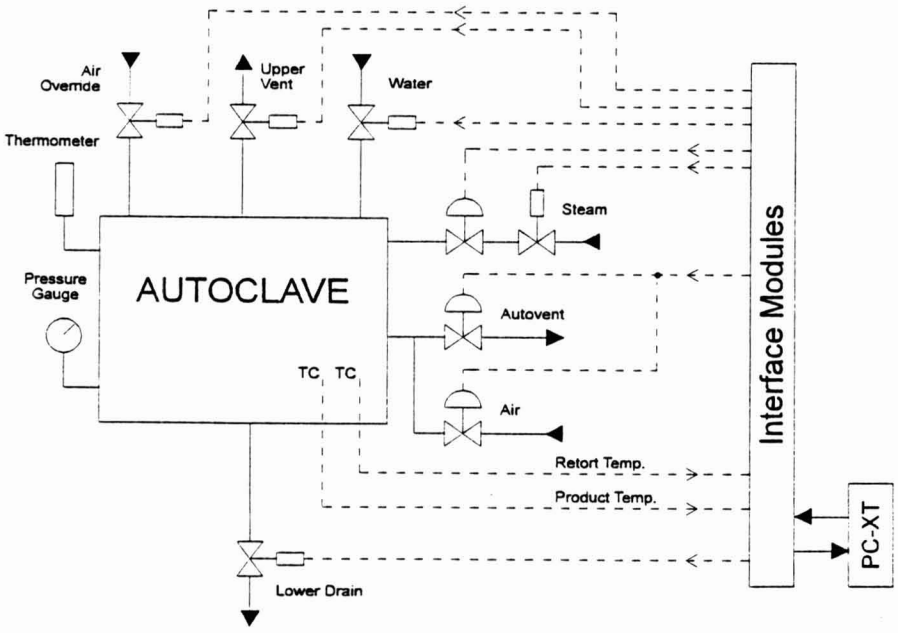

FIG. 1. COMPUTER-BASED RETORT CONTROL SYSTEM

venting temperature, product temperature after cooling, etc.; controller parameters, such as controller gain, integration time constant, and initial control signal; and a filename for data logging. After initialization, the program waits for a key press to begin the process. The display continuously indicates the state of the process, (i.e., date, time, on-off valves status, retort and product temperatures, accomplished lethality, control signal to D/P transducers), updating every second.

The control logic used was developed by Mulvaney (1984), Fig. 3. The pressure was not controlled by the program; instead, the retort's original analog controller maintained the given set point by regulating an on-off air valve. Venting was regulated by the computer program for 2 min after the retort temperature reached 100C. A predefined temperature profile followed the heating process. The cooling process started when the lethality reached the set point, and the process finished when the product temperature achieved the desired cooling temperature. Since water level and pressure sensors were not used during the cooling process, excess water simply overflowed through the vent or drain pipes. At any time, the process could be switched to manual

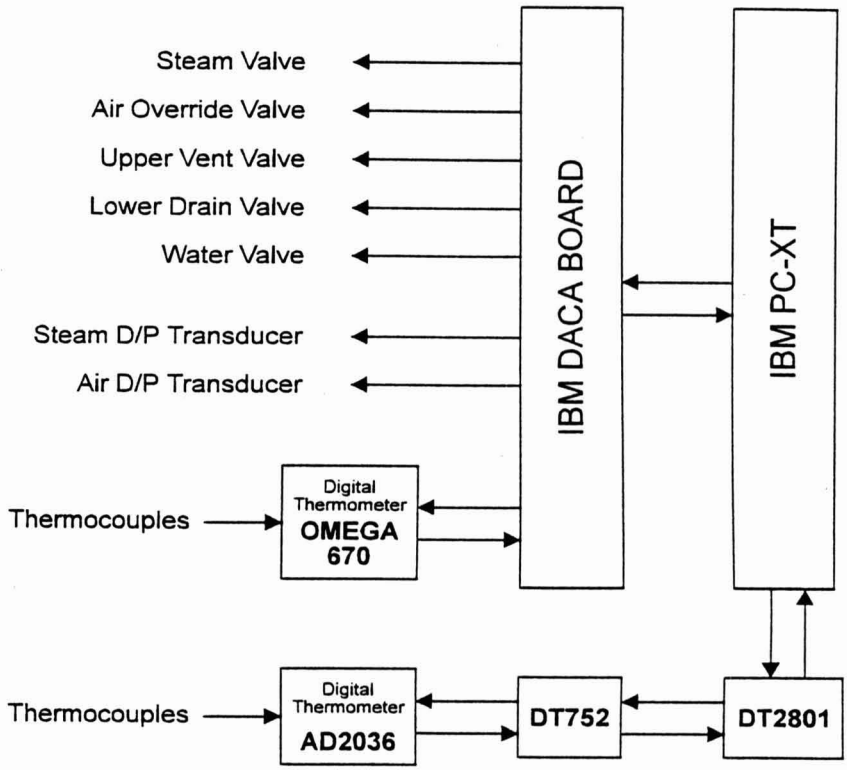

FIG. 2. INTERFACE MODULES

operation or stopped completely. At the end of the process, all temperature, control signal, and process condition data were saved to the disk by the program.

Experimental

Pea puree was chosen for measurement of nutrient retention because of its high thiamine content and because thiamine destruction rate data are available. The puree was prepared from frozen, sweet peas purchased from a local food market. The peas were rapidly thawed by placing them in boiling water for 2 min. They were then blended with sufficient water to obtain a puree containing 20% additional water by weight (Teixeira *et al.* 1975a). The retort processing was carried out in 211 × 400 cans. Type T thermocouples were placed in the center of the can for product temperature measurement. Product temperature was recorded by the computer control system and a portable hybrid recorder (Model 3087, Yokogawa Hokushin Electric, Tokyo, Japan) simultaneously.

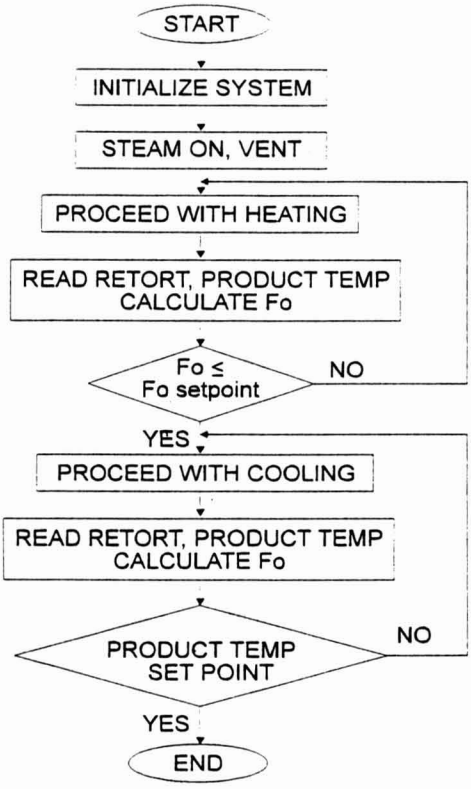

FIG. 3. FLOW DIAGRAM OF RETORT CONTROL PROGRAM

The process control program allowed to change retort temperature-time profiles by modifying a program file. The digital PI controller was set at K (controller gain) = 150, TI (integration time constant) = 100, and initial control signal = 0.

Six arbitrarily chosen temperature profiles, including three isothermal, one sinusoidal, one step, and one ramp, were examined (Fig. 4). The retort temperature range was 215 to 250F. These processes were carried out by the process control program with manual cooling. For each process, condensed steam at the drain was collected and weighed to estimate the energy consumption. After the process, the pea puree was stored in a freezer until the thiamine measurement. The measurement of thiamine was done by the fluorometric method (AOAC 1984).

Numerical Simulation

A finite difference program was developed, based on Teixeira *et al.* (1969), to simulate thiamine retention. The program implements variable temperature

retort profiles and takes into account come-up time and cooling, uses a windows-based user interface, and provides both numerical and graphical output. Total nutrient retention and lethality values are calculated, as well as mass average values and center point values. The model assumes that $f_c = f_h =$ constant throughout the process (including venting). The simulation conditions are summarized in Table 1.

TABLE 1.
SELECTED SIMULATION PARAMETERS FOR THIAMINE RETENTION PROGRAM

Parameter	Present Study	Teixeira *et al.* (1975)
Can size	307 × 409[a]	307 × 409
Radial increments	10	10
Vertical increments	10	10
Time increment (min)	0.125	0.125
Thermal diffusivity (in^2/min)	0.0211	0.0143
Initial food temp. (°F)	85	160
Cooling water temp. (°F)	55	unknown
Cut off temperature (°F)	100	unknown
Venting time (min)	2	not simulated
Process time (min)	48.0-162.0	70.0-89.0
D-246F thiamine (min)	178.6	178.6
z-value thiamine (°F)	46	46
D-250F *C. botulinum* (min)	2.4	unknown
z-value *C. botulinum* (°F)	18	unknown

[a] 211×400 and 603×700 can sizes were also simulated, with thermal diffusivity values adjusted accordingly.

RESULTS AND DISCUSSION

Experimentally obtained retort temperature profiles are shown in Fig. 4. At any given time, the retort temperature error was less than 1.8F. This accuracy may not be enough for product temperature acquisition. An error in temperature of 0.18 to 1.8F results in a corresponding error in accomplished lethality of 2.3 to 26 % (Navankasattusas and Lund 1978). Type T thermocouples produce a maximum error of ± 1.4F (Lappo and Povey 1986). The digital PI controller reached its operational limit if the retort temperature step change was more than 5F at any given time. An antiwindup algorithm could be added to the controller to prevent the larger overshoot which was caused by a larger step change. To avoid overshoot, the set temperature was gradually increased at the beginning of the isothermal process. The sampling rate had a 30% error which was brought about by the polling method to count the time. This error did not

seriously affect the system performance, since this error does not accumulate. At the end of the process the system time error was always less than 0.3 s.

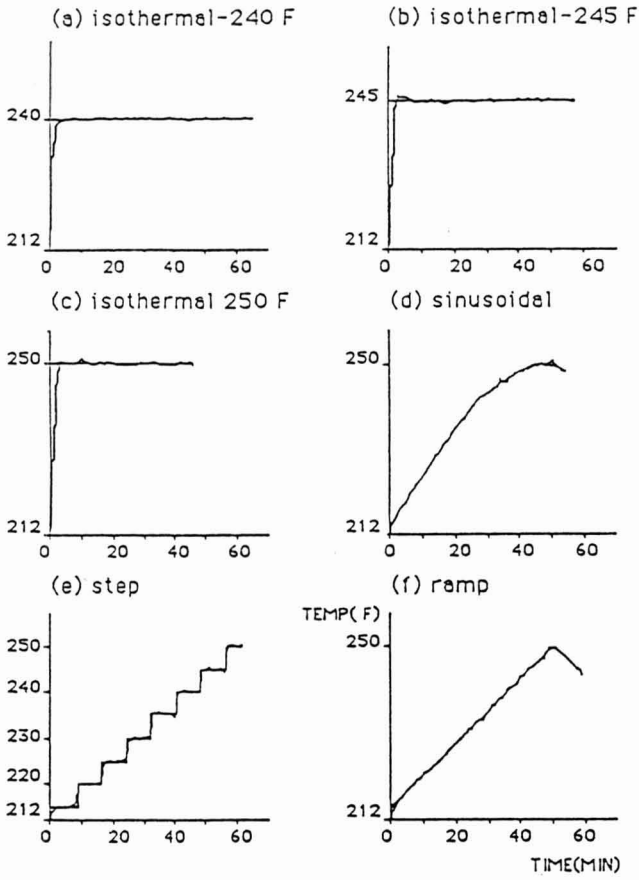

FIG. 4. RETORT TEMPERATURE PROFILE CURVES OBTAINED BY RETORT CONTROL SYSTEM

A summary of the nutrient retention and steam consumption is shown in Table 2. Resulting lethality (F_o) varied from 7.33 to 7.60 min. Thiamine retention for the isothermal processes was 66%, 65%, and 64% for 240F, 245F and 250F, respectively. For the nonisothermal processes the values were 72%, 72% and 70% for step, ramp, and sinusoidal functions, respectively. The nonisothermal processes generally had smaller F_o than isothermal processes, while thiamine retention improved significantly for the nonisothermal processes.

TABLE 2.
EXPERIMENTAL RESULTS OF LETHALITY, THIAMINE RETENTION, AND STEAM CONSUMPTION AND SIMULATION RESULTS OF LETHALITY AND THIAMINE RETENTION FOR A 211×400 CAN

		EXPERIMENTAL				SIMULATION (mass average)		
Retort Profile	Process Time (min)	Fo (min)	Fs (min)	Thiamine Retention (%)	Steam (kg)	Fo (min)	Fs (min)	Thiamine Retention (%)
Isothermal								
240°F	66.0	7.49	10.8	66	16.5	6.44	9.2	65.7
245°F	57.8	7.33	11.6	65	15.8	8.23	13.1	64.6
250°F	47.8	7.56	12.7	64	14.3	7.80	15.6	66.7
Step	62.4	---	---	72	16.8	4.73	7.2	71.5
Ramp	60.3	---	---	72	15.3	3.65	6.1	74.5
Sinusoidal	56.1	---	---	70	15.6	6.24	12.4	69.3

Regarding energy efficiency, there were no significant differences in the steam consumption. The higher the isothermal retort temperature or the shorter the process, the less the steam consumption, suggesting that process time affected the use of steam rather than the temperature profiles.

The center (F_o) and integrated (F_s) lethalities calculated by the simulation program are also shown in Table 2, together with their corresponding simulated thiamine retention, using the experimental process times. The differences between the experimental and simulated thiamine retention values are not significant, but the program seems to underestimate most of the lethality values. If these results are compared to those reported by Teixeira *et al.* (1975b), most of them will be found to be different. Their simulation was done for a larger can size (307×409 instead of 211×400), taking longer processing time (70-89 min), and for a higher integrated lethality (F_s = 20 min) than those for the present study. Their initial product temperature was 160F compared to 85F for this study, and furthermore, the come-up time and venting phases were not included in their simulation. However, our simulation results for the 307×409 can do compare favorably with those reported by Teixeira (1975b), especially for the isothermal profile processes.

Process time and thiamine retention values were also determined by the simulation program for lethalities between 5 and 20 min, for 211×400, 307×409, and 603×700 can sizes, and for each heating profile under investigation. The results are plotted in Fig. 5 and 6, grouped by can size, and in Fig. 7 grouped by heating regime. In all cases, curves converge to 100% thiamine retention as the lethality approaches zero (no processing), as expected. The differences in thiamine retention between the different heating profiles increase as the F_s values become larger, especially for smaller can sizes. This is most evident in the top of Fig. 5, where thiamine retention ranges from 45% for the 240F isothermal process, to 62% for the 250F isothermal process, for a mass average F_s value of 20 min. For large lethality values, thiamine retention was highest for the 250F isothermal process and lowest for the 240F isothermal process, with the non-isothermal profiles in between. But for lower lethality values, some of the nonisothermal processes, in particular the sinusoidal profile, results in higher thiamine retention for a given lethality value, as in the bottom of Fig. 6. The ramp and step heating regimes result in similar residual thiamine for a given F value, since the latter can be thought of as a rough approximation of the first.

Comparing Fig. 5 and 6, we note that the differences in residual thiamine for the various heating profiles are less prominent for any given F_o value than for an F_s value. This, as expected, indicates that heat conduction to reach the can center buffers the differences in heating regimes, especially as the can size increases.

In general, the heating regime has a diminishing effect on nutrient retention as the can size increases. Figure 7 shows that for any given F_s value and fixed

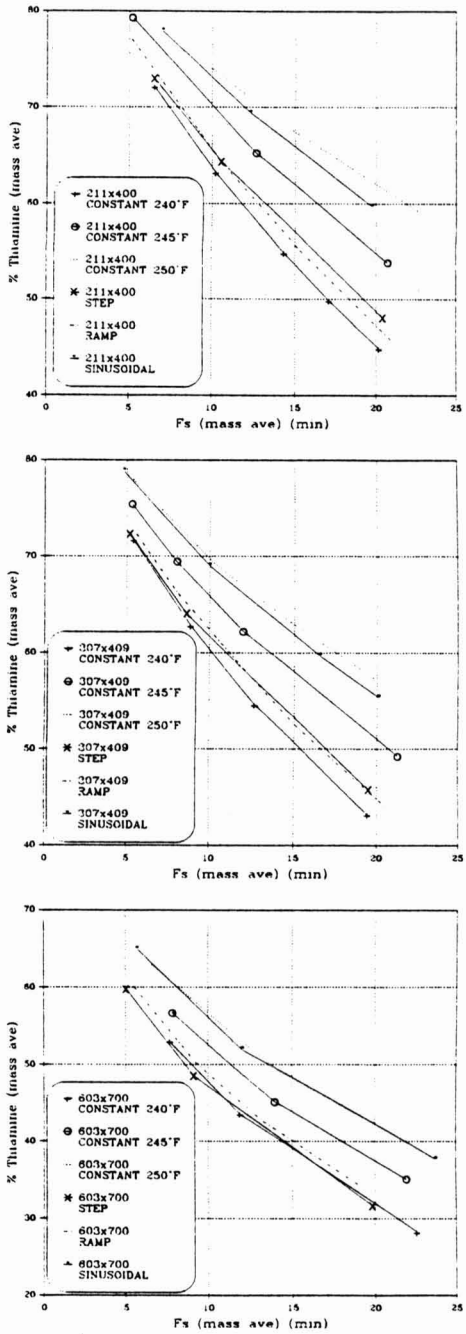

FIG. 5. MASS AVERAGE THIAMINE RETENTION VERSUS MASS AVERAGE F_s, BY SIMULATION, GROUPED BY CAN SIZE

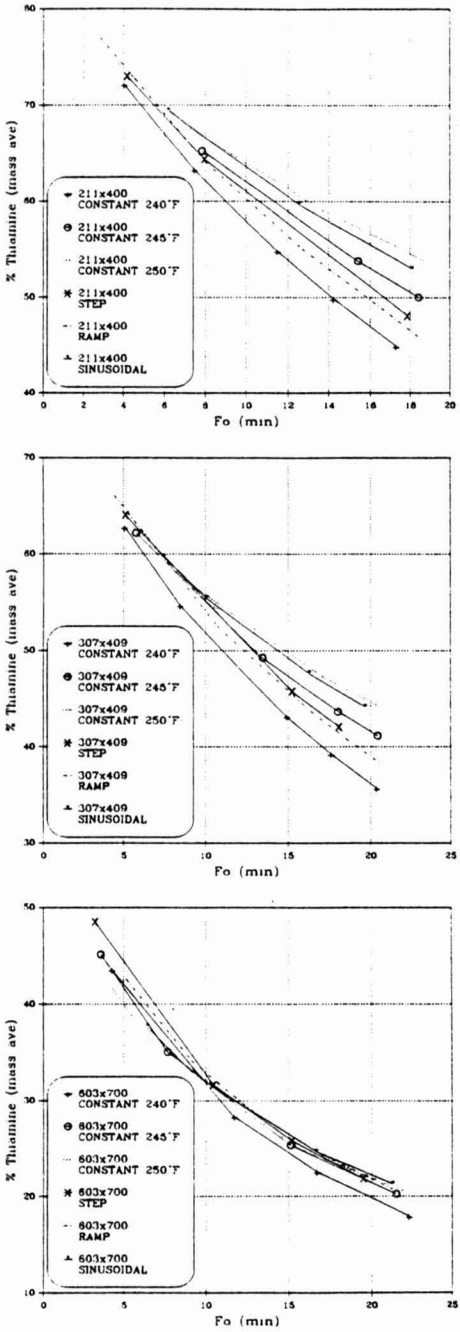

FIG. 6. MASS AVERAGE THIAMINE RETENTION VERSUS F_o, BY SIMULATION, GROUPED BY CAN SIZE

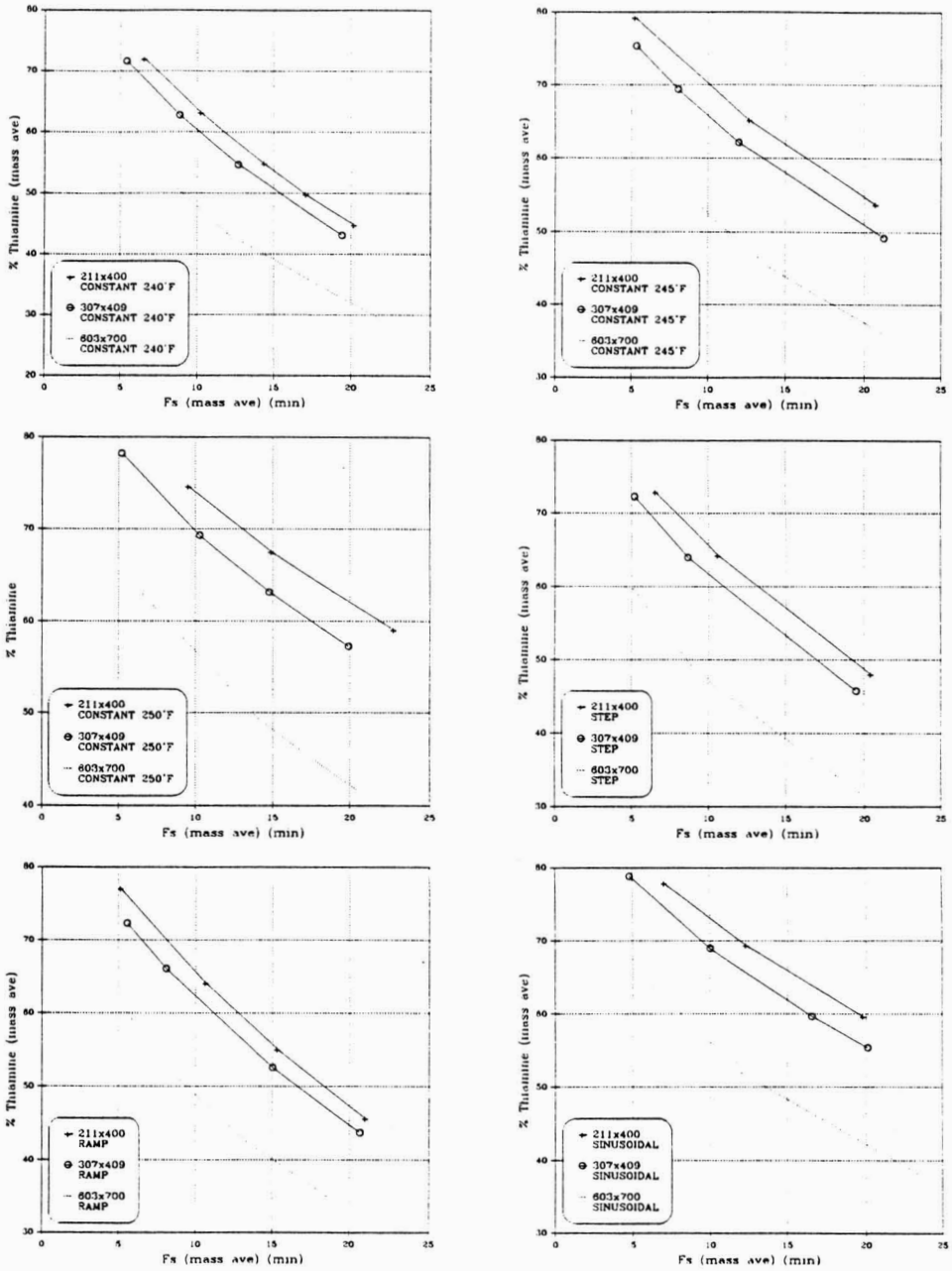

FIG. 7. MASS AVERAGE THIAMINE RETENTION VERSUS MASS AVERAGE F_s, BY SIMULATION, GROUPED BY HEATING REGIME

heating profile, thiamine retention is higher for smaller cans, due to shorter process times to achieve the same lethality and less severe treatment of the outer layers than that which larger cans require.

These simulations did not take into account any temperature dependence of food properties. All food materials should be considered variable diffusivity products as the thermal diffusivity of water alone increases 12.4% over the temperature range of 140 to 248F (Mulvaney 1987). The difference in the retort temperature profile affects thermal diffusivity and thus also the thiamine retention. It seems worthy to develop a variable diffusivity model to simulate nutrient retention and validate experimental results. A knowledge of the physical property changes during both the heating and cooling processes is needed for further improvement of the simulation program. Besides, the assumption of infinite surface heat transfer coefficient of the can is not acceptable during the cooling process, especially if the cans sit in a stagnant pool of water. And these parameters are also assumed constant during venting, even though the presence of air significantly modifies these physical properties. Discrepancy between the simulated and experimental integrated lethality results might arise from these assumptions. Finally, finding the profile that optimizes both nutrient retention and energy efficiency, along with any other quality factors simultaneously, should prove worthwhile.

REFERENCES

AOAC. 1984. *Official Methods of Analysis of the Association of Analytical Chemists*, Washington, DC.

DATTA, A.K., TEIXEIRA, A.A. and MANSON, J.E. 1986. Computer-based retort control logic for on-line correction of process deviations. J. Food Sci. *51*, 480.

KOIDE, H. 1989. M.S. Thesis, Cornell University, Ithaca, New York.

LAPPO, B.P. and POVEY, M.J.W. 1986. A microprocessor control system for thermal sterilization operations. J. Food Eng. *5*, 31.

MULVANEY, S.J. 1984. M.S. Thesis, Cornell University, Ithaca, New York.

MULVANEY, S.J. 1987. Ph.D. Dissertation, Cornell University, Ithaca, New York.

NAVANKASATTUSAS, S. and LUND, D.B. 1978. Monitoring and controlling thermal processes by on-line measurement of accomplished lethality. Food Tech. *32*, 79.

TEIXEIRA, A.A., DIXON, J.R., ZAHRADNIK, J.W. and ZINSMEISTER, G.E. 1969. Computer optimization of nutrient retention in thermal processing of conduction-heated foods. Food Tech. *23*, 137.

TEIXEIRA, A.A., STUMBO, C.R. and ZAHRADNIK, J.W. 1975a. Experimental evaluation of mathematical and computer models for thermal process evaluation. J. Food Sci. *40*, 653.

TEIXEIRA, A.A., ZINSMEISTER, G.E. and ZAHRADNIK, J.W. 1975b. Computer simulation of variable retort control and container geometry as possible means of improving thiamine retention in thermally processed foods. J. Food Sci. *40*, 656.

EFFECTS OF DIPPING AND WASHING PRE-TREATMENTS ON MICROWAVE DRYING OF GRAPES

T.N. TULASIDAS, G.S.V. RAGHAVAN[1] and E.R. NORRIS

Department of Agricultural Engineering
Macdonald Campus of McGill University
21 111, Lakeshore Road, Ste. Anne-de-Bellevue
H9X 3V9, Quebec, Canada

Accepted for Publication February 12, 1995

ABSTRACT

The effects of different dipping pretreatments on microwave drying of grapes was studied in a multimode cavity. Grapes pretreated with 2% ethyl oleate in 0.5% sodium hydroxide (NaOH) solution resulted in comparatively good quality raisins with lowest drying times. Pretreatment with 3% ethyl oleate in 0.5% NaOH solution led to similar product without any major advantage over the former. Grapes treated with 3% ethyl oleate in 2.5% potassium carbonate solution took longer time to dry. Grapes treated with only NaOH solution resulted in raisins of inferior quality in terms of color and appearance. The interphase mass transfer coefficients also described the effect of these chemical pretreatments. Studies conducted on the effect of washing and time of holding after the pretreatment indicated that both of these factors had no influence on drying time.

INTRODUCTION

Drying of grapes is an important activity in the grape industry. Though sun drying is the common method employed, it has several inherent problems such as being time consuming and prone to contamination with dust and insects, besides being weather dependent (Berna *et al.* 1991; Jacob 1944). Hot air drying of grapes is a slow process owing to the resistance offered by the waxy outer skin of the fruit for moisture transfer (Chambers and Possingham 1963). The potential of dielectric heating with microwaves (MW) for drying of grapes has been reported (Tulasidas *et al.* 1993). Several pretreatments have been developed to reduce the drying time of grapes and to enhance the quality of raisins in terms of color and appearance. In most of the pretreatment methods, the fruits are first fumigated with sulphur dioxide to attain a concentration of

[1]To whom correspondence should be addressed.

Journal of Food Process Engineering **19** (1996) 15–25.

about 900 ppm. This sulphuring treatment is mainly aimed at obtaining a bright yellow color in the finished product. The fumigated fruits are then dipped in hot alkaline solutions to make the outer skin more permeable to water for rapid drying. The effects and effectiveness of these pretreatments on hot air drying of grapes are reported in literature (Ponting and McBean 1970; Riva *et al.* 1986; Saravacos and Marousis 1988). However, there is no information on the effects of chemical pretreatments on MW drying of grapes. The present study was therefore undertaken to investigate and quantify the effect of pretreatments and washings on MW drying of grapes.

MATERIALS AND METHODS

Grapes were dried into raisins using combined hot air forced convection and microwaves utilizing the drying apparatus shown in Fig. 1. The apparatus consisted of a 600 W microwave oven which represents a multimode cavity. The MW oven was modified by providing a hot air supply system to work as a drier. The duty cycle of the MW oven was variable in steps of 10% (power levels 1 to 10). The 10% duty cycle (power level 1) was essentially an intermittent operation of the oven and it was found that in this mode of operation the oven was on for 2 s for every 30 s off period. However, following a water load calibration it was estimated that 10% duty cycle provided a power of about 15 W. All the drying studies were conducted at this power level (10% duty cycle or power level 1) as higher levels were found to be unsuitable for grapes (Tulasidas *et al.* 1993). At higher levels bursting and burning of the product was noticed. An air temperature of 50C and an air velocity of 2.0 m/s was used in all the tests as this combination of air temperature and velocity was found to be suitable for grapes (Tulasidas *et al.* 1993). Thompson seedless variety of grapes of uniform size were selected and used in the drying studies (average berry weight = 4.0 $\pm$ 0.25 g). Each sample utilized in the experiment weighed about 50.0 $\pm$ 1.5 g. The moisture contents (m.c.) of grapes during drying at different interval of time were calculated using the observed mass loss for a given run. The drying was concluded when the final m.c. reached about 0.18 kg/kg dry mass as it is the safe storage m.c. for raisins (Winkler *et al.* 1974). The m.c. was determined using vacuum oven method at 70C until a constant weight was attained, which took about 24 h (Canellas *et al.* 1993; Boland 1984). The initial moisture content (m.c.) of grapes varied from 78.0% to 81.0%, wet basis (w.b.). An analysis of initial m.c. of the population showed that the variation within them was small (CV = 1.2%). The initial m.c. was expressed as the mean of the three replicates within each treatment. The temperature inside the grape berry (at the center of the fruit) during drying in the MW field was measured with the help of a fiber optic temperature sensor (755 Multichannel Fluro optic Thermometer, Luxtron, CA, USA). The sample holder was made

of perforated polyethylene tray and the hot air was admitted through its bottom side (Fig. 1) which offered negligible resistance to air flow. A mode stirrer fixed at the ceiling of the oven provided an even distribution of absorbed MW power in the material (Metaxas and Meredith 1983). Mass loss was measured by taking out and weighing the tray on a digital balance at 30 min intervals.

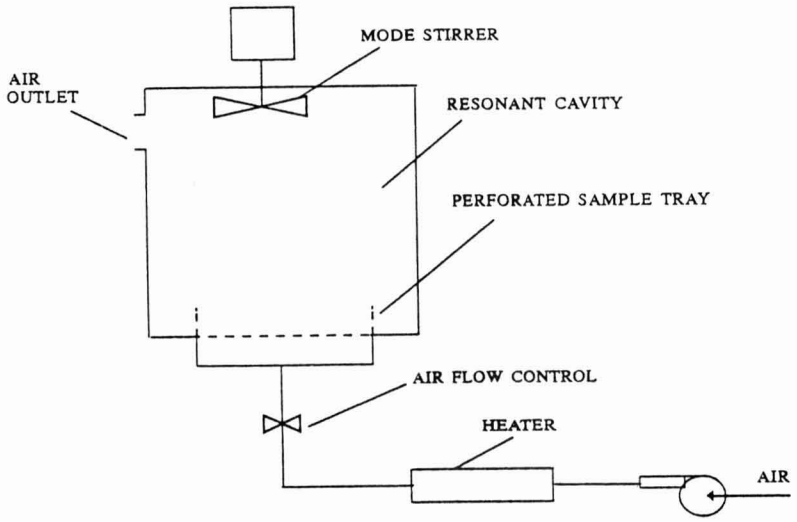

FIG. 1. SCHEMATICS OF THE MICROWAVE DRYING SETUP

Based on earlier studies of chemical pretreatments to enhance grape drying by forced convection (Ponting and McBean 1970; Riva *et al.* 1986; Saravacos and Marousis 1988), we chose the following chemical pretreatments for the MW drying experiments:

C_1 - Dipping for 30 s at 80C in 0.5% sodium hydroxide (NaOH) solution, (0.5% NaOH only).

C_2 - Dipping for 30 s at 80C in 2.0% ethyl oleate (EO) in 0.5% NaOH solution, (2% EO + 0.5% NaOH).

C_3 - Dipping for 30 s at 80C in 3.0% EO in 0.5% NaOH solution, (3% EO + 0.5% NaOH).

C_4 - Dipping for 3 min at 40C in 3.0% EO in 2.5% potassium carbonate (K_2CO_3) solution, (3% EO + 2.5% K_2CO_3).

Groups of berries were subjected to different dipping pretreatments and then dried in single layers in the sample holder. Color and appearance, the main quality attributes, were evaluated by visual observation of each sample after drying. Sulphur dioxide fumigation, which is a normal practice in commercial raisin production (Riva *et al.* 1986), was not performed in this study since the color and appearance of raisins obtained by MW drying was comparable to that of commercial raisins which were sulphured (Tulasidas *et al.* 1993). After each specified pretreatment, the grapes were washed twice in tap water, drained and immediately taken for drying tests.

Washing the grapes and holding them for some time after the pretreatment is done to remove residual chemicals from the surface (Riva *et al.* 1986). Considering this, the effects of washing and the holding time after a pretreatment on the drying characteristics of grapes was also investigated. Based on the results obtained from the pretreatment tests, the best treatment combination was selected for further investigation. The chemical pretreatment applied in these tests was C_2. These washing treatments were:

T_1 - Pretreated grapes washed twice in tap water, free gravity drained and immediately taken for drying with no holding time, (wash, 0 h).

T_2 - Pretreated grapes not washed, free gravity drained and were immediately taken for drying with no holding time (no wash, 0 h).

T_3 - Pretreated grapes not washed and were kept for 1 h holding time before drying, (no wash, 1 h).

To quantify the importance of the outer skin to the drying kinetics, a few tests were also conducted on de-skinned grapes. In one of the tests, the C_2 pretreatment was applied to peeled grapes (PC_2). In another test, no chemical pretreatment was applied (PC_0). Care was taken not to disturb the contents of the fruit while peeling. An experiment was also conducted under forced hot air convective conditions with pretreatment C_2 (CC_2). These tests were carried out for the sake of comparison and were conducted under the same drying conditions as mentioned earlier.

The experiments were performed in a randomized complete block design (RCBD) with three replicates to study the effect of different treatments as discussed. The response parameter, drying time, was the time required to dry grapes to a final moisture content of 0.18 kg/kg. Analysis of variance was conducted to determine whether significant differences existed between different treatments. Treatment differences were determined using Tukey's test (Steel and Torrie 1980; SAS 1989). Dimensionless moisture ratios (MR) were calculated as described in Eq. 1:

$$MR=(X-X_e)/(X_o-X_e) \quad (1)$$

where, X = moisture content, kg/kg dry mass,
X_o = initial moisture content, kg/kg dry mass and
X_e = equilibrium moisture content of raisins, kg/kg dry mass.

X_e values were computed using the GAB equation for raisins (Maroulis *et al.* 1988). Drying curves (plot of MR against time) were utilized to compare the difference in drying behavior amongst different treatments.

RESULTS AND DISCUSSION

Chemical Pre-treatments

The times required to dry grapes under different pretreatments to a final m.c of 0.18 kg/kg in the MW dryer with a 10% duty cycle mode (power level 1) and an air temperature of 50C, are given in Table 1, along with the results from Tukey's means separation test (SAS, 1989).

TABLE 1.
DRYING TIME, IN HOURS, UNDER PRETREATMENTS C_1, C_2, C_3 AND C_4

Blocks(R)	C_1	C_2	C_3	C_4
1	12.0	8.5	8.0	11.0
2	11.5	9.0	8.5	10.5
3	11.5	8.5	8.5	11.5
Mean	11.7^a	8.7^b	8.3^b	11.0^a

Note: Means with a common letter are not significantly different.

The analysis of variance indicated that the drying time was significantly different among treatments (F value = 52; d.f. = 3; $P < 0.001$). Two pairs of treatments emerged as not having significantly different drying times: C_1 and C_4, and C_3 and C_2. The quality of raisins obtained was similar for all the treatments except C_1 which resulted in pale and dull colored raisins rather than bright ones. Riva *et al.* (1986) have observed similar effects of these chemical pretreatments on drying kinetics of grapes under convective drying conditions. Figure 2 show the drying curves for grapes under these pretreatments. The tests conducted on de-skinned grapes showed that they dried fastest (4.5 h) after the C_2 pretreatment (PC_2), while unpeeled grapes (C_2) dried in 8.7 h. The drying time for de-skinned fruits (PC_0) without C_2 pretreatment was 5.5 h. Further, the grapes with skin intact and treated with C_2 (CC_2) dried by forced convection (without MW power) in about 20 h.

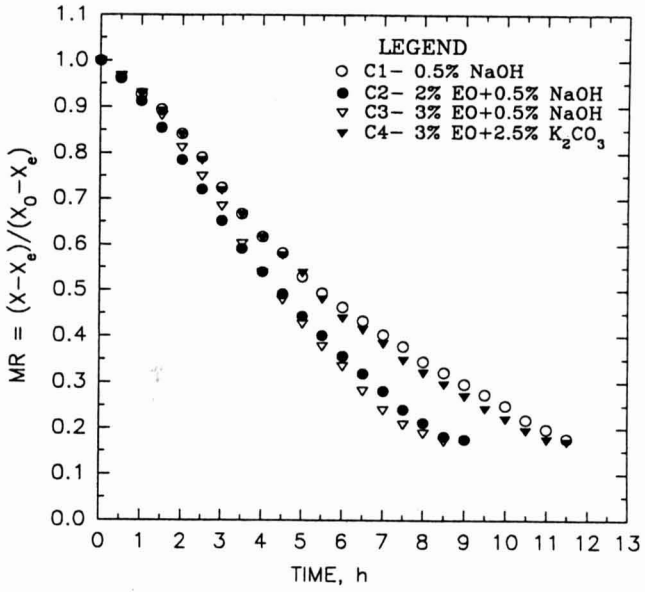

FIG. 2. EFFECT OF DIFFERENT DIPPING PRE-TREATMENTS ON MW DRYING OF GRAPES; POWER LEVEL 1, AIR: 50C, 2.0 M/S

It is interesting to note that the peeled fruit that was not pretreated (PC_0) dried more slowly than the peeled fruit treated with ethyl oleate (PC_2). This confirms earlier claims that ethyl oleate not only decreases skin resistance to diffusion but also enhances the internal moisture diffusion process (Saravacos and Marousis 1988; Riva *et al.* 1986).

Interphase Overall Mass Transfer Coefficients

As the grapes were exposed to MW radiation, they absorbed energy and heat was generated within the fruit. In consequence, the temperature of the fruit rose above that of the surrounding air which was at 50C. Due to application of MW power with a 10% duty cycle, the power absorbed by the fruit was not steady and therefore the heat generated within the fruit was obviously not uniform. The power absorbed by a material depends on its dielectric properties, and these are dependent on moisture content (Metaxas and Meredith 1983; Decareau and Peterson 1986). In the case of grape drying, the amount of power absorbed must have changed with time according to the time-dependent change in moisture content. These factors lead to highly complex and transient heat conditions inside the fruit. The temperature measured inside a grape berry was found to range from 56-64C. A mean temperature of 60C was assumed to

represent the average temperature inside the fruit. MW power absorption was assumed to be uniform throughout the fruit at any given instant of time.

An expression for rate transfer, as given by Geankoplis (1993), is:

$$J=k_c\Delta C=k_c\frac{\Delta p}{RT} \tag{2}$$

where,

J = mass flux of water, kg/m^2s
k_c = over-all inter phase mass transfer coefficient, m/s
ΔC = moisture concentration difference, kg/m^3
Δp = partial water vapor difference, kPa
R = gas constant for water vapor, 461.5 J/kg K and
T = absolute temperature at the mass transfer surface, K

In order to apply Eq. 2 it was assumed that the fruit surface attained the same temperature as that of its interior; this assumption is valid because of volumetric nature of heating due to microwave absorption. This represented a situation of a spherical object with its wet surface at 60C subjected to forced convection in a stream of drying air. The driving force term Δp in Eq. 2 is the vapor pressure difference between saturation vapor pressure at 60C at the surface and partial water vapor pressure of drying air at 50C and 12% RH. The over-all inter phase mass transfer coefficient k_c between the wet grape surface and the bulk air stream is given by a Sherwood relation of the type (Geankoplis 1993):

$$S_h=2+0.6Re^{1/2}Sc^{1/3} \tag{3}$$

where,

S_h = Sherwood No. = $k_c\, d/D_e$
R_e = Reynolds No. = $dV\rho/\mu$
S_c = Schmidt No. = $\mu/\rho D_e$
ρ = density of air = kg/m^3
V = velocity of air, m/s
μ = viscosity of air, kg/ms
D_e = effective diffusion coefficient, m^2/s
d = characteristic length, equivalent diameter of grape, m

For moisture diffusion in a sphere of 2.1 cm diameter evaporating into an air stream at 60C at 2 m/s, Saravacos and Marousis (1988) estimated the mass transfer coefficient (using Eq. 3) and this value was found to be close to their experimentally determined value using Eq. 2 under similar drying conditions, thus indicating the validity of the procedure applied. This technique was extended to compute the mass transfer coefficient (k_c) at the grape skin-air

interphase. With all other drying conditions being similar, the difference in drying rates between treatments was mainly due to the skin surfaces as modified by particular pretreatments. The interphase mass transfer coefficients reflect the extent of the change in skin surface resistance to moisture transport. The overall mass transfer coefficients at the interphase, were thus computed using Eq. 2 to illustrate the effect of different pretreatments under MW drying conditions.

In the MW drying process the initial moisture transport is higher than in convective drying (Lyons *et al.* 1974; Turner and Jolly 1991). This phenomenon was observed for MW drying of grapes (Tulasidas *et al.* 1993) and should essentially keep the evaporating surface wet for some time. Thus, application of Eq. 2 was justified for the initial drying period. The over-all mass transfer coefficients at the interphase, as calculated through Eq. 2 for the first hour of drying, were 0.00152, 0.00205, 0.00164 and 0.00154 m/s for treatments C_1, C_2, C_3 and C_4, respectively. The difference in the observed values reflected the effect of pretreatments they received since all other drying conditions were similar. The highest value of k_c was observed in the case of pretreatment C_2 which indicated that it offered a minimum resistance. This was followed by pretreatments C_3, C_4 and C_1. Comparison of these values and results given in Table 1 showed that the pretreatments influenced the drying rate of raisins under microwaves. Although pretreatment C_3 resulted in a slightly shorter mean drying time (8.33 h) than C_2 (8.67 h), the difference was not significant and the quality was the same. It is therefore concluded that there is no advantage in using 3% EO rather than 2% EO in terms of reducing the drying time and that treatment C_2 is the best since less chemical is used. The other treatments considered resulted in significantly longer drying times and are therefore not effective in reducing the time required for MW drying.

Washing and Holding Treatments

The drying time in hours required to dry grapes after pretreatment C_2 combined with washing of fruits and holding for various times are given in Table 2. Since none of these treatments was significantly different from the others (Tukey's test, hsd @ 1%, SAS 1989), neither washing or holding after a chemical pretreatment significantly affects the drying time. The drying behavior under these washing treatments was found to be identical (Fig. 3). Washing of the fruits immediately after a chemical pretreatment is always preferred from the standpoint of removal of residual chemicals left on the fruit surfaces. However, no chemical analysis was done in this study to measure the residual chemicals. Holding the fruits for some time after a chemical pretreatment necessitates extra equipment, space and time in the processing plant. Since the study indicated that there was no advantage derived from such a holding, the grapes could be washed, drained and immediately dried.

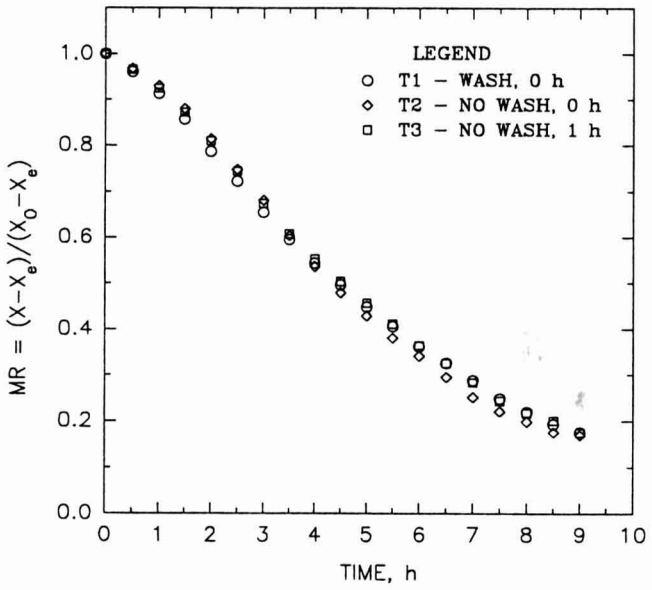

FIG. 3. EFFECT OF WASHING TREATMENTS ON MW DRYING OF GRAPES; POWER LEVEL 1, AIR: 50C, 2.0 M/S

TABLE 2.
DRYING TIME, IN HOURS, UNDER TREATMENTS T_1, T_2 AND T_3

Blocks	T_1	T_2	T_3
1	8.5	8.5	9.5
2	9.5	9.0	8.0
3	9.0	8.5	8.5
Mean	9.0[a]	8.7[a]	8.7[a]

NOTE: Means with the same letter are not significantly different at the 0.01 level

SUMMARY AND CONCLUSIONS

The effects of different pretreatments on drying of grapes under microwaves was studied. Grapes pretreated with 2% ethyl-oleate in 0.5% NaOH solution resulted in comparatively good quality raisins at shorter drying times. Pretreat-

ment with 3% ethyl oleate in 0.5% NaOH solution led to similar product quality and drying time. Treatment of grapes with 3% ethyl oleate in 2.5% potassium carbonate solution resulted in slower drying and was comparable to the treatment with 0.5% NaOH solution and no ethyl oleate. Grapes treated only with NaOH solution resulted in raisins of inferior quality in terms of color and appearance. Interphase mass transfer coefficients also described the effect of these chemical pretreatments. Studies conducted on the effect of washing and time of holding after a pretreatment indicated that neither factor influenced drying time.

ACKNOWLEDGMENT

The authors gratefully acknowledge the Canadian International Development Agency for funding through their Institutional Cooperation and Development Services Division for the study; the University of Agricultural Sciences, Bangalore, India, for the study leave granted to the first author and to the Quebec Ministry of Education for the FCAR grant.

REFERENCES

BERNA, A., ROSELLO, C., CANELLAS, J. and MULET, A. 1991. Drying kinetics of a majorcan seedless grape variety. In *Drying 91*, (A.S. Mujumdar, ed.) pp. 455–461, Elsevier Science Publishers, Amsterdam.

BOLAND, F.E. 1984. Fruits and Fruit Products. In *AOAC Official Methods of Analysis, Fruits and Fruit Products*, (W. Horwitz, ed.) pp. 413–418, AOAC, Washington.

CANELLAS J., ROSELLO, C., SIMAL, S. and MULET, A. 1993. Storage conditions affect quality of raisins. J. Food Sci. *58*, 4, 805–809.

CHAMBERS, T.C. and POSSINGHAM, J.V. 1963. Studies of the fine structure of the waxy layer of sultana grapes. Aust. J. Biol. Sci. *16*, 818–825.

DECAREAU, R.V. and PETERSON, R.A. 1986. *Microwave Process Engineering*, Ellis Horwood Ltd., Chichester, England.

JACOB, H.E. 1944. Factors influencing the yield, composition, and quality of raisins. Bulletin No. 683, Agricultural Experiment Station, Univ. of California, Berkeley, California.

LYONS, D.W., HATCHER, J.D. and SUNDERLAND, J.E. 1972. Drying of a porous medium with internal heat generation. Int. J. Heat and Mass Transfer *15*, 897.

MAROULIS, Z.B., TSAMI, E. and MARINOS-KOURIS, D. 1988. Application of the GAB model to the moisture sorption isotherms for dried fruits. J. Food Engng., *7*,1, 63–78.

METAXAS, A.C. and MEREDITH, R.J. 1983. *Industrial Microwave Heating*, Peter Peregrinus Ltd., London, U.K.

PONTING, J.D. and McBEAN, D.M. 1970. Temperature and dipping treatment effects on drying rates and drying times of grapes, prunes and other waxy fruits. Food Tech. *24*, 84–88.

RIVA, M., PERI, C. and LOVINO, R. 1986. Effects of pretreatments on kinetics of grape drying. In *4th Int. Congress on Food Engineering and Applications*, Vol. 1, (M. Le Maguer and P. Jelen, eds.) Elsevier Applied Science Publ., Amsterdam.

SARAVACOS, G.D. and MAROUSIS, S.N. 1988. Effect of ethyl oleate on the rate of air-drying of foods. J. Food Engn. *7*, 263–270.

SAS. 1989. SAS INSTITUTE INC., *SAS/STAT User's Guide*, Version 6, 4th Ed. Vol. 2, Cary, NC.

STEEL, G.D. and TORRIE, J.H. 1980. *Principles and Procedures of Statistics*, McGraw-Hill Book Co., New York.

TULASIDAS, T.N., RAGHAVAN, G.S.V. and NORRIS, E.R. 1993. Microwave and convective drying of grapes. Trans. ASAE, *36*, 6, 1861–1865.

TURNER, I.W. and JOLLY, P.G. 1991. Combined microwave and convective drying of a porous material. Drying Tech. *9*,5, 1209–1269.

WINKLER, A.J., COOK, W.M., KLIEWER, W.M. and LIDER, L.A. 1974. *General Viticulture*, Univ. of California Press, Berkely, CA.

SIMULTANEOUS DIFFUSION OF CITRIC ACID AND ASCORBIC ACID IN PREPEELED POTATOES

A.M. LOMBARDI and N.E. ZARITZKY[1]

Centro de Investigación y Desarrollo en Criotecnología de Alimentos, CIDCA
Facultad de Ciencias Exactas, Dpto. de Ingeniería Química, Facultad de Ingeniería
Universidad Nacional de La Plata. CONICET

Accepted for Publication February 12, 1995

ABSTRACT

The study of the simultaneous diffusion of chemical preservatives in vegetable tissues permits the determination of the time required to complete this process and the concentration distributions of the preservatives.

The individual or simultaneous diffusion of citric and ascorbic acids in pre-peeled potatoes was analyzed; the effect of pH decrease on the diffusive flux of ascorbic acid and the interaction between both acids was considered as the multicomponent diffusion problem.

Potato spheres of different radii were immersed in individual solutions or mixtures of citric and ascorbic acids in concentration ranging from 0.5% to 2% W/V for different immersion times and agitation conditions. The residual concentration of citric acid was determined by titrable acidity (22058 AOAC method) and that of ascorbic acid by 2-6 dichlorophenol-indophenol method.

Experimental data were fitted to the mathematical models and the effective diffusion coefficients were determined for citric ($D_e = 4.3 \pm 0.2 \times 10^{-10}$ m^2/s) and ascorbic acids ($D_e = 5.45 \pm 0.4 \times 10^{-10}$ m^2/s) diffusing individually. When mixtures of two acids were used, multicomponent analysis was adopted and interaction coefficients were evaluated ($D_{12} = 6.67 \pm 0.8 \times 10^{-11}$ m^2/s and $D_{21} = 8.33 \pm 0.8 \times 10^{-11}$ m^2/s); they were an order of magnitude lower than binary diffusion values.

The pH effect on the diffusive flux of ascorbic acid was decoupled from the interaction of both acids during simultaneous diffusion by studying the diffusion of the first acid in potatoes preacidified with the second acid.

[1]Correspondence: Dra. N.E. Zaritzky, CIDCA - Fac. Ciencias Exactas, Univ. Nac. La Plata, Calle 47 y 116, La Plata (1900) ARGENTINA.

Journal of Food Process Engineering **19** (1996) 27-48. *All Rights Reserved.*

INTRODUCTION

Prepeeled potatoes are a product characterized by a short shelf-life. Preservation from browning reactions must consider chemical treatments and storage at temperatures around 10C.

Numerous works have dealt with methods to prevent potatoes browning (Feinberg *et al.* 1975; Smith 1977). The most common chemical preservatives used to inhibit enzymatic browning are sodium sulfite and bisulfite. These salts are also known to retard microbial growth in prepeeled vegetables. However, since 1987 the FDA (Food and Drug Administration) has limited their use as food ingredients to 10 ppm. Consequently, during the last years the tendency to replace bisulfite as a preservative has moved towards the use of other preservatives like citric acid, ascorbic acid, sorbic acid and their salts, sodium erythorbate and phosphate, stand alone or in mixtures (Labell 1983; Golan-Goldhirsch and Whitaker 1984; Duxbury 1986, 1988; Giannuzzi and Zaritzky 1991; Sperber 1992).

Citric acid is used as an enzymatic browning inhibitor in fresh vegetables because it inhibits the polyphenol oxidase action. Citric acid acts in two ways: it lowers the medium pH to a value far from the optimum enzyme pH (5.6 to 6.7) and it captures cupric ions necessary for the enzymatic activity. Besides, citric acid shows antimicrobial effect.

Ascorbic acid is an effective reducing agent. It reduces the quinones formed by polyphenol oxidase action to dihydroxyquinones (Kertesz and Zito 1962) and acts as a chelating agent of specific metals found in foods; it also captures oxygen. However, ascorbic acid has a low stability and is not very effective as an antimicrobial agent.

Ascorbic acid is highly susceptible to various forms of degradation caused by temperature, salt concentration, sugar concentration, pH, oxygen, enzymes, metals and ascorbic acid/dehydroascorbic acid ratio. L-ascorbic acid is readily oxidized to dehydroascorbic acid.

To reduce L-ascorbic acid losses, presence of oxygen should be limited (e.g. vacuum packaging, nitrogen purge, sulfites addition, etc.) and presence of Cu^{+2} and Fe^{+2} which act as catalyzers (e.g. citrate complex formation, EDTA addition, etc.) should also be limited; water activity and pH should also be reduced (Liao and Seib 1988).

Labell (1983) reported that the shelf-life of vegetables treated with ascorbic acid was 3 to 4 days. However, when sulfites were used the product remained acceptable for 7 to 8 days.

The use of ascorbic acid together with citric acid makes it more stable and effective. Labell (1983) working on apples, lettuce, and potatoes, also found that adding a small amount of calcium chloride (0.1%-0.3% W/V) makes ascorbic acid (1%-5% W/V) treatments more effective.

Duxbury (1988) found that the use of alternative preservatives of sulfite such as ascorbic acid and citric acid allowed a product shelf-life of approximately 5 days and recommended dipping prepeeled potatoes for 15 to 20 min in 3-4% W/V preservative solution. The product was notably improved and the shelf-life was extended if the product was packaged with plastic films under vacuum to avoid any contact with iron, aluminum, copper or zinc.

Giannuzzi and Zaritzky (1991) working with low gas permeability films, reported that SO_2 can be replaced by 2% W/V citric acid, 2% W/V ascorbic acid or a mixture of citric acid/ascorbic acid (1%/1% W/V) with immersion times of 60 s. With these treatments a shelf-life of 20 days was reported. The quality of the product considering microbial growth, color and texture was improved with the combined use of both acids.

The study of simultaneous diffusion of the mentioned preservatives through the vegetable tissue becomes necessary. The transfer of a substance from the surface to the center of the foodstuff can be accomplished either through the extracellular space or by a substance interchange through the cell walls and membranes. A combination of both mechanisms is also possible. Potato can be considered as an insoluble matrix of starch, cellulose and pectic substances and an aqueous phase through which ascorbic acid and/or citric acid diffuse.

Effective or apparent coefficients are normally assumed; these coefficients are determined experimentally (Stahl and Loncin 1979). Solute diffusivities in leaching processes have been reported by Schwartzberg and Chao (1982). Ascorbic acid losses in potatoes during blanching in water were studied by various authors and apparent diffusivities of ascorbic acid were obtained (Luna and Garrote 1987; Kinkal and Kaymak 1989).

When simultaneous diffusion of citric and ascorbic acids into the tissue matrix occurs, the diffusion process of each component in the mixture is affected by the presence of the other component. It can be accurately described only with generalizations of Fick's law (Cussler 1976).

The study of chemical preservatives diffusion in potatoes allowed the determination of process time and whether the preservative distribution is uniform or not.

The objectives of the present work were:

(1) to analyze the diffusion of citric acid and ascorbic acid either individually or simultaneously in a vegetable tissue like prepeeled potatoes,
(2) to determine the binary and multicomponent diffusion coefficients by fitting the mathematical models to the experimental concentration values,
(3) to identify the effect of pH decrease in the diffusive flux of ascorbic acid, and

(4) to analyze both acids' interaction in the multicomponent diffusion process.

MATERIALS AND METHODS

Experimental Procedure

Sample Preparation. Potatoes (Kennebec variety, ρ = 1070 kg/m^3) of semi-late production from Balcarce, Buenos Aires, Argentina, without storage, were used. The potatoes were washed, hand-peeled, cut into spheres (R = 1.3 cm) and dipped into different concentration solutions of citric and/or ascorbic acids at 25C for different immersion times and agitation conditions. External solution to sample volume ratio was 100:1 to maintain constant concentration of acids during the experiment. Citric acid (Timper) and L(+) ascorbic acid (Merck) were of analytical grade.

Firstly, the diffusion coefficients of the acids diffusing individually into the samples were determined. To calculate the diffusion coefficient of citric acid, a group of spherical potatoes were dipped in 1% W/V acid solution for 5, 15, 25, and 35 min with maximum agitation (360 rpm, RK-I Rolco SRL, Argentina). The agitation conditions used allowed assumption of constant concentration at the interface that notably simplifies the mathematical resolution. This assumption was previously verified on experiments of sodium bisulfite diffusion in prepeeled potatoes (Rodriguez and Zaritzky 1986).

A second group was dipped in a 2% W/V citric acid solution agitated by a blade stirrer at 30 rpm (F.B.R. SACIF, Argentina) for 30, 60, 90 and 120 s. These conditions were selected to verify the validity of the proposed models in a wide range of agitation conditions.

A third group of spheres was dipped into a 2% W/V ascorbic acid solution for 30, 60, 90 and 120 min to evaluate the diffusion of ascorbic acid. Agitation was not applied to prevent oxidation of the ascorbic acid.

Facing the possibility that any degradation of ascorbic acid may occur due to its diffusion into a medium with pH higher than 4.0, the potato tissue was acidified. With that purpose, samples were first dipped into 2% W/V citric acid solution with no agitation for different periods until potatoes reached a pH $\leq$ 4. Then samples were dipped into 2% W/V ascorbic acid solution with no agitation for 30, 60, 90 and 120 min to quantify the diffusion coefficient.

To analyze the interaction of both acids in the multicomponent diffusion process, another group of samples was dipped into an ascorbic acid/citric acid (1%/1% W/V) solution with maximum agitation: 360 rpm (RK-I, Rolco SRL, Argentina) for 5, 15, 30, 40 and 60 min.

Finally, a group of spheres (R = 1.1 cm) with a different size to the former ones, were dipped in an ascorbic acid/citric acid (1%/0.5% W/V) solution with

the same agitation conditions for 5, 15, 30, 45 and 60 min. These conditions were used to experimentally verify the validity of the proposed model for other concentration values.

After immersion, samples were shaken gently to remove the remaining solution from the potato surface. Afterwards, the amount of the residual citric acid was determined on the first and second groups, the amount of the residual ascorbic acid on the third and fourth groups, and the amount of both acids on the last two groups.

In all cases determinations were performed in triplicate and mean values were used to calculate the diffusion coefficients.

Determination of Residual Citric Acid. Residual citric acid was determined as titratable acidity according to the 22058 AOAC method (AOAC 1984). The percentage of citric acid content in the sample was calculated assuming that 1 mL of 0.1N NaOH neutralizes 0.064g citric acid. The same procedure was followed with the control that corresponded to a potato sample without any treatment.

Determination of Residual Ascorbic Acid. Titration of 2-6 dichlorophenol-indophenol method was followed. This method is based on the reduction of the dye agent by acid action (AOAC 1984). The same procedure was followed with the control that corresponded to a potato sample without any treatment. Albrecht and Schafer (1990) compared the titration method of 2-6 dichlorophenol-indophenol against the high performance liquid chromatography (HPLC) method to determine ascorbic acid on different vegetables. The first method gave satisfactory results whenever interfering substances (copper, iron, etc.) were not present. The advantages of this method are its simplicity and low cost.

Augustin *et al.* (1981) determined ascorbic acid on potatoes and did not find differences between HPLC and the titration method for raw potatoes. However, they found different results for some potato products. Bushway *et al.* (1984), when comparing both methods, reported similar observations working on different varieties of potatoes.

Percent Recovery of the Dosage Methods. A known amount of citric or ascorbic acid in the corresponding diluent was added to potatoes without any treatment to determine the percent recovery of the different dosage techniques. The reported values were means of three replicates.

Determination of the Experimental Conditions for the Previous Acidification of the Tissue. The pH of the potato tissue ranged between 5.6 and 6.0 (Weast 1975). As discussed previously, a pH $>$ 4.0 makes ascorbic acid susceptible to degradation.

To compare individual diffusion of ascorbic acid within systems with and without acidification, potato spheres were dipped in a 2% W/V citric acid solution (pH = 2.3) to decrease the sample pH; no agitation was provided. Samples were dipped in the solution for different periods. Afterwards, samples were finely ground to measure their pH and to determine the time necessary to reach pH $\leq$ 4.0.

Determination of Solid Moisture. Potato moisture was determined by the 32083 AOAC method (AOAC 1984).

Potatoes were cut into thin slices. Approximately 10g of slices were dried at 105C until constant weight (tolerance difference < 0.5 mg). An infrared drying unit (Mettler LP 16, Switzerland) with a balance (Mettler PE 300, Switzerland) was used. Moisture values were recorded every 10 min.

Mathematical Modeling

Binary Diffusion. The diffusion mechanism in symmetric porous materials can be analyzed by the general form of the microscopic mass balance:

$$\frac{\partial c}{\partial t} = \frac{1}{r^{\phi-1}} \frac{\partial}{\partial r} \left(r^{\phi-1} D_e \frac{\partial c}{\partial r}\right) \quad (1)$$

where c is the solute concentration in the solid expressed as ascorbic acid or citric acid weight per solid volume unit, with $\phi = 1$ for an infinite flat plate, 2 for an infinite cylinder, 3 for a sphere; r is the distance measured from the center of the solid and D_e is the diffusion coefficient of citric acid or ascorbic acid in the potato matrix. The diffusion coefficient can be expressed in terms of molecular diffusivity (D_{AB}) porosity (ε) and tortuosity factor (Ω) (Sherwood *et al.* 1975):

$$D_e = \frac{D_{AB}\varepsilon}{\Omega} \quad (2)$$

Prepeeled potatoes are frequently processed in spheres, cubes and parallelepiped shapes. In the case of spheres (radius R) at initially c_0 concentration and with the following boundary condition:

$$\text{at } t>0; \quad D_e \frac{\partial c}{\partial r} = k_L(c_f' - c') = \frac{k_L}{\epsilon}(c_f - c); \quad \text{when} \quad r=R \quad (3)$$

where k_L is the mass transfer coefficient at the potato-solution interface, c'f is the bulk concentration and c' is the concentration of ascorbic acid or citric acid in the dipping solution (weight of ascorbic acid or citric acid per unit volume of solution), and ϵ is the potato porosity (water content on wet basis). The ratio of the equilibrium distribution between the solute concentration in the dipping

solution (c′) and the concentration in the solid was calculated as $c = c'\epsilon$ assuming that the partition coefficient equals one.

The solution of Eq. 1, which was integrated over the total sample volume (V) (Rodriguez and Zaritzky 1986) is:

$$F=\frac{M_t}{M_\infty}=1-\sum_{n=1}^{\infty}\frac{6Bi^2\exp(-\alpha_n^2 t^*)}{\alpha_n^2(\alpha_n^2+Bi(Bi-1))} \tag{4}$$

where $M_\infty = c'_f \epsilon V$, the Biot number is $Bi = (k_L R)/(D_e \epsilon)$, $t^* = (D_e t)/R^2$ and α_n $n = 1, 2\ldots$ are the roots of:

$$\alpha_n \cot \alpha_n = 1-Bi \tag{5}$$

If $Bi > 200$ the error in diffusion coefficient estimation due to neglected external resistance is less than 1% (Schwartzberg and Chao 1982).

When the concentration at the interface can be assumed as constant the boundary condition (Eq. 3) is replaced by $c = c_f$. The amounts of the residual acid were calculated as follows:

$$F = \frac{M_t}{M_\infty} = 1-\frac{6}{\pi^2}\sum_{n=1}^{\infty}\frac{1}{n^2}\exp(-t^* n^2\pi^2) \tag{6}$$

The mass transfer coefficients (k_L) of the solution were calculated using the following equation (Sherwood *et al.* 1975) in terms of Reynolds and Schmidt numbers and evaluating the potato-fluid relative velocity:

$$\frac{k_L 2R}{D_{AB}} = 2+0.6Re^{1/2}Sc^{1/3} \qquad \text{(spheres)} \tag{7}$$

These equations were previously verified in experiments of sodium bisulfite diffusion (Rodriguez and Zaritzky 1986).

Multicomponent Flux Equations. There are two approaches to describe the multicomponent diffusion: one is experimental and the other is theoretical (Cussler 1976). The last one, suggested by Maxwell on the basis of the kinetic theory of ideal gases is described by:

$$\nabla x_i=\sum_{j=1}^{n}\frac{x_i x_j}{D_{ij}}(v_j-v_i) \qquad i=1\ldots n \tag{8}$$

where x_i, x_j, v_i and v_j are the molar fractions and velocities of each component, respectively, and D_{ij} is the binary diffusion coefficient.

The mathematical alternative supported by experiment was suggested by Onsager in 1945:

$$J_i = \sum_{j=1}^{n-1} D_{ij} \nabla c_j \tag{9}$$

and is known as the generalized Fick's law form. The D_{ii} are called the main-term coefficients and generally equal the binary coefficients. The D_{ij} are the cross-term coefficients, generally of a lower value than the main-term coefficients.

The disadvantages of this equation are that one of the components must be chosen as solvent (n) and that the D_{ij} tend to depend strongly on concentration. However, this approach is recommendable by its simple mathematical and experimental treatment. It is frequently used in systems where density may be assumed constant. This equation was applied to multicomponent systems as in the isothermal evaporation of ethanol and toluene into stagnant air (Cussler and Lightfoot 1963) and to estimate the diffusion coefficients of LiCl-KCl and LiCl-NaCl mixtures in aqueous solution (Fujita and Gosting 1956).

Onsager's equation was used in the present work to analyze the simultaneous diffusion of both citric and ascorbic acids assuming the presence of two solutes and a solvent, absence of chemical reaction, one-dimensional diffusion, diffusion coefficients independent of solute concentration and that the diffusive flux was more important than the convective flux. Thus, the equations that govern the phenomenon are:

$$\frac{\partial c_i}{\partial t} = \frac{1}{r^2} \frac{\partial}{\partial r}\left(r^2 \sum_{j=1}^{2} D_{ij} \frac{\partial c_j}{\partial r} \right) \quad r \leq R \quad i=1,2 \tag{10}$$

for a sphere immersed in a perfectly agitated solution. The solutes with concentrations c'_{1f} and c'_{2f} diffuse from the solution.

The following initial and boundary conditions were considered:

$$\begin{aligned} &t \leq 0 \quad c_i = c_{i0} \quad r \leq R \\ &t > 0 \quad c_i = c_{if} \quad r = R \\ &i = 1,2 \end{aligned} \tag{11}$$

where i indicates each participating species.

The system of Eq. 10 has an associated $\underline{\underline{D}}$ coefficients matrix:

$$\underline{\underline{D}} = \begin{bmatrix} D_{11} & D_{12} \\ D_{21} & D_{22} \end{bmatrix}$$

This matrix can be converted into a diagonal form by an adequate transformation, thus the original system is decoupled (Paul and Di Benedetto 1965; Zorrilla and Rubiolo 1992). The eigenvalues of the $\underline{\underline{D}}$ matrix are:

$$\lambda_{1,2} = \frac{D_{11} + D_{22} \pm \sqrt{(D_{11}-D_{22})^2+4D_{12}D_{21}}}{2} \qquad (12)$$

and are real and different.

The equation system of 10 and 11 is represented in matrix form.

Defining a new concentration $\underline{\psi}$:

$$\underline{\psi} = \underline{\underline{V}}^{-1} \bullet \underline{c}$$

where $\underline{\underline{V}}$ is called the modal matrix (Cussler 1976):

$$\underline{\underline{V}} = \begin{bmatrix} 1 & \dfrac{D_{12}}{D_{22}-\lambda_1} \\ \dfrac{D_{22}-\lambda_2}{D_{12}} & 1 \end{bmatrix}$$

a decoupled system was obtained.

Crank (1957) presents the solution for spheres initially at c_o concentration and constant concentration at the surface (c_f). Working with the $\underline{\psi}$ variable under matrix form, the solution is:

$$\frac{\underline{\psi}-\underline{\psi}_0}{\underline{\psi}_f-\underline{\psi}_0} = \underline{\underline{I}} + \frac{2R}{\pi r}\sum_{n=1}^{\infty}\frac{(-1)^n}{n}\sin\frac{n\pi r}{R}\exp\left[\frac{-\underline{\Lambda} n^2\pi^2 t}{R^2}\right] \qquad (13)$$

where $\underline{\Lambda}$ is a diagonal matrix whose elements are the eigenvalues of $\underline{\underline{D}}$.

When this equation is integrated over the total sample volume (V) and considering the variable transformation used, it results in:

$$\frac{\underline{M}_t}{\underline{M}_\infty} = \underline{\underline{I}} - \frac{6}{\pi^2}\sum_{n=1}^{\infty}\frac{1}{n^2}\exp\left[\frac{-\underline{\underline{D}} n^2\pi^2 t}{R^2}\right] \qquad (14)$$

Determination of the Diffusion Coefficients of Ascorbic and Citric Acids in Potato Tissue. The uptake of ascorbic and/or citric acid was experimentally measured and compared to the results of the residual acid concentration calculated from the theoretical models. Diffusion coefficients were calculated

from computational programs of the models using FORTRAN (Microsoft, FORTRAN) language.

The models were also used to predict the results for other situations like different concentrations of the acid solution and different sphere sizes.

When less than perfect agitation was reached, experimental values were fitted to the theoretical curves of Eq. 4. The Biot number and t*, both contain in an implicit form the diffusion coefficient, thus, the best fit was obtained by selecting the D_e value that leads to the least percent deviation between both theoretical and experimental values for residual concentration.

The α_n roots of Eq. 5 were determined from an iterative computational algorithm. A modified Regula Falsi method was used; for short contact times, more than twenty-five roots were calculated to get convergence of the Series. Convergence criterion was established as $S_n - S_{n+1} < 1$ ppm, with S_n being the summation of n terms in Eq. 4.

In the case of simultaneous diffusion, Eq. 14 was fitted to the experimental values of residual concentrations of both acids. D_{11} and D_{22} were calculated as the binary coefficients and different D_{12} and D_{21}, were selected to get the least percent deviation (%E) between theoretical (W_T) and experimental (W_e) concentrations of the residual content of citric or ascorbic acids and N is the number of experimental data considered.

To determine whether the interaction of the diffusion of both acids is a relevant factor or not, experimental values were fitted in parallel to the theoretical curves considering $D_{12} = D_{21} = 0$. The percent relative error (%e) was compared for each preservative in both situations.

$$\%e = \frac{\sum_{n=1}^{N} \left[\frac{W_t - W_e}{W_e} \right]}{N}$$

RESULTS AND DISCUSSION

Moisture Determination

The mean moisture value for potato samples was 80%, expressed as $(g_{water}/g_{total})*100$ with a variability of 1.1%.

Citric Acid

Determination of Citric Acid Uptake in Potatoes. Experimental data of total uptake of citric acid in spherical potato samples (R = 1.3 cm) as a function of immersion time in citric acid solution (1% W/V) are shown in Fig. 1 for an agitation condition of 360 rpm. The average residual concentration values in ppm for different immersion times were calculated subtracting the total acidity

value of the corresponding nontreated potatoes. The percent recovery of the extraction method was 89%.

Citric acid is the most abundant acid found in potatoes. Reported values of citric acid of Russet Burbank potatoes stored at 15.5C are 292 ppm for the apical zone and 221.8 ppm for the basal zone (Silva *et al.* 1991). Bushway *et al.* (1984), studying different organic acids in some potato varieties, found by chromatographic techniques that the value for citric acid of Kennebec variety was 481 ± 21.4 mg per 100 g of fresh material for the apical zone and 474.9 ± 25.8 mg for the basal zone. Lisinska and Amiolowsky (1990) reported values between 131 and 208 mg of citric acid per 100 g of fresh product depending on potato variety.

The selected technique used to determine citric acid allowed the calculation of the residual uptake by simple subtraction between concentration values of treated and nontreated samples.

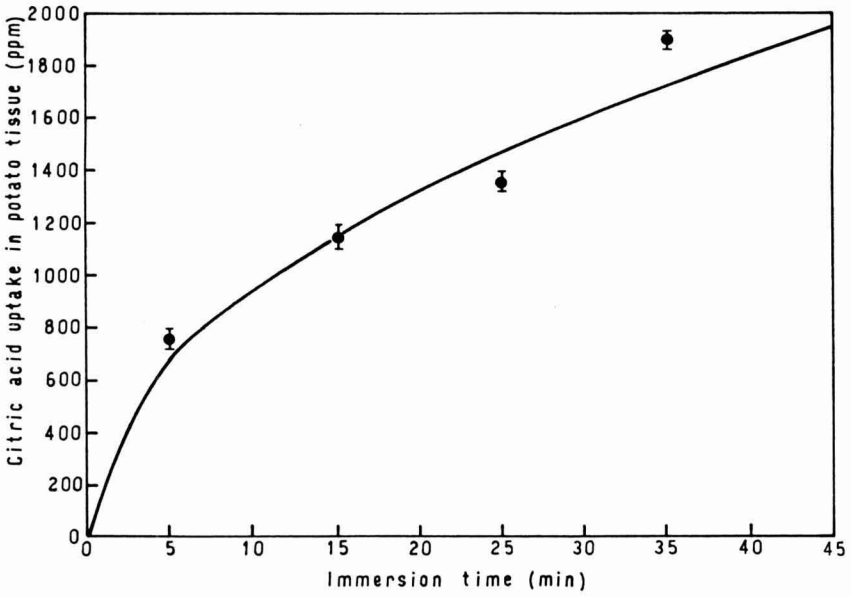

FIG. 1. COMPARISON OF PREDICTED (—) AND EXPERIMENTAL (•) CITRIC ACID UPTAKE (PPM) IN SPHERICAL PREPEELED POTATOES (R = 1.3 CM)
Concentration of dipping solution: 1% W/V citric acid. Constant interfacial concentration (Bi > 700).

Determination of Diffusion Coefficient of Citric Acid. As previously mentioned, the assumption of constant concentration at the interface notably simplifies the calculation of the diffusion coefficient.

To calculate the diffusion coefficient of citric acid the results shown in Fig. 1 were used. These results correspond to constant interfacial concentrations (Biot > 700).

For samples with 20% total solids content, the effective diffusion coefficient which minimized differences between theoretical and experimental values (Fig. 1) was $D_e = 4.3 \pm 0.2 \times 10^{-10}$ m^2/s. The diffusion coefficient value was verified performing another experiment (Fig. 2).

A satisfactory fit was observed when the mass transfer coefficient (k_L) of this experiment, (corresponding to an agitation condition of 30 rpm) was $k_L = 1.32 \times 10^{-6}$ m/s. This value was obtained from Eq. 7 that led to Bi = 50.

Replacing the obtained value of D_e in Eq. 2 and considering $D_{citr.-water} = 6.61 \times 10^{-10}$ m^2/s (Perry and Chilton 1973), $\epsilon = 0.8$ (total solids content = 20%) a tortuosity value of $\Omega = 1.23$ was calculated. This value is similar to those reported by Calvelo and Califano (1983), Stahl and Loncin (1979) and Rodriguez and Zaritzky (1986).

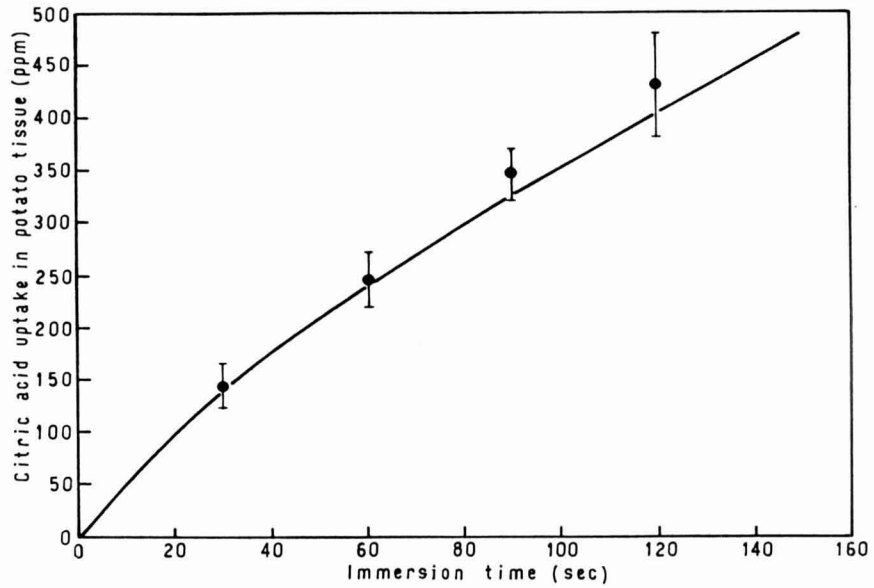

FIG. 2. COMPARISON OF PREDICTED (—) AND EXPERIMENTAL (•) CITRIC ACID UPTAKE (PPM) IN SPHERICAL PREPEELED POTATOES (R = 1.3 CM)
Concentration of dipping solution: 2% W/V citric acid, 30 RPM (Bi = 50).

Ascorbic Acid

Determination of Ascorbic Acid Uptake in Potatoes. The concentration of ascorbic acid in nontreated potatoes was determined and the obtained value was 121 ± 24 ppm according to literature data (Shekhar and Iritani 1979; Augustin *et al.* 1981; Bushway *et al.* 1984; Keijbets and Ebbenhars-Seller 1990; Mullin *et al.* 1991). Ascorbic acid content in potatoes depends on the soil characteristics and potato variety (Mullin *et al.* 1991; Vanderslice and Higgs 1991). The percent recovery of the dosage method used was 88%. The values of residual ascorbic acid content in spherical samples are shown in Table 1. These values were used in an attempt to model ascorbic acid diffusion and consequently calculate the effective diffusion coefficient. However, the experimental values of Table 1 were so small that no one ϵ/Ω ratio allowed a satisfactory fit of the theoretical curve of Eq. 4. This fact suggested that oxidation reactions of ascorbic acid may have occurred.

Considering that the dosage method used does not detect the oxidized form of ascorbic acid, it was decided to use diffusion data of previously acidified potatoes as detailed later.

TABLE 1.
VALUES OF RESIDUAL ASCORBIC ACID IN SPHERICAL POTATOES SAMPLES (R = 1.3 CM) FOR DIFFERENT IMMERSION TIMES
Concentration of dipping solution 2% W/V ascorbic acid, without agitation.

Immersion Time (min)	Residual Ascorbic Acid (ppm)
30	437 ± 14
60	634 ± 35
90	1006 ± 10
120	1150 ± 17

Determination of Immersion Time in the Acidifying Solution. Table 2 shows the pH values of the potato tissue after different immersion times in a 2% W/V citric acid solution.

The pH of nontreated samples was 5.8 ± 0.2. This value is within the range reported by other authors (Lisinska and Amiolowski 1990). According to the results of Table 2, spheres were dipped for more than 3 h 30 min in a 2% W/V citric acid solution to reach the desired pH (pH < 4.0).

TABLE 2.
TISSUE PH OF SPHERICAL POTATO SAMPLES (R = 1.3 CM), FOR DIFFERENT IMMERSION TIMES IN 2% W /V CITRIC ACID SOLUTION WITHOUT AGITATION

Immersion Time (min)	pH of Vegetable Tissue
non-treated	5.8 ± 0.20
60	5.0 ± 0.25
90	4.5 ± 0.20
210	4.0 ± 0.15
1080	3.5 ± 0.10

Effect of Previous Tissue Acidification on Ascorbic Acid Diffusion. Results shown in Fig. 3 correspond to ascorbic acid diffusion (2% W/V ascorbic acid solution, stagnant conditions) in spherical samples (R=1.3cm) previously acidified with citric acid (pH = 3.5).

These results showed a marked increase of ascorbic acid concentration compared to samples without acidification (pH = 5.8) shown in Fig. 4; degrading reactions were inhibited at pH ≤ 4.0.

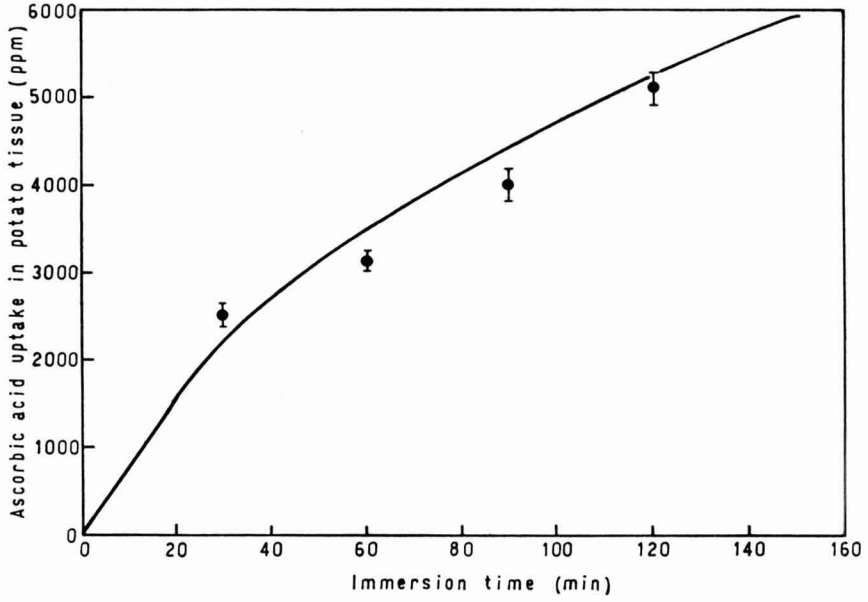

FIG. 3. COMPARISON OF PREDICTED (—) AND EXPERIMENTAL (•) ASCORBIC ACID UPTAKE (PPM) IN SPHERICAL PREPEELED POTATOES (R = 1.3 CM) PREVIOUSLY ACIDIFIED IN 2% W/V CITRIC ACID FOR 3 H 30 MIN
Concentration of dipping solution: 2% W/V ascorbic acid without agitation.

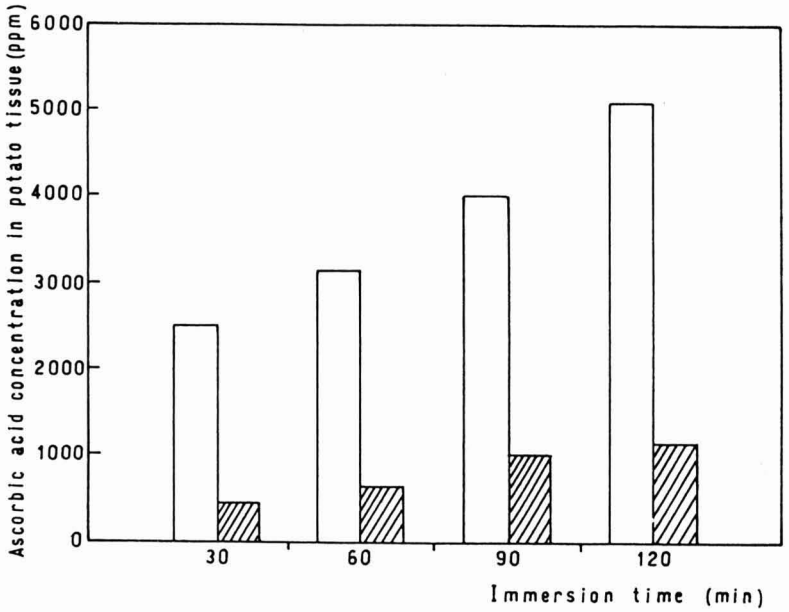

FIG 4. ASCORBIC ACID UPTAKE IN SPHERICAL POTATO SAMPLES ACIDIFIED IN 2% W/V CITRIC ACID SOLUTION FOR 3 HR 30 MIN (□) AND WITHOUT ACIDIFICATION (▨)
Concentration of dipping solution: 2% W/V ascorbic acid without agitation.

Determination of Diffusion Coefficient of Ascorbic Acid in Potato. Diffusion coefficient of ascorbic acid was calculated from the data shown in Fig. 3. A finite Biot number had to be used because of the inconvenience in working with ascorbic acid solutions highly agitated that leads to instability problems. For the given experimental conditions a $k_L = 6.37 \times 10^{-7}$ m/s (Bi = 19) was calculated from Eq. 7.

The effective diffusion coefficient which minimized differences between theoretical curves and experimental data was $D_e = 5.45 \pm 0.4 \times 10^{-10}$ m^2/s (Fig. 3).

From this value of D_e with a known $D_{asc\text{-}water} = 8.4 \times 10^{-10}$ m^2/s (Perry and Chilton 1973), and being $\epsilon = 0.8$, a similar tortuosity coefficient $\Omega = 1.23$ was obtained, in agreement with the one previously calculated.

With the D_e of citric acid previously calculated, the acidifying time was evaluated considering the same agitation conditions in order to verify whether or not enough time was used in the acidifying experiments with citric acid. An immersion time of 3 h 30 min gave a concentration at the center of the sphere

corresponding to 95% of that of the surface. Thus, the targeted pH was reached in the entire sphere during the immersion time.

Determination of Ultimate Ascorbic Acid and Citric Acid Content of Potatoes Dipped in a Mixture of Both Acids. Fig. 5a shows the results for the simultaneous diffusion of both acids after dipping the sample in a citric acid/ascorbic acid solution (1%/1% W/V, R = 1.3cm) with agitation (RK-I Shaker, 360 rpm, ROLCO SRL).

A good agitation was provided to assure a constant interface concentration which notably simplifies the multicomponent diffusion equations.

For each component, theoretical curves of Eq. 14 were fitted to the experimental values presented in Fig. 5a. The cross coefficients D_{12} and D_{21}, were determined assuming that D_{11} and D_{22} equaled the previously calculated binaries.

Considering $D_{11} = 4.3 \pm 0.2 \times 10^{-10}$ m^2/s for citric acid and $D_{22} = 5.45 \pm 0.4 \times 10^{-10}$ m^2/s for ascorbic acid, values of $D_{12} = 6.67 \pm 0.8 \times 10^{-11}$ m^2/s and $D_{21} = 8.33 \pm 0.8 \times 10^{-11}$ m^2/s were obtained using a computational program. The values of the cross diffusion coefficients were approximately an order of magnitude smaller than the binary coefficients. Fujita and Gosting (1956) presented similar findings for aqueous solutions of LiCl-KCl and LiCl-NaCl, like Zorrilla and Rubiolo (1992) did for diffusion of salts in cheese.

To validate the model, the theoretical curves were fitted to the experimental values shown in Fig. 5b. These values corresponded to spheres with a smaller diameter (R = 1.1.cm), immersed in a solution of different concentration (ascorbic acid/citric acid, 1%/0.5% W/V) but the same agitation conditions. These conditions still allow the assumption of constant concentration at the interface. Curves of Fig. 5b show a satisfactory fitness with percent errors (%e) of 1.0% for citric acid and 2.5% for ascorbic acid.

It must be emphasized that if D_{22} coefficient had not been calculated from experiments with ascorbic acid uptake of previously acidified potatoes, much larger values for the interaction coefficients (D_{ij}) would have been found.

To quantify the error introduced when negligible cross-term coefficients are considered, theoretical curves of Eq. 14 were fitted to the experimental values of Fig. 5a but assuming $D_{ij} = 0$. The percent error between experimental and theoretical values was in that case 7% for citric acid and 9% for ascorbic acid. These errors were higher than those previously calculated considering the interaction; however, the higher mathematical complexity of multicomponent diffusion introduced by the cross-term coefficients can only be justified when very small errors are admitted.

A comparison between experimental values of citric and ascorbic acids uptake and the predicted ones, using the calculated diffusion coefficients are shown in Fig. 6.

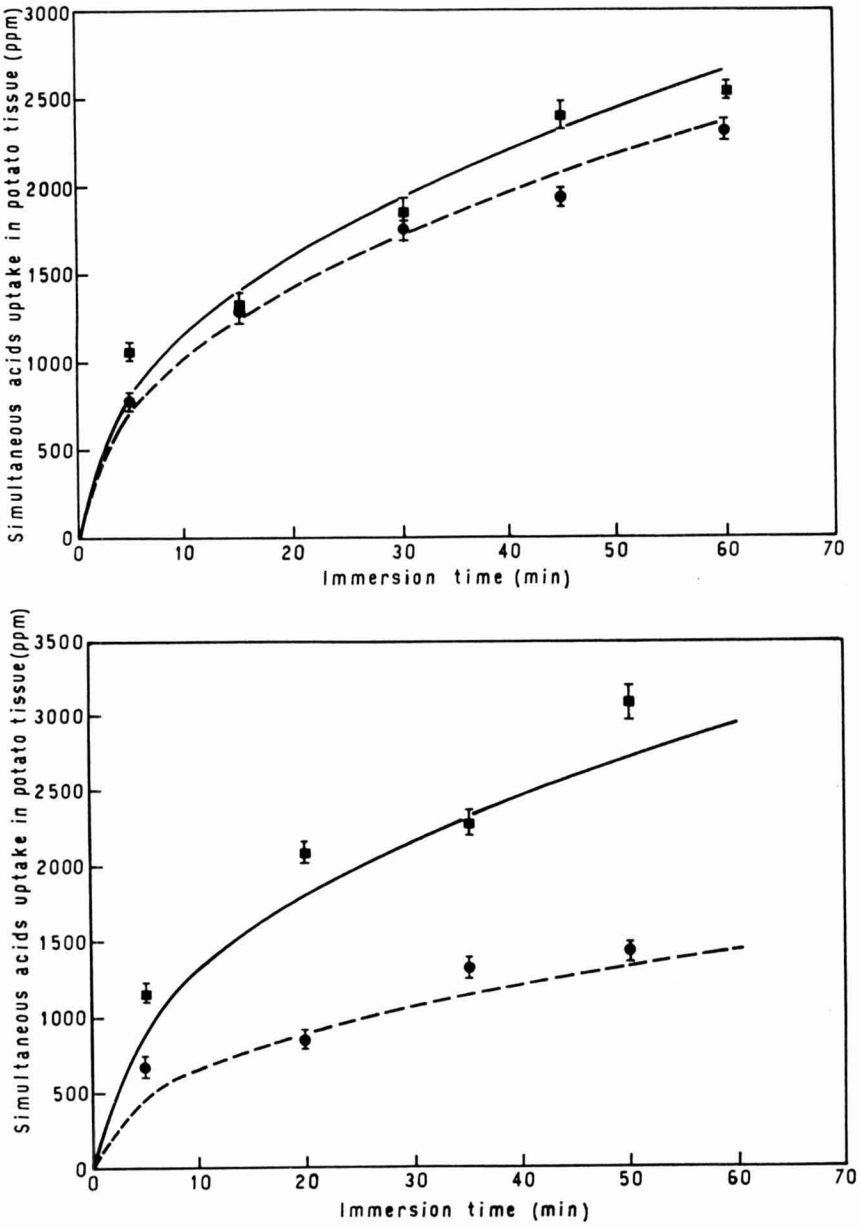

FIG. 5: COMPARISON OF PREDICTED AND EXPERIMENTAL SIMULTANEOUS ACIDS UPTAKE IN SPHERICAL PREPEELED POTATOES

Constant interfacial concentration (Bi > 700, 360 rpm). Experimental data: citric acid (●), ascorbic acid (■) in ppm; predicted curves citric acid (--) and ascorbic acid (—) uptake (ppm)
a) R = 1.3 cm, concentration of dipping solution 1%/1% W/V citric acid/ascorbic acid;
b) R = 1.1 cm, concentration of dipping solution 0.5%/1% W/V citric acid/ascorbic acid.

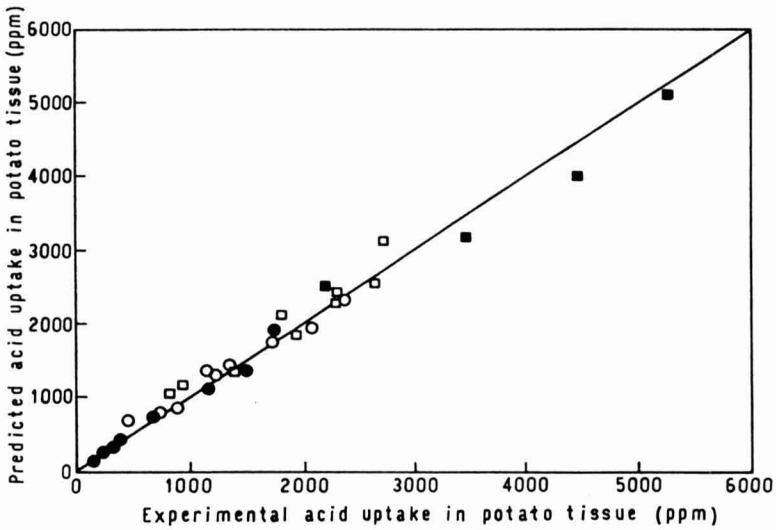

FIG. 6. COMPARISON BETWEEN PREDICTED AND EXPERIMENTAL ACIDS UPTAKE IN INDIVIDUAL DIFFUSION (● CITRIC ACID, ■ ASCORBIC ACID) AND SIMULTANEOUS DIFFUSION (○ CITRIC ACID, □ ASCORBIC ACID)
The 45° straight line corresponds to the ideal situation.

The tested cases included different radii of samples, acids concentration in external solution and agitation conditions in binary and multicomponent diffusion according to the described experiments. This plot showing deviations from the 45° straight line (ideal situation) is helpful to appreciate the goodness of fit.

CONCLUSIONS

(1) The diffusion models considering effective coefficients satisfactorily describe the ascorbic acid and/or citric acid uptake in prepeeled potatoes dipped in the acidified solutions.

(2) The fit of the mathematical models to the experimental concentration data allowed the calculation of the values of the binary ($D_{11} = 4.3 \pm 0.2 \times 10^{-10}$ m^2/s for citric acid and $D_{22} = 5.45 \pm 0.4 \times 10^{-10}$ m^2/s for ascorbic acid) and multicomponent diffusion coefficients ($D_{12} = 6.67 \pm 0.8 \times 10^{-11}$ m^2/s and $D_{21} = 8.33 \pm 0.8 \times 10^{-11}$ m^2/s).

(3) The effect of pH on the diffusion flux of ascorbic acid was decoupled from the acids' mutual interaction during multicomponent diffusion.

(4) Even when ascorbic and citric acids interaction during multicomponent diffusion do exist, the use of cross-term coefficients is justified only when errors lower than 7% are permitted.

ACKNOWLEDGMENT

The authors gratefully acknowledge the Consejo Nacional de Investigaciones Científicas y Técnicas (CONICET), Argentina for providing financial support to this work.

NOMENCLATURE

Bi Biot number, $Bi = (k_L R)/(D_e \epsilon)$
c solute concentration in the solid (weight of citric or ascorbic acid per unit volume of potato)
c′ solute concentration in solution (weight of citric or ascorbic acid per unit volume of solution, $c' = c/\epsilon$
$\underline{c}$ concentration vector
D_{AB} molecular diffusivity (m^2/S)
D_e effective diffusion coefficient of citric or ascorbic acid in the potato matrix (m^2/s)
$\underline{\underline{D}}$ diffusion coefficients matrix
%E percent deviation
%e percent standard error
F fractional uptake ($F = M_t/M_\infty$
k_L mass transfer coefficient at the potato fluid interface (m/s)
$\underline{\underline{I}}$ identity matrix
M_t amount of diffusing substance in the sample at time t
M_∞ amount of diffusing substance in the sample at infinite time
N number of experimental data
r distance measured from the center of the solid (m)
R sphere radius (m)
V potato sample volume (m^3)
$\underline{\underline{V}}$ modal matrix
$\underline{\underline{W}}$ residual ascorbic or citric acid (ppm)

Greek Letters

α_n positive roots of Eq. 8
ϵ porosity, water content on wet basis
μ solution viscosity (kg/m s)
ø shape factor in Eq. 2
Ω tortuosity factor
ρ potato density (kg/m^3)
ψ transformed variable
$\underline{\psi}$ transformed variable vector

λ eigenvalue
$\underline{\underline{\Lambda}}$ matrix of associated eigenvalues to $\underline{\underline{D}}$

Superscripts

* dimensionless variables

Subscripts

$_i$ i component
$_j$ j component
$_0$ at initial time
$_f$ in bulk dipping solution
$_1$ citric acid
$_2$ ascorbic acid
$_e$ experimental values
$_t$ theoretical values

REFERENCES

ALBERECHT, J.A. and SCHAFER, H.W. 1990. Comparison of two methods of ascorbic acid determination in vegetables. J. Liquid Chrom. *13* (13), 2633–2641.

AOAC. (1984) Official Methods of Analysis 13th Ed. Association of Official Analytical Chemists, Washington, DC.

AUGUSTIN, J., BECK, C. and MAROUSEK, G.I. 1981. Quantitative determination of ascorbic acid in potatoes and potato products by high performance liquid chromatography. J. Food Sci. *46*, 312–313, 316.

BUSHWAY, R.J., BUREAU, J.L. and MACGANN, D.F. 1984. Determinations of organic acids in potatoes by high performance liquid chromatography. J. Food Sci. *49*, 75–77, 81.

CALIFANO, A.N. and CALVELO. 1983. Heat and mass transfer during the warm water blanching of potatoes. J. Food Sci. *48*, 220–225.

CRANK, J. 1957. *The Mathematics of Diffusion*, Oxford University Press, London.

CUSSLER, E.L. 1976. *Multicomponent Diffusion*, Vol 3. Elsevier Scientific Publishing, Amsterdam.

CUSSLER, E.L. and LIGHTFOOT, E.N. 1963. Multicomponent diffusion in restricted system. AIChE J. *9* (6), 783–785.

DUXBURY, D. 1986. Sulfite alternative blend extends fruit, vegetable freshness. Food Processing, *Nov.*, 64–66.

DUXBURY, D. 1988. Stabilizer blend extends shelf-life of fresh fruit, vegetables. Food Processing, *Sept.*, 98–99.

FEINBERG, B., OLSON, R. and MULLINS, W.R. 1975. Pre-peeled potatoes. In *Potato Processing*, Ch. 18, (W. Talburt and O. Smith, eds.) Van Nostrand Reinhold/AVI, New York.

FUJITA, H. and GOSTING, L.J. 1956. An exact solution of equations for free diffusion in three-component system with interacting flows and its use in evaluation of diffusion coefficients. J. Am. Chem. Soc. *78*, 1099–1106.

GIANNUZZI, L. and ZARITZKY, N.E. 1991. The effect of packaging film on the shelf-life of treated refrigerated pre-peeled potatoes. Packaging Tech. and Sci. *4*, 69–76.

GOLAN-GOLDHIRSH, A. and WHITAKER, J.R. 1984. Effect of ascorbic acid, sodium bisulfite and thiol compounds on mushroom polyphenol oxidase. J. Agric. Food Chem. *32*, 1003-1009.

KEIJBETS, M.J.H. and EBBENHARST-SELLER, G. 1990. Loss of vitamin C (L - ascorbic acid) during long-term cold storage of duch table potatoes. Potato Res. *33*, 125–130.

KERTESZ, D. and ZITO, R. 1962. Phenolase, In *Oxygenases*, (O. Hayoishi, ed.) pp. 307, Academic Press, New York.

KINKAL, N.S. and KAYMAK, F. 1989. Simultaneous diffusion and degradation of ascorbic acid in potato blanching. *Engineering and Food* (Vol. 1): *Physical Properties and Process Control*, (W.E.L. Spiess and H. Shubert, eds.) pp. 512–520, Elsevier Applied Science, London.

LABELL, F. 1983. Sulfite alternatives. Food Process., *Nov.*, 54.

LIAO, M. and SEIB, P.A. 1988. Chemistry of L-ascorbic acid to foods. Food Chemistry *30*, 289–312.

LISIŃSKA, G. and AMIOLOWSKI, K. 1990. Organic acids in potato tubers: Part 1 - The effect of storage temperatures and time on citric and malic acid contents of potato tubers. Food Chem. *38*, 255–261.

LUNA, J.A. and GARROTE, R.L. 1987. Prediction of vitamin C retention of potato strips blanched in water. J. Food Sci. *52* (3), 634–638, 672.

MULLIN, W.J., JUI, P.Y., NADEAU, L. and SMYRIL, T.G. 1991. The vitamin C content of seven cultivars of potatoes grown across Canada, Canadian Inst. Food Sci. and Tech. J. *24*, 169–171.

ONSAGER, L. 1945. Theories and problems of liquid diffusion. Ann. N.Y. Acad. Sci. *46*, 241.

PAUL, D.R. and DI BENEDETTO, A.T. 1965. Diffusion in amorphous polymers; J. Polym. Sci. Part. C, *10*, 17–44.

PERRY, R.H. and CHILTON, C.H. 1973. *Chemical Engineers Handbook* (5th), Ind. Student (McGraw-Hill Kogakusha, Ltd., ed.) Tokyo, Japan.

RODRIGUEZ, N. and ZARITZKY, N.E. 1986. Modeling of sulfur dioxide uptake in pre-peeled potatoes of different geometrical shapes. J. Food Sci. *51* (3), 618–622.

SCHWARTZBERG, H.G. and CHAO, R.Y. 1982. Solute diffusivities in leaching processes. Food Technol. *2*, 73–86.

SHEKHAR, V.C. and IRITANI, W.M. 1979. Changes in malic and citric acid contents during growth and storage of Solanun Tuberosum L. Am. Potato J. *56*, 87–94.

SHERWOOD, T.K., PIGFORD, R.L. and WILKE, C.R. 1975. *Mass Transfer*. International Student (McGraw-Hill Kogakusha, Ltd., ed.) Tokyo, Japan.

SILVA, G.H., CHASE, R.W., HAMMERSCHANICH, R. and CASH, J.N. 1991. After-cooking darkening of spartan pearl potatoes as influenced by location, phenolic acids, and citric acid. J. Agric. Food Chem. *39*, 871–873.

SMITH, O. 1977. Potato, Production, Storing, Processing, 2nd Ed. Van Nostrand Reinhold/AVI, New York.

SPERBER, B. 1992. Sulfite-free potatoes. Food Process., *Nov.*, 107–108.

STAHL, R. and LONCIN, M. 1979. Prediction of diffusion in solid foodstuffs. J. Food Processing and Preservation *3*, 313.

VANDERSLICE, J.T. and HIGGS, D.J. 1991. Vitamin C content of foods: sample variability. Am. J. Clin. Nutr. *54*, 1323S–7S.

WEAST, R.C. 1975. *Handbook of Chemistry and Physics* 56th Ed.

ZORRILLA, S.E. and RUBIOLO, A.C. 1992. A model for using the diffusion cell in the determination of multicomponent diffusion coefficients in gels or foods. Chemical Engineer. Sci. *49* (13), 2123-2128.

IMPLEMENTATION OF AN AUTOMATED REAL-TIME STATISTICAL PROCESS CONTROLLER

J. TAN[1], Z. CHANG and F. HSIEH

Dept. of Biological & Agricultural Engineering
University of Missouri
Columbia, MO 65211

Accepted for Publication February 12, 1995

ABSTRACT

Through a simple application, this research demonstrates the potential and procedure of applying computer vision and control techniques in developing automated real-time statistical process controllers (SPC). A computer vision system was developed to sample and measure quality variables (area, length, and width) of an extruded food product. Shewhart control charts were used to monitor the state of statistical control. Corrective actions were determined by using a PI control algorithm to minimize the product size variation caused by material inconsistency in moisture content. The system was implemented and tested. Considerable improvement was achieved in product size uniformity.

INTRODUCTION

Statistical process control (SPC) has been regaining acceptance and popularity in the past few years as a result of the increasing consumer demand for quality products and the intensifying global economic competition. Statistical process control is being employed as a major quality control mechanism for more and more manufacturing processes. It has become an indispensable tool to the manufacturing industry for improving productivity and product quality (Rauwendaal 1993).

Statistical process control is a strategy for monitoring and modifying a manufacturing process on the basis of product quality measurements. An SPC system consists of two major parts. The first includes means and activities involved to collect, store, summarize and statistically analyze quality-related data. The second is a mechanism by which necessary process corrections can be made when quality problems are detected (Sturm *et al.* 1991).

[1]To whom correspondence should be addressed.

Journal of Food Process Engineering **19** (1996) 49–61. *All Rights Reserved.*

Applications of SPC are found predominantly in discrete or batch manufacturing processes. In such a process, quality variables or attributes are evaluated for either all product units produced or product samples taken periodically. Techniques such as the Shewhart and cumulative sum (CUSUM) control charts are used to monitor the production process (Messina 1987). If a quality variable deviates excessively from its target, appropriate corrective actions are determined and implemented. Depending on the product and process, one or more steps of the SPC procedure may require human involvement. These may include manual evaluation of quality characteristics, process analysis involving production personnel, and manual implementation of corrective actions. The need for human intervention often leads to a considerable time lag between problem detection and correction, i.e., the process control is not in real-time.

For high-throughput processes, it is very desirable to have real-time process control because any time delay in process adjustment can result in significant amount of low-grade products or wastes. This is especially true for continuous processes which cannot be stopped and restarted frequently. A good example of such a process is food extrusion, which requires constant attention of experienced operators for prompt process adjustments (Harper 1979). Implementation of real-time SPC often encounters two major difficulties. One is the lack of automated means for on-line assessment of quality variables or attributes, the other is the difficulty in deriving a simple control law for determining corrective actions based on product quality measurements.

The rapid development of computers in recent years has brought about tremendous advances in measurement, process modeling, and control implementation. Computer vision has emerged as an extremely promising technology for on-line measurement of product quality. Image processing techniques have been used to quantify quality attributes of extruded and many other food products (e.g., Tan *et al.* 1994). Various computer control algorithms can be readily implemented for discrete or continuous processes. With the ability for on-line acquisition of product quality information, corrective actions can be determined by applying existing control theories and implemented digitally. It has great potential to integrate computer vision and control techniques into the development of automated real-time SPC.

In this research, computer vision and control techniques were applied in developing an automated real-time statistical process controller for improving the size uniformity of an extruded product. A computer vision system was developed to sample the product and measure the product size (area, length and width). A proportional and integral (PI) control scheme was used to determine the corrective actions. The system was implemented and tested.

PROCESS AND EQUIPMENT

The Process

In the food extrusion process, materials are driven by a set of screws through a barrel in which the materials are mixed, pressurized, heated, and subjected to shear. This process transforms the materials into a gelatinized melt in a high-pressure and high-temperature state. When the melt exits through a die orifice, it expands and is cut into a desirable size by a rotating cutter. The final product size depends on the cutter speed, material feed rate, and degree of expansion. The degree of expansion is in turn a function of several process and material property variables. These include screw speed, feed rate, material composition, moisture content, barrel temperature, extrudate pressure and temperature in the die (Kulshreshtha *et al.* 1991).

Because of inevitable variability and inconsistencies in food materials, extruded product quality varies continuously (Wiedmann and Strecker 1988). Product size, whose consistency is desirable for some extruded products, can vary considerably as a result of variations in, for example, material moisture content. Controlled extrusion performance requires constant process monitoring and adjustments by trained operators. Manual controls are slow, tedious, and unreliable. In large-scale productions, considerable off-specification wastes result from tardy process adjustments.

Equipment and Materials

An APV Baker MPF-50/25 twin-screw food extruder (APV Baker, Grand Rapids, MI) was used. The extruder was driven by a 27.96 kW (37.5 hp) DC motor. The material feeder was a K-TRON model T35 twin-screw volumetric unit (K-Tron Corp., Pitman, NJ). An IVEK Digifeeder system (IVEK Corp., North Springfield, VT) was used to inject water into the barrel. The extruder had nine zones with independent barrel temperature controllers. The cutter was driven by a DC motor with a speed range from 0 to 2000 rpm.

Corn puffs made from yellow corn meal were used as the test product. The screw speed was set at 300 rpm and feed rate at 45 kg/h. The barrel temperature profile and screw configuration were fixed as described in Chang and Tan (1993).

The computer vision system consisted of a Cohu model 4815 camera (Cohu, Inc., San Diego, CA), Data Translation DT-2851 image grabber and DT-2858 auxiliary frame processor (Data Translation, Inc., Marlboro, MA), a SONY model PVM-1271Q video monitor (VMI of St. Louis, St. Louis, MO) and an IBM-AT host computer. The system was supported by a Data Translation DT-Iris image processing library and programmed in Turbo C. The system

furnished the capabilities of real-time image acquisition and processing for the research.

VISION SYSTEM DEVELOPMENT

Since only the product size (profile area, length, and width) was of interest, binary images were used for fast processing. The left part of Fig. 1 shows the original image of a corn puff. Based on the gray level difference between the object and background, a thresholding operation converts the original image into a binary image as shown by the middle part of Fig. 1.

The profile area can be easily found from the binary image of the product. If the gray level of the product area is denoted by b(x, y), where x and y are the pixel coordinates, the profile area (A) is

$$A = K\sum b(x,y) \tag{1}$$

where K is a calibration factor. The profile area was used as a measure of product size for SPC development in this study.

To simplify the computation of length and width, a high-pass mask was applied to detect the edge of the product. An edge image is shown in the right part of Fig. 1. The edge pixel coordinates and gray level, g(x, y), were then stored in a matrix. This matrix was much smaller than the original or binary image matrix, thus improved processing speed was achieved.

To find the product length and width, the product geometric center and orientation must be first determined. The geometric center, (x_0, y_0), can be found by computing the first moments as shown below.

$$x_0 = \frac{\sum xg(x,y)}{A} \tag{2}$$

$$y_0 = \frac{\sum yg(x,y)}{A} \tag{3}$$

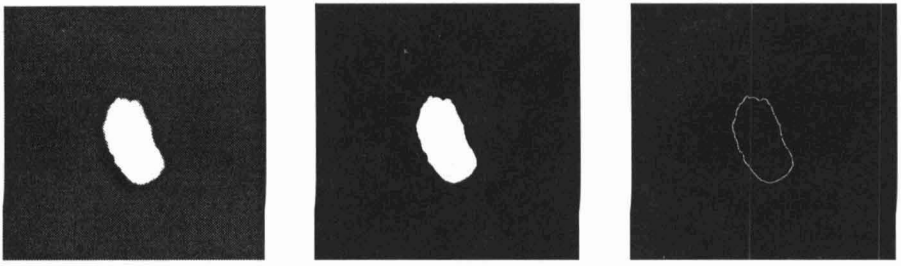

FIG. 1. PRODUCT IMAGE PROCESSING (LEFT: ORIGINAL IMAGE; MIDDLE: BINARY IMAGE AFTER THRESHOLDING; RIGHT: EDGE IMAGE AFTER HIGH-PASS EDGE DETECTION)

For an oblong object, the long axis is in the direction of the least second moment. The direction angle θ (Fig. 2) of the long axis is thus given by

$$\tan 2\theta = \frac{b}{a-c} \tag{4}$$

where

$$a = \sum [(x')^2 b(x,y)] \tag{5}$$

$$b = 2\sum [x'y'b(x,y)] \tag{6}$$

$$c = \sum [(y')^2 b(x,y)] \tag{7}$$

with $x' = x - x_0$, and $y' = y - y_0$. The long axis is the line going through (x_0, y_0) in the θ direction, and the short axis is the line going through the same point but perpendicular to the long axis. The product length was found by computing the distance between the two points where the long axis intersects the product edge (Fig. 2). Since the product profile had a convex shape, the product width was measured as the distance between the two points where the short axis intersects the product edge. For products of other shapes, a different width may be more appropriate.

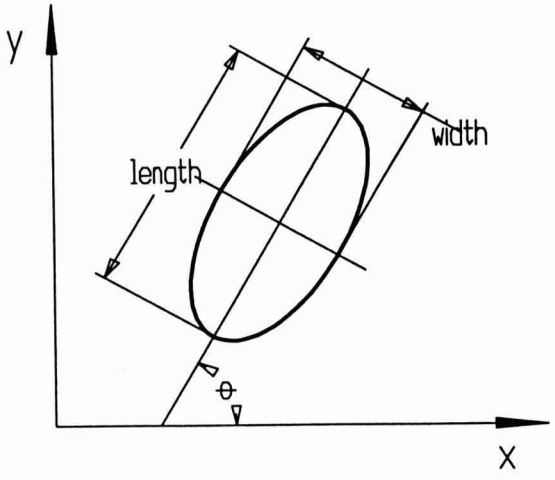

FIG. 2. PRODUCT ORIENTATION AND DIMENSIONS

To express the size measurements in engineering units, the vision system was calibrated. Square and circular objects of known dimensions were measured with the vision system. A spatial calibration factor was then found from the measured and known sizes of the objects.

A sampler was designed and fabricated to bring product samples to the camera focus area at a specified sampling rate. It consisted primarily of a hopper and a spoon-shaped catcher attached to an arm. The hopper channels the products into a continuous flow. The catcher reaches into the flow and catches a puff. The puff is then unloaded into a fenced area with a uniform black background. The sampler was driven with a solenoid controlled by the host computer. Necessary computer interfacing and control hardware was constructed. A multi-channel 8-bit D/A card was made to control the product cutter and water injection pump.

PROCESS VARIATIONS

In a long-term extrusion run, feed material properties can vary considerably. For example, the moisture content of corn meal used in this research could vary from 9 to 13% (wet basis) as a result of differences in batch, supply source, and storage conditions. This variation can significantly affect the product size and other quality attributes. To shorten the experimental run time, the effects of material moisture variation on product size was demonstrated by introducing a disturbance into the flow of added water. The disturbance was a square wave as shown in Fig. 3, which caused the overall moisture content to vary from 17 to 21%.

The variations in product area (profile area A given by Eq. 1) are shown in Fig. 3. The dotted line in the figure shows the area variations when a single sample was measured at every sampling instant. The plot indicates that the variations consisted of two major components: a fast or high-frequency variation on top of a slow trend. The fast component of variation was due to random or common causes, and the slow component was due to assignable or special causes. The primary assignable cause was moisture change in this case.

Random causes are undeterminable. For process control, it is important to detect the effects of assignable causes. Subgrouping is often used to separate the effects of the two types of causes. Subgroups are chosen so that within a subgroup variations are considered to be only due to random causes, and between two subgroups variations are due to assignable causes. A rational subgroup is chosen in various ways depending on the manufacturing process. For a continuous process, the key factor for a subgroup is the subgroup size (number of samples), which determines if the subgroup possesses the properties described above. Proper selection of the subgroup size usually requires many trials. For this development, a subgroup size of 10 was found appropriate

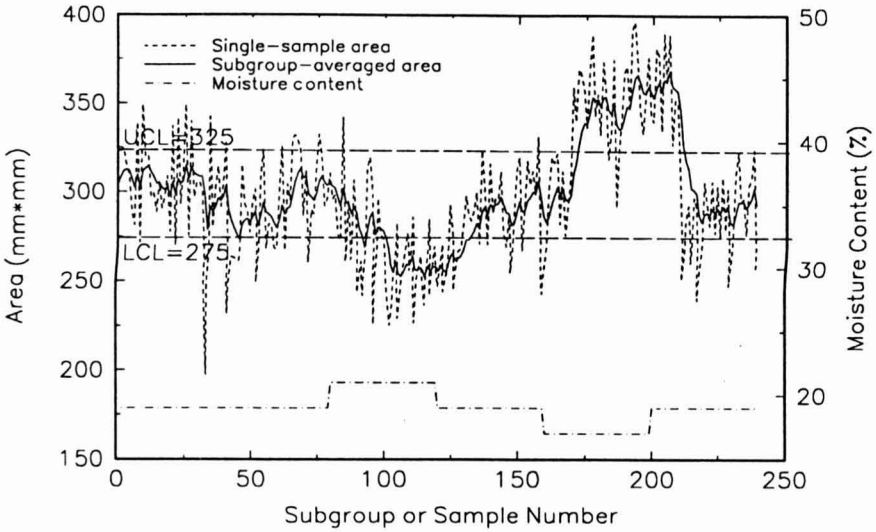

FIG. 3. PRODUCT AREA VARIATIONS RESULTING FROM RANDOM CAUSES AND ASSIGNABLE CAUSES (CHANGES IN MOISTURE CONTENT)

through experiments. When ten samples were taken to compute a subgroup-averaged area at every sampling instant (actually a short time interval as the process was continuous), the area variations are as shown by the solid line in Fig. 3. The fast or high-frequency variations associated with random causes are largely filtered out by the averaging operation. It is clear from the solid line that the subgroup-averaged area was inversely related to moisture content.

In SPC, control charts are used to determine if a process exhibits a state of statistical control. The $\bar{x}$ Shewhart control chart is widely employed to monitor the subgroup mean of a quality variable by examining if it is between an upper control limit (UCL) and a lower control limit (LCL). The UCL and LCL are usually expressed as (Messina 1987):

$$UCL = X + \alpha R \tag{8}$$

$$LCL = X - \alpha R \tag{9}$$

where X is the grand average of a measured quality variable over a long run (average of subgroup means), α is a constant depending on the subgroup size, and R is the average of within-subgroup ranges. Since R indicates the magnitude of random variations in a process, the control limits defined by Eq. 8 and 9 reflect the process capability to maintain uniformity in a quality variable.

The control limits were determined through trial experiments. For the product area, $X = 300$ mm^2 and $R = 80$ mm^2. For a subgroup size of 10, $\alpha = 0.308$ (Messina 1987). Then,

$$UCL = 325 \text{ mm}^2 \text{ and } LCL = 275 \text{ mm}^2$$

for the subgroup-averaged product area (the solid line in Fig. 3). Figure 3 is the Shewhart control chart for the product area without implementation of corrective actions. The area was out of the control limits because of the moisture variation and the process was not in a state of statistical control.

The product length and width variations are shown in Fig. 4. The length reduced with an increase in moisture content or vice versa. For the product length, X = 22 mm, R = 6 mm, and $\alpha = 0.308$ (subgroup size = 10), which give

$$UCL = 23.8 \text{ mm and } LCL = 20.2 \text{ mm}$$

As shown in Fig. 4, the product length was also out of its control limits as a result of the moisture variation.

The product width exhibited little variation relating to moisture change as shown by Fig. 4. The size variations were almost exclusively reflected on the product length. As a result, further control of the product width was unnecessary for minimizing the effects of moisture variation on size uniformity of the test product.

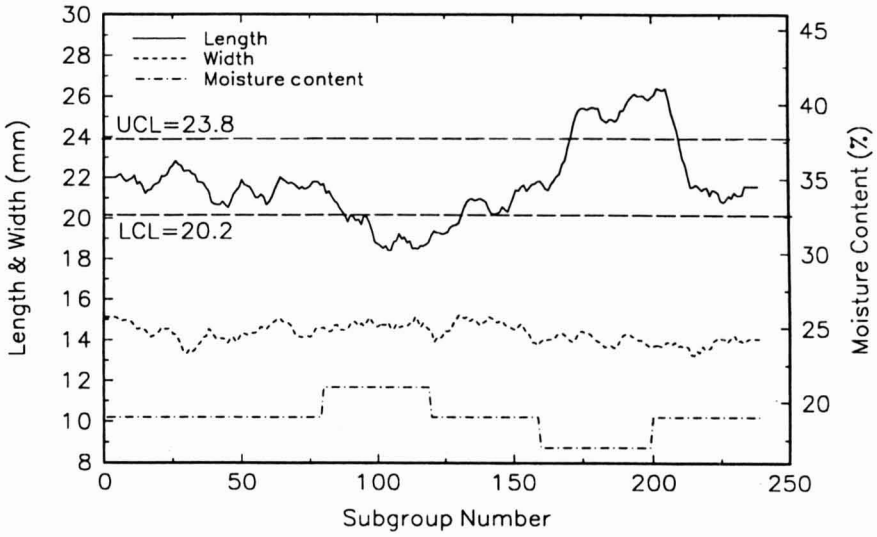

FIG. 4. PRODUCT DIMENSION VARIATION RESULTING FROM MOISTURE CONTENT CHANGES

CONTROL IMPLEMENTATION

To bring the process to a state of statistical control, appropriate corrective actions must be implemented. Since the process was continuous and dynamic, automated on-line process correction would be very important for control effectiveness. Based on the size measurement by the vision system, the cutter speed was varied to compensate for the effects of moisture variations.

The block diagram of the control system implemented is shown in Fig. 5. In the figure, product size refers to either product area or length depending on which one of the two is of interest for control. The process block stands for the transfer function from the control signal for cutter speed to product size. The disturbance effect block represents the unknown transfer function from moisture content to product size. The purpose of the controller was to minimize product size variation under the disturbance of moisture variations.

The process block in Fig. 5 could be modeled through either theoretical analysis or experimental identification; but a rigorous modeling effort was considered unnecessary as the block consisted primarily of the dynamics of the cutter motor. It is a well known fact that a DC motor can be closely described with a second-order model and second-order systems can be effectively controlled with proportional, integral and derivative (PID) controllers.

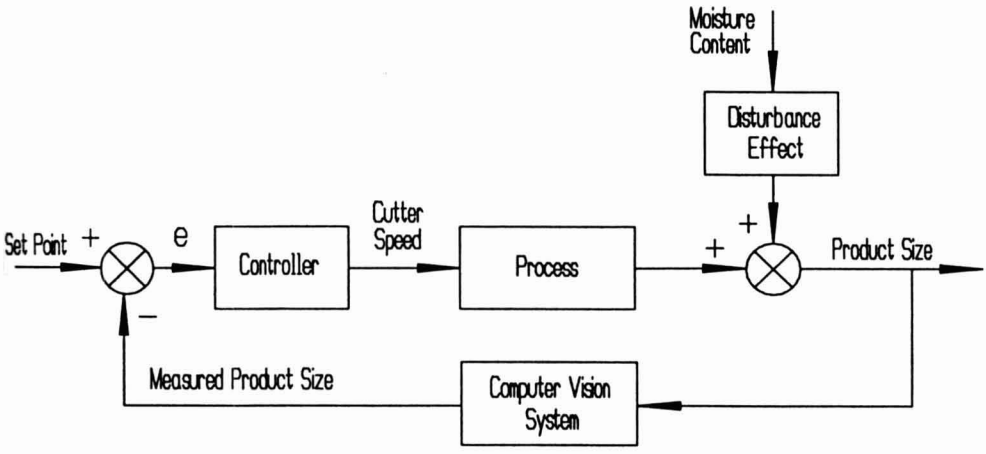

FIG. 5. BLOCK DIAGRAM OF THE VISION-BASED CONTROL SYSTEM

Therefore, the following PI (proportional and integral) controller was employed:

$$u(t) = u(t-1)+K_p[e(t)-e(t-1)]+K_i e(t) \quad (11)$$

where u is the cutter speed control signal, e is the difference (error) between the desired product size and the measured size, K_p and K_i are gain constants, and t stands for the current sampling instant or subgroup number.

The proportional and integral gains, K_p and K_i, can be designed if the process model is known. They can also be determined through experimental tuning as widely practiced in industry. The Ziegler-Nichols tuning procedure was used in this research (Seborg *et al.* 1989). The two controller gains were determined as $K_p = 0.01$, $K_i = 0.03$ for product area control, and $K_p = 0.14$ and $K_i = 0.42$ for product length control.

The vision-based control system was implemented on-line and tested against moisture disturbances. Figure 6 shows a control chart for both product area and length when the process was subjected to the same moisture disturbance shown in Fig. 3 and 4. The control chart illustrates the performance of the controller.

In comparison with the uncontrolled curves in Fig. 3 and 4, the controller improved the product size uniformity significantly. The controlled product area and length were always within UCL and LCL, meaning that the process was in a state of statistical control in spite of the moisture variation. The controlled curves do not have a clearly identifiable pattern, indicating that the controller largely eliminated the variations caused by the moisture disturbance.

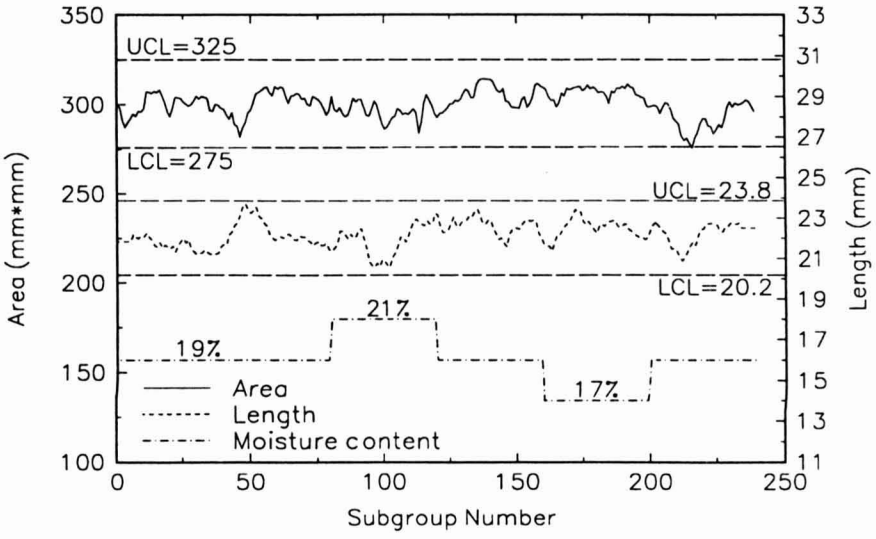

FIG. 6. SHEWHART CONTROL CHART SHOWING PERFORMANCE OF THE AUTOMATED REAL-TIME SPC

Figures 7 and 8, respectively, are the product area and length histograms with and without the vision-based controller. The histograms show that the uncontrolled product area and length gathered in three clusters corresponding to the three distinct levels of the moisture disturbance. Within a cluster, the product size also varied; but the roughly normal shape of the histogram for each cluster shows that the within-cluster variation was a result of random causes. The standard deviations of uncontrolled product were 27.7 mm^2 for area and 1.96 mm for length, indicating considerable ranges of variation. The controlled histograms, on the other hand, are essentially limited to the middle clusters despite the presence of the disturbance. Their roughly normal shapes indicate that the effects of assignable causes were mostly eliminated or the process performance was near optimal in terms of product size uniformity. The standard deviations of the controlled product were 7.6 mm^2 for area and 0.64 mm for length, which were respectively, 73% and 67% reductions over the uncontrolled. The results show a considerable improvement of product size uniformity by the application of the vision-based controller.

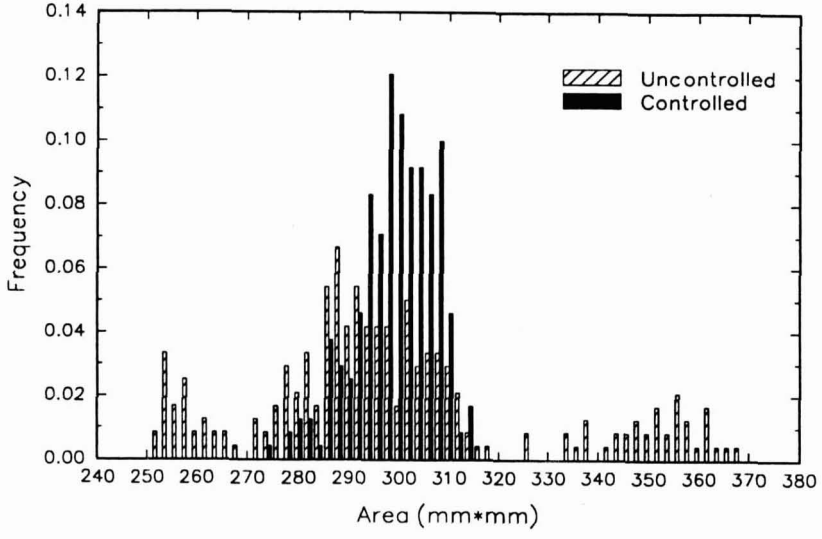

FIG. 7. HISTOGRAMS OF PRODUCT AREA WITH AND WITHOUT THE AUTOMATED REAL-TIME SPC

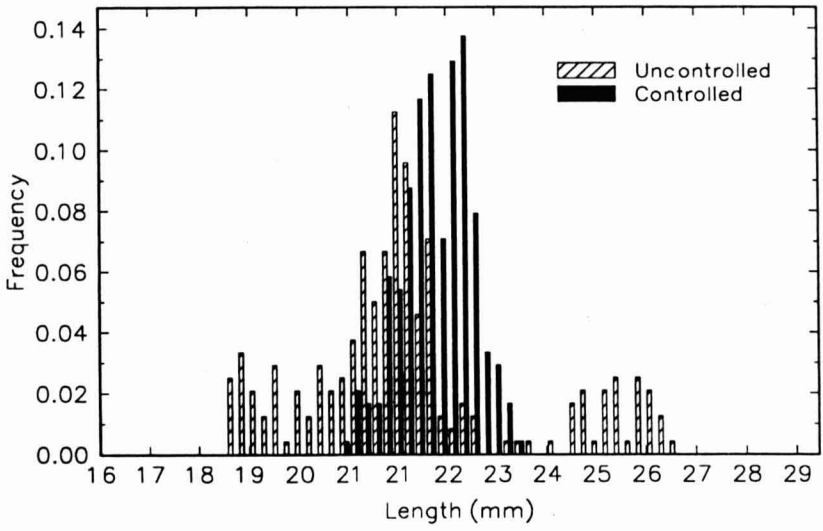

FIG. 8. HISTOGRAMS OF PRODUCT LENGTH WITH AND WITHOUT THE AUTOMATED REAL-TIME SPC

SUMMARY

By applying machine vision techniques, an automated real-time statistical process control system was successfully implemented. The system significantly improved the uniformity of two product quality variables, which can result in improved overall product quality and reduced production costs. The automated control system reduced the need for close monitoring and process adjustments by human operators, which leads to enhanced productivity. Though the process studied was simple and the quality variables used are not necessarily important for all food products, the results of this research demonstrate the great potential of vision-based process control in enhancing product quality and productivity in the processing industry. The same procedure can be followed to control similar quality variables or attributes.

ACKNOWLEDGEMENT

Contribution from the Missouri Agricultural Experiment Station. Journal Series No. 12,134. Mr. David Owens and Mr. Harold Huff are gratefully acknowledged for their help with hardware fabrication and experimental data collection.

REFERENCES

CHANG, Z. and TAN, J. 1993. Determination of model structure for twin-screw food extrusion I: multi-loop, Food and Bioproducts Processing, Trans. of IChE, *71*(C), 11–19.

HARPER, J. M. 1979. Food extrusion. In *CRC Critical Reviews in Food Science and Nutrition*, Vol 11(2), pp. 115–215, CRC Press, Cleveland, OH.

JABLONSKY, C.M., DAVIS, J.R. and HICHINGS, G. 1991. Monitoring the effectiveness of refinery advanced controls with a statistical process control scheme. In *Statistical Process Control in Manufacturing*, (J.B. Keats and D.C. Montgomery, eds.) Marcel Dekker, New York.

KLAUS, B. and HORN, P. 1991. Robot Vision, MIT Press, Cambridge, MA.

KULSHRESHTHA, M.K., ZEROR, C.A. and JUKES, D.J. 1991. Automatic control of food extrusion: problems and perspectives. Food Contr., *1*, 80–85.

MESSINA, W.S. 1987. *Statistical Quality Control for Manufacturing Managers*, Wiley, New York.

MILLER, T. and BALCH, B. 1989. Statistical process control in food processing. Proc. ISA Int'l. Conf. and Exhibit, *44*(3).

RAUWENDAAL, C. 1993. *SPC - Statistical Process Control in Extrusion*, Hanser Publishers, New York.

SEBORG, D., EDGAR, T.F. and MELLICHAMP, D.A. 1989. *Process Dynamics and Control*, Wiley, New York.

STURM, G.W., MELNYK, S.A., YOUSRY, M.A., FELTZ, C.L. and WOLTER, J.F. 1991. Sufficient statistical process control: measuring quality in real time. In *Statistical Process Control in Manufacturing*, (J.B. Keats and D.C. Montgomery, eds.) Marcel Dekker, New York.

TAN, J., GAO, X. and HSIEH. F. 1994. Extrudate characterization by image processing, J. Food Sci. *59* (6), 1247–1250.

WIEDMANN, W. and STRECKER, J. 1988. Process control of cooler-extruder. In *Automatic Control and Optimization of Food Processes*, (M. Remard and J.-J. Bimbenet, eds.) Elsevier Applied Science Publ., London.

YOURSTONE, S.A. 1991. Real-time process quality control in a computer integrated manufacturing environment. In *Statistical Process Control in Manufacturing*, (J.B. Keats and D.C. Montgomery, eds.) Marcel Dekker, New York.

MILK COAGULATION CUT-TIME DETERMINATION USING ULTRASONICS

SUNDARAM GUNASEKARAN[1]

Biological Systems Engineering Department
University of Wisconsin - Madison
460 Henry Mall, Madison, WI 53706

and

CHYUNG AY

National Chiayi Institute of Agriculture
Chiayi, Taiwan

Received for Publication June 9, 1995

ABSTRACT

A nondestructive method of determining milk coagulation cut-time was investigated. Velocity and attenuation of ultrasonic waves through coagulating skim milk were measured after rennet addition. The ultrasonic attenuation measurements were found suitable for distinguishing the effect of different experimental variables (three levels of temperature, rennet and $CaCl_2$). Based on the rate of change of attenuation during coagulation, a turning point was defined at which the attenuation rate change was −0.1 neper/m/min. The cut-time was proposed to be 20 min from the time the turning point was observed. The cut-times predicted by this criterion were statistically similar to those predicted by the manual method currently used in the industry.

INTRODUCTION

In the manufacture of almost all varieties of cheese, milk proteins are coagulated to form a continuous, solid curd in which milk fat globules, water and water-soluble materials are entrapped. The most popular method of milk coagulation is with an enzyme extract from calf stomachs (rennet) or by microbially-produced enzymes. These enzymes cleave and hydrolyze k-casein and begin milk coagulation. Hydrolysis of k-casein leads to destabilization of the colloidal system followed by aggregation of protein micelles into clusters. The clusters grow in size, followed by crosslinking between chains which eventually

[1]Author to whom correspondence should be sent.

Journal of Food Process Engineering **19** (1996) 63–73.

transform the milk into a gel or curd. The textural strength or formation of crosslinks firms the gel.

When a certain curd firmness has been reached, the gel is cut by traversing with wire knives to slice the gel into approximately 7 mm cubes. This promotes drainage of whey (syneresis) from the curd. Cutting when the coagulum is too soft decreases cheese yield due to increased loss of fat and curd fines. Cutting when the coagulum is too firm retards syneresis and results in high moisture cheese (Hori 1985; Scott 1986). Therefore, it is important in cheesemaking to determine the optimal cut-time.

Current practice in the dairy industry is to cut the coagulum after a set enzymatic reaction time or rely on the subjective judgment of an operator. Cutting the curd after a set time is questionable because many factors affecting curd strength do not remain constant. Therefore, a more objective determination of cut-time than the current practice should help refine cheesemaking and maximize yield (Bynum and Olson 1982).

The optimal time for cutting the coagulum depends on its rheological properties which Scott Blair and Burnett (1958) have shown to be related to several physical parameters. A number of researchers have investigated the coagulum firmness (Scott Blair and Burnett 1963; Burgess 1978; Bynum and Olson 1982; and Douillard 1973). Several curd firmness testers and/or cut-time detectors have been proposed. They include use of penetrometers (Thomason and Voss 1977; Burgess 1978; Yun *et al.* 1981; Storry and Ford 1982); suspended bodies (Steinsholt 1973); torsion viscometers (Thomason and Voss 1977); rotational viscometers (Scott Blair and Oosthuizen 1961; Kopelman and Cogan 1976). However, all these methods destroy the coagulum and make multi-sample evaluations at different locations within a cheese vat difficult.

Nondestructive evaluation of cut-time was investigated using optical methods (McMahon *et al.* 1984; Hardy and Fanni 1981; Payne *et al.* 1993) and the hot-wire method (Hori 1985). The hot-wire method is now commercially available. However, its effectiveness has not been well documented.

In this paper, a nondestructive method of milk coagulation cut-time determination using ultrasonics is described. Ultrasonics are high frequency (> 18 kHz) sound waves that can travel in a continuous medium. Everson and Winder (1968) made the first attempts to use ultrasonics for studying milk coagulation. However, their investigation has not resulted in any useful findings. There are several other ultrasonic studies on milk (Bachman *et al.* 1980; Fitzgerald and Winder 1961; Hueter *et al.* 1953; Saraf and Samal 1984; Miles *et al.* 1990). But none of these was to determine the milk coagulation cut-time.

The objective of this investigation was to develop an ultrasonic measurement system for nondestructive determination of milk coagulation cut-time.

MATERIALS AND METHODS

Ultrasonic System

The experimental ultrasonic measurement system is schematically presented in Fig. 1. It consists of two ultrasonic longitudinal wave transducers (Panametrics, P/N V302; I MHz central frequency), an ultrasonic pulser-receiver (Panametrics, 5055PR), a digital storage oscilloscope, DSO (Tektronix 2430A) and a personal computer. The transducers were placed in the middle of a milk tank (24 × 17 × 12 cm) 25 mm apart to avoid diffraction effects (Herzfield and Litovitz 1959). The voltage signals from the receiver were acquired by the DSO using a GPIB-PC interface.

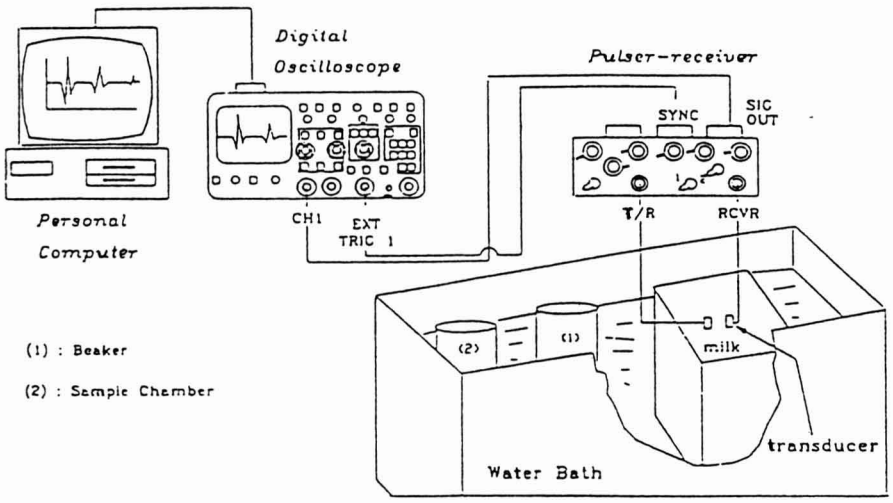

FIG. 1. SCHEMATIC OF THE ULTRASONIC MEASUREMENT SYSTEM

Experiments

The milk tank was filled with skim milk submerging the transducers. Grade A pasteurized, nonfat dry milk powder obtained from the Dairy Plant at UW-Madison was used as the substrate for fluid milk. This was to avoid the

effect of fat and variations due to milk source and process conditions. The fluid milk was prepared by stirring 600 g of milk powder in 5 L of warm water. Three levels of temperature, rennet and $CaCl_2$ were considered as the experimental variables. All these factors strongly influence the rate of coagulation and/or curd strength (Scott 1986). These levels represent a standard (corresponding to current industry practice for Cheddar cheesemaking) and one above and one below the standard levels (Table 1). Four replications were performed at each level.

TABLE 1.
EXPERIMENTAL TREATMENTS

Treatment (notation)	Temperature (°C)	Rennet Concentration (mL/454 kg milk)	$CaCl_2$ Concentration (mL/454 kg milk)
Standard (ST)	32	90	15
High Rennet (HR)	32	110	15
Low Rennet (LR)	32	70	15
High Temperature (HT)	37	90	15
Low Temperature (LT)	27	90	15
High $CaCl_2$ (HC)	32	90	25
Low $CaCl_2$ (LC)	32	90	5

The milk was stirred and heated to the desired coagulation temperature, then $CaCl_2$ was added. This substrate was poured into the milk tank placed in water set at the coagulation temperature. After 30 min (allowing for temperature equilibration), rennet, diluted with distilled water 1 to 10, was added. The ultrasonic pulser was turned on and the ultrasonic signals received at the receiver were collected continuously for 75 min. Additional details of the system and experimentation are presented in Ay and Gunasekaran (1994).

RESULTS AND DISCUSSIONS

Ultrasonic Velocity

The average velocities of ultrasonic waves through milk coagulating at different temperatures are presented in Fig. 2. The ultrasonic velocity decreased at the beginning (under 6 min after rennet addition) and then increased. But after 12 min, the velocity fluctuated a great deal with a small increasing trend. This pattern of velocity change during coagulation is similar to that of milk density. Because of the strong dependence of ultrasonic velocity on the medium density, the observed changes seem justifiable. Similar results were obtained from

experiments at different levels of rennet and $CaCl_2$. For each experimental variable, the differences due to different experimental levels were not statistically significant. Therefore, ultrasonic velocity measurements were not considered further for cut-time determination.

Ultrasonic Attenuation

Ultrasonic attenuation data obtained in experiments with different temperatures are presented in Fig. 3. Similar data were obtained in experiments with different levels of rennet and $CaCl_2$. Unlike ultrasonic velocity, the attenuation showed steady decrease with coagulation time. The effect of experimental levels was statistically significant. Thus attenuation measurement was targeted as a potential cut-time indicator.

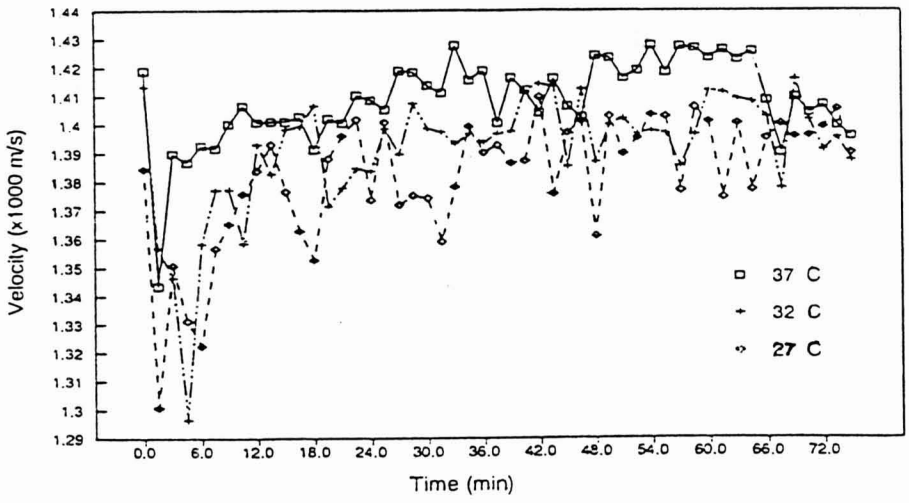

FIG. 2. ULTRASONIC VELOCITY THROUGH MILK COAGULATING AT DIFFERENT TEMPERATURES
(rennet = 90 mL/454 kg of milk; $CaCl_2$ = 15 mL/454 kg of milk)

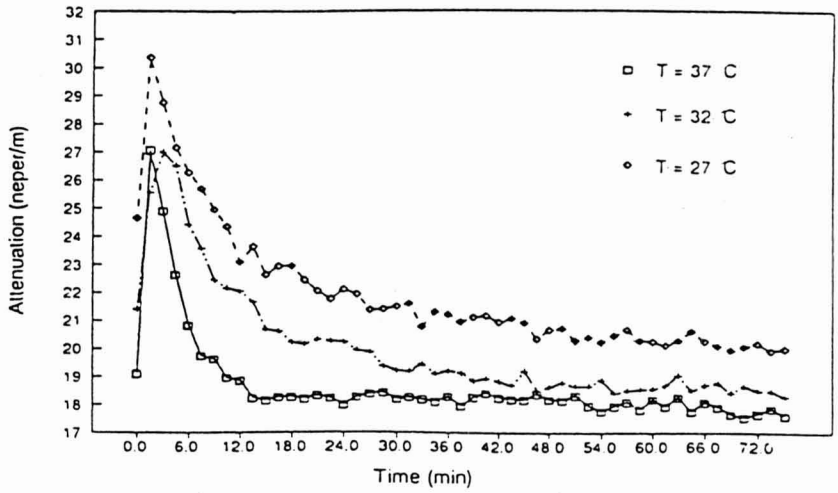

FIG. 3. ULTRASONIC ATTENUATION THROUGH MILK COAGULATION AT DIFFERENT TEMPERATURES
(rennet = 90 mL/454 kg of milk; $CaCl_2$ = 15 mL/454 kg of milk)

Cut-time Determination

Even though attenuation decreased steadily, it was hard to identify a point at which optimal cut-time might have been reached. This is because of the nature of the coagulation process, a slow and continuous change in gel strength. However, the rate of change of attenuation appeared to have two phases, first, a rapid change until about 20 min after rennet addition, followed by a slow change toward a steady state situation. This corresponded to some extent to the two phases of coagulation, first the enzymatic and second the physicochemical (Brule and Lenoir 1987). Therefore, polynomial regression lines were fitted to the attenuation data, and, using successive data points on the regression line 1.5 min apart, the first derivatives were calculated. A typical plot of rate of change of attenuation versus time is shown in Fig. 4. As can be seen in Fig. 4, most of the rate of change of attenuation data was in the -0.1 to 0.1 neper/m/min range. Thus, the slope of -0.1 neper/m/min was considered to signify the first phase of attenuation change with coagulation time. Accordingly, the time at which the slope was -0.1 neper/m/min was labeled as the turning point (P_t). In Fig. 5, the P_t of several attenuation versus time plots are presented. The P_t was fairly influenced by the different experimental variables and levels. For example, the P_t at high temperature (37C) was earlier than at the standard temperature

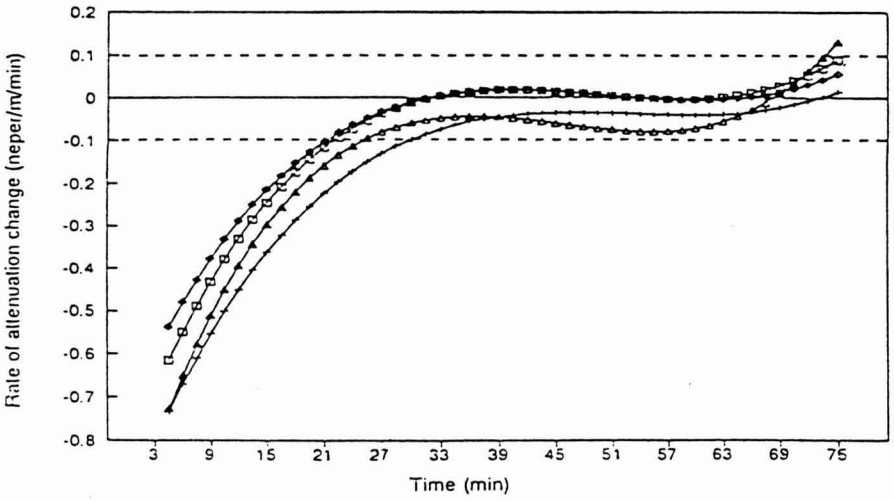

FIG. 4. RATE OF CHANGE OF ATTENUATION VERSUS COAGULATION TIME -- FOUR REPLICATIONS OF COAGULATION AT:
(temperature = 32C, rennet = 90 mL/454 kg of milk;
$CaCl_2$ = 15 mL/454 kg of milk)

(32C). It indicates that the coagulation rate was faster at higher temperatures. Similarly, P_t, at high rennet concentration (110 mL/454 kg milk) was earlier than at low rennet concentration (70 mL/454 kg milk). These trends conformed to expected results and validated the potential for P_t to be an indicator of coagulation rate. In fact, P_t correlated well with coagulation time or clotting time which signified the end of the enzymatic phase and the beginning of coagulation proper (Ay and Gunasekaran 1994).

Some researchers specified the cutting time to be a certain time after a reference time, the clotting time (Kowalchyk and Olson 1977). Therefore, a similar approach was taken to specify a cut-time with reference to P_t. Evaluating manual cut-time predictions and P_t for all the experiments, an empirical criterion was established. That is, cut-time is 20 min after the P_t. Comparison of manually determined cut-times and those obtained based on ultrasonic attenuation measurement criterion are presented in Table 2. An advantage of this method is that close monitoring of the coagulation process is necessary only during the initial phase of coagulation. The control units could be assigned other tasks in a typical automatic control situation.

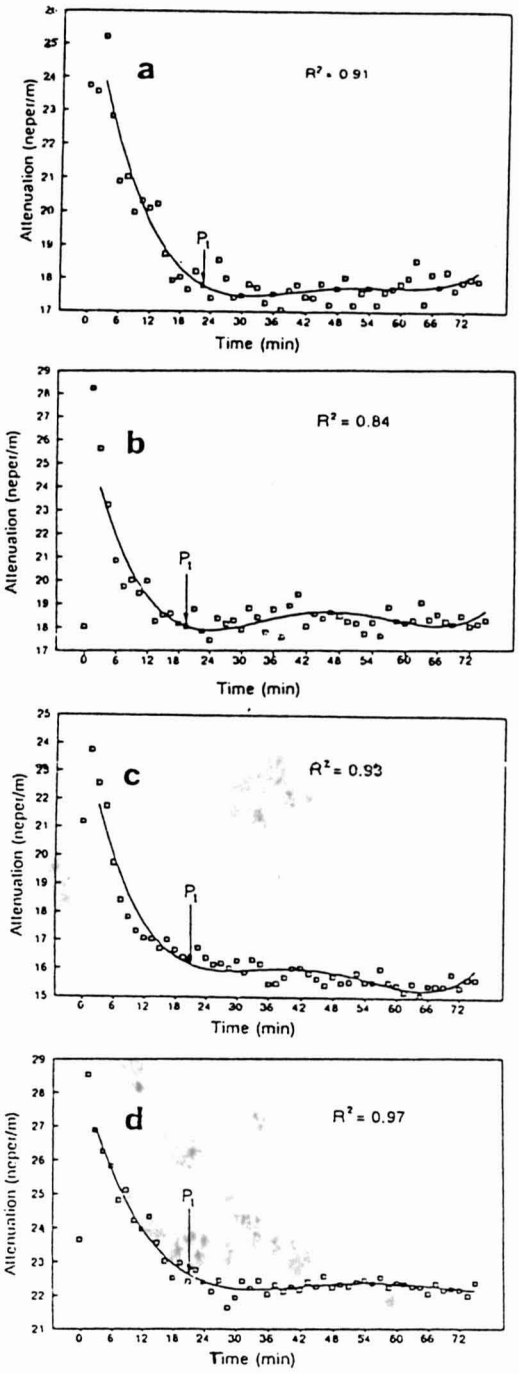

FIG. 5. ULTRASONIC ATTENUATION VERSUS COAGULATION TIME WITH TURNING POINT (P_t) INDICATED
Experimental treatments used were: a) ST; b) HT; c) HR; d) LR.

TABLE 2.
COMPARISON OF CUT-TIMES DETERMINED BY MANUAL AND ULTRASONIC METHODS

Experimental Treatment	Cut-time, min (avg. ± std. error) Manual Method*	Ultrasonic Method
ST	45.0 ± 2.9	45.1 ± 4.9
HR	39.8 ± 1.2	38.8 ± 2.7
LR	47.2 ± 2.1	47.1 ± 3.5
HT	37.5 ± 2.9	39.1 ± 1.0
HC	42.4 ± 3.1	42.1 ± 5.2
LC	43.5 ± 1.7	39.3 ± 9.3

*According to the current industry practice.

For standard conditions of Cheddar cheesemaking, the manually determined cut-time averaged 45.0 min compared to 45.1 min. The mean cut-times at other experimental variables were also very close to the corresponding manual determinations (within about 2 min) except at low rennet (within 4 min). However, the standard errors associated with ultrasonic measurements were always higher than with the corresponding manual measurements. This indicated that the precision of ultrasonic cut-time predictions should be improved. An hypothesis t-test of paired data was used to verify the statistical difference between the two methods. Since the difference between each set of paired data from the two methods approximated normal distribution (verified by the stem-and-leaf plot), the null hypothesis (H_0) of assuming that the difference between the means is zero was tested. The result of the hypothesis t-test run using STATGRAPHICS (Table 3) validated this assumption. That is, the ultrasonic method can be used to predict cut-times comparable to the current industry practice of manual determination.

TABLE 3.
PAIRED-DATA HYPOTHESIS TEST TO EVALUATE VALIDITY OF ULTRASONIC DETERMINATION OF MILK COAGULATION CUT-TIME

Sample Statistics:	Number of obs.	24
	Average	1.02083
	Variance	16.4235
	Standard deviation	4.05259
	Median	1.75

Confidence Interval for Difference in Means = 95%

Hypothesis	H_0:	Difference Mean = 0
	H_a:	Difference Mean ≠ 0

Computed t Statistic = 1.23404 < $t_{(23,0.05)}$ = 2.069

Result: Do not reject H_0; i.e., the cut-times determined by ultrasonic and manual methods were similar.

CONCLUSIONS

An ultrasonic measurement system was set up. The velocity and attenuation of ultrasonic waves through coagulating milk were continuously monitored. The ultrasonic attenuation measurements provided a useful indicator for predicting milk coagulation cut-time nondestructively. The cut-times predicted using the ultrasonic method were comparable to those predicted by the manual method currently used in the industry.

REFERENCES

AY, C. and GUNASEKARAN, S. 1994. Ultrasonic attenuation measurements for estimating milk coagulation time. Transactions of the ASAE *37*(3), 857–862.

BACHMAN, S., KLIMCZAK, B. and GASYNA, Z. 1980. Non-destructive viscometric studies of enzymic milk coagulation. II. The secondary phase of milk coagulation. Acta Aliment. Pol. *4*(3), 239–246.

BRULE, G. and LENOIR, J. 1987. The coagulation of milk. In *Cheesemaking: Science and Technology* (A. Eck, ed.) Lavoisier Publishing, New York.

BURGESS, K.J. 1978. Measurement of the firmness of milk coagulum. Ir. J. Food Sci. Technol. *2*, 129–134.

BYNUM, D.G. and OLSON, N.F. 1982. Influence of curd firmness at cutting on cheddar cheese yield and recovery of milk constituents. J. Dairy Sci. *65*, 2281–2290.

DOUILLARD, R. 1973. Rheological analysis of curd formation. J. of Texture Studies *4*, 158–165.

EVERSON, T.C. and WINDER, W.C. 1968. Rennet coagulation test with a recorded output. J. Dairy Sci. *51* (6) 940.

FITZGERALD, J.W. and WINDER, W.C. 1961. An ultrasonic method for measurement of solids-not-fat and milk fat in fluid milk. J. Dairy Sci. *44*, 1165.

HARDY, J. and FANNI, J. 1981. Application of reflection photometry to the measurement of milk coagulation. J. Food Sci. *46*, 1956–1957.

HERZFIELD, F.K. and LITOVITZ, T.A. 1959. Absorption and Dispersion of Ultrasonic Waves. Academic Press. New York.

HORI, T. 1985. Objective measurements of the process of curd formation during rennet treatment of milks by the hot wire method. J. Food Sci. *50*, 911.

HUETER, T.F., MORGAN, H. and COHEN, M.S. 1953. Ultrasonic attenuation in biological suspensions. J. Acoust. Soc. Am. *25*(6), 1200–1201.

KOPELMAN, I.J. and COGAN, U. 1976. Determination of clotting power of milk clotting enzymes. J. Dairy Sci. *59*, 196–199.

KOWALCHYK, A.W. and Olson, N.F. 1977. Effect of pH and temperature on the secondary phase of milk clotting by rennet. J. Dairy Sci. *60*, 1256–1259.

MCMAHON, D.J., BROWN, R.J. and ERNSTROM, C.A. 1984. Enzymatic coagulation of milk casein micelles. J. Dairy Sci. *67*, 745–748.

MILES, C.A., SHORE, D. and Langley, K.R. 1990. Attenuation of ultrasound in milks and creams. Ultrasonics *28*, 394–400.

PAYNE, F.A., HICKS, C.L., MADANAGOPAL, S. and SHEARER, S.A. 1993. Fiber optic sensor for predicting the cutting time of coagulating milk for cheese production. Transactions of the ASAE *36*(3), 841–847.

SARAF, B. and SAMAL, K. 1984. Ultrasonic velocity absorption in reconstituted powdered milk, part II. Acustic *56*, 61–66.

SCOTT, R. 1986. *Cheesemaking Practice*. 2nd Ed., p. 193, Elsevier Applied Science, New York.

SCOTT BLAIR, G.W. and BURNETT, J. 1958. Physical changes in milk caused by the action of rennet: I. Description of apparatus for measuring rigidity moduli and internal viscosities, tests of reliability and some observations on syneresis. J. Dairy Res. *25*, 297.

SCOTT BLAIR, G.W. and BURNETT, J. 1963. A simple method for detecting an early stage in coagulation of renneted milk. J. Dairy Res. *30*, 383–390.

SCOTT BLAIR, G.W. and OOSTHUIZEN, J.C. 1961. A viscometric study of the breakdown of casein in milk by rennin and rennet. J. Dairy Res. *28*, 165–173.

STEINSHOLT, K. 1973. The use of an Instron universal testing instrument in studying the rigidity of milk during coagulation by rennin. Milchwissenschaft *28*, 94–97.

STORRY, J.E. and FORD, G.D. 1982. Development of coagulum firmness in renneted milk -- a two-phase process. J. Dairy Res. *49*, 343–346.

THOMASON, J. and VOSS, E. 1977. Methods for the determination of the firmness of milk coagulum. I.D.F. Annual Report Dec. #99.

YUN, S.E., OHMIYA, K. KOBAYASHI, T. and SHIMIZU, S. 1981. Increase in curd tension of milk coagulum prepared with immobilized proteases. J. Food Sci. *46*, 705-707.

FLUID TO PARTICLE CONVECTIVE HEAT TRANSFER COEFFICIENT IN A HORIZONTAL SCRAPED SURFACE HEAT EXCHANGER DETERMINED FROM RELATIVE VELOCITY MEASUREMENT[1]

V.M. BALASUBRAMANIAM[2] and S.K. SASTRY[3]

Department of Agricultural Engineering
The Ohio State University
590 Woody Hayes Drive
Columbus, OH 43210

Received for Publication February 27, 1995

ABSTRACT

Liquid-to-particle convective heat transfer coefficient (h_{fp}) between fluid and particle was investigated in continuous flow through a horizontal scraped surface heat exchanger. The relative velocities between fluid and particle were measured, and h_{fp} calculated from well known correlations. Heat transfer coefficients increased with increasing flow rate, rotational speed, and decreased with increasing carrier medium viscosity and particle size. The measured relative velocities during flow visualization studies ranged from 0.04 to 0.29 m/s with corresponding h_{fp} values of 597 W/m²°K and 1975 W/m²°K, respectively. Even with the most conservative correlation, Nusselt numbers ranged from 12.1 to 49.7; significantly greater than the value of 2.0 for a sphere in a stagnant fluid.

INTRODUCTION

Characterization of convective heat transfer coefficient (h_{fp}) between fluids and particles will help improve understanding of the complex heat transfer mechanism in continuous flow through aseptic processing systems. Data on h_{fp}

[1] Salaries and research support provided in part by State and Federal Funds appropriated to the Ohio Agricultural Research and Development Center, The Ohio State University, and in part by a grant from the Center for Aseptic Processing and Packaging Studies, North Carolina State University. References to commercial products and trade names are made with the understanding that no discrimination and no endorsement by The Ohio State University is implied.

[2] Present address: The National Center for Food Safety and Technology, Illinois Institute of Technology, Summit-Argo, IL 60501.

[3] Corresponding author.

in continuous flow is critical for development of process schedules for aseptic processing of low acid foods containing particulates. The schedules should be conservatively prepared to guarantee microbial sterility; and yet be realistic enough to avoid overprocessing. Recently several studies reported h_{fp} for continuous tube flow conditions (Heppell 1985; Sastry *et al.* 1990; Balasubramaniam and Sastry 1994a; Mwangi *et al.* 1993; Zitoun and Sastry 1994). However, to the best of our knowledge, no studies (other than our own) have attempted to determine h_{fp} in continuous flow through heat exchangers, although wall-fluid heat transfer has been extensively investigated (e.g., Trommelen 1967; Bott *et al.* 1968; Weisser 1972; Cuevas and Cheryan 1982; and Härröd 1990). Studies on scraped surface heat exchangers have been conducted by Balasubramaniam and Sastry (1994b) using liquid crystal temperature sensors. It is desirable and important to cross-validate such experiments with other techniques such as relative velocity measurement. Although individual methods may have their own inaccuracies, they may be used to compare and lend a measure of credibility to each other (Balasubramaniam and Sastry 1994a). Hence this study had the following objectives: (1) to characterize h_{fp} in continuous flow through scraped surface heat exchangers by measuring relative velocities between fluid and particle, and (2) to study the factors influencing the liquid-to-particle heat transfer under these conditions.

Principle

The relative velocity method is a flow field visualization technique, wherein the motion of fluid tracers and the particle are videotaped to experimentally determine the relative velocity. Values of h_{fp} can be back calculated using well-known correlations such as those of Ranz and Marshall (1952), Kramers (1946), or Whitaker (1972) given by Eq. 1 to 3, respectively.

$$Nu = 2.0 + 0.6Re_{G,S}^{0.5}Pr_{G,A}^{0.33} \tag{1}$$

$$Nu = 2.0 + 1.3Pr_{G,A}^{0.15} + 0.66Pr_{G,A}^{0.31}Re_{G,S}^{0.5} \tag{2}$$

$$Nu = 2.0 + (0.4Re_{G,S}^{0.5} + 0.06Re_{G,S}^{2/3})Pr_{G,A}^{0.4}(\mu/\mu_p)^{0.25} \tag{3}$$

The first two relations have been chosen since they are readily available in heat transfer textbooks, and are widely cited in the literature. They also deal with a finite spherical object, which (unlike correlations for flat plates or tubes) is at least a modest approximation of the situation encountered in aseptic processing. The third relation is relatively recent, and incorporates more data in establishing the correlation. All three relations were developed for idealized conditions, and flows in aseptic processing may deviate considerably from these

situations; nevertheless, they will serve to show whether h_{fp} measured by other methods are consistent with observed relative velocities.

Further details of the experimental method are available elsewhere (Balasubramaniam and Sastry 1994a). This approach has been compared with other heat transfer based experimental techniques (moving thermocouple and liquid crystal methods) and found to yield results that are slightly conservative in comparison to the liquid crystal method, but somewhat higher than the conservative moving thermocouple approach (Balasubramaniam and Sastry 1994a,b; Zitoun and Sastry 1994). However, all three techniques yield results that are not in marked, inexplicable disagreement with each other; thus the extra measure of verification is truly useful. In addition, this approach provides further insight into fluid flow surrounding particles in continuous flow systems.

MATERIALS AND METHODS

Experimental Setup and Conditions

Figure 1 presents the schematic diagram of the experimental setup. The scraped surface heat exchanger consisted of a hollow transparent glass test section (0.152 m ID and 1.0 m in length) through which the motion of the particle and the fluid was videotaped. The mutator was made of plastic, and driven by a variable speed power drive (Dayton Electric Mfg. Co., Chicago). A digital tachometer (Shimpo America Corp., Lincolnwood, IL) was used to measure rotational speed of the mutator shaft. Table 1 presents relevant heat exchanger dimensions.

Aqueous solutions of sodium carboxymethylcellulose (CMC, 7HF; Aqualon Company, Wilmington, DE) were used as the carrier medium. Experiments were conducted for three concentrations of CMC (0.5%, 0.8%, and 1.0%), three flow rates of 0.000221, 0.000315, and 0.000505 m^3/s (corresponding to 3.5, 5.0, and 8.0 gal/min, respectively), three mutator shaft speeds (50, 70, and 120 rpm), and three different sizes of spheres (0.01703, 0.01603, and 0.01295 m diameter). All experiments were conducted at atmospheric pressure with a fluid temperature of 45C. A maximum variation of ± 1.5C in fluid temperature was observed between inlet and outlet thermocouples. At least three replications were performed for each of the conditions described above. The particles used were hollow aluminum spheres, with an apparent density adjusted to be similar to that of a real food particle. Properties and dimensions of the spheres are presented in Table 2.

The experiment consisted of introducing a spherical particle into the fluid medium from the upstream end, and videotaping its motion as it moved downstream. Finely ground polystyrene particles ($\approx$ 1 mm size) suspended in the carrier fluid were used as tracers to visualize the flow field around the

particle. The particle and tracer locations at any given instant of time were located using square grids drawn over a transparency sheet wound over the outer

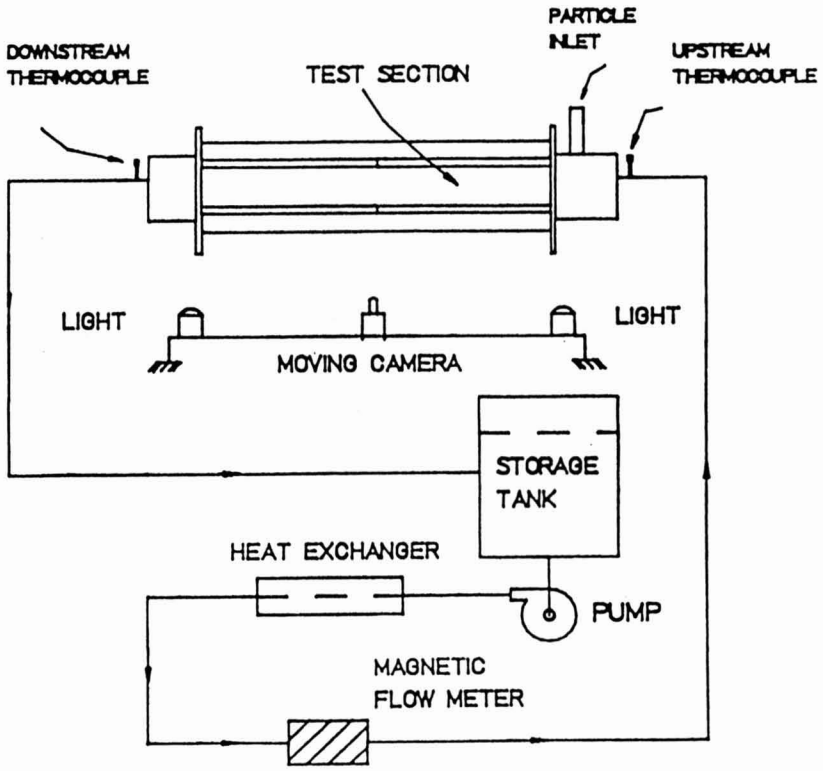

FIG. 1. SCHEMATIC DIAGRAM OF THE EXPERIMENTAL SETUP

TABLE 1.
SCRAPED SURFACE HEAT EXCHANGER DIMENSIONS

Dimension	Value
Inside diameter	0.1524 m (6 in.)
Shaft diameter	0.077 m (3.06 in.)
Shaft length	1.0 m (3.3 ft)
Configuration of blades	Straight
Number of blades	2

TABLE 2.
DIMENSIONS AND PROPERTIES OF TRANSDUCERS USED DURING THE FLOW VISUALIZATION STUDIES

Material	Diameter m	Apparent Density kg/m^3
Aluminum	0.01703	1005.8
Aluminum	0.01603	1006.1
Aluminum	0.01295	1004.5

tube. Later the videotape was replayed in still mode at selected instants to determine the relative velocity by noting the time required for a selected tracer to pass over the transducer particle. In this procedure, it was necessary to identify those tracers that did not have significant velocities perpendicular to the plane of observation. This was attempted by using a mirror installed at a 45° angle behind the system to obtain a view from a perpendicular plane. This approach was of limited usefulness because the particle was in the field of the mirror only part of the time, the view being obstructed by the mutator shaft. This provided some degree of verification regarding the absence of perpendicular velocities; however the possibility of error exists. It is important to note that ignoring the perpendicular velocity component would be conservative.

Values of h_{fp} were back calculated from relative velocity using a suitable Nusselt number correlation (Eq. 1 to 3).

Measurement of Particle Slip Revolution Speed. Further analysis was also done to determine particle revolution speed ($V_{p,r}$) at selected instants from the videotape of relative velocity experiments. This was done by noting the time required for a particle to complete one revolution around the mutator shaft (Eq. 4). The particle slip revolution speed ($V_{p,s,r}$) was then calculated as the difference between the mutator rotational speed and the particle revolution speed (Eq. 5).

$$V_{p,r} = \frac{1}{\Delta t_{p,r}} \tag{4}$$

$$V_{p,s,r} = V_{m,r} - V_{p,r} \tag{5}$$

Rheological Characterization. The rheological characteristics of the CMC solution were studied using a coaxial cylinder type rotational viscometer (Contraves RHEOMAT Model 115, Contraves, AG, Zurich, Switzerland) equipped with a jacket for temperature control. The data were fitted using the Ostwald-de Waele power law model.

$$\tau = K\dot{\gamma}^n \tag{6}$$

The values of the consistency coefficients (K) and flow behavior index (n) for different experimental conditions are tabulated in Table 3. The range of dimensionless numbers for the study are presented in Table 4.

TABLE 3.
PROPERTIES OF CARRIER FLUID (CMC) AT 45C.

		Rheological Characteristics	
Concentration %	Density kg/m^3	Consistency Coefficient (K) Pas^n	Flow behavior index (n)
0.5	988.8	0.432	0.643
0.8	990.5	1.134	0.622
1.0	993.8	2.712	0.549

TABLE 4.
RANGE OF DIMENSIONLESS NUMBERS FOR THE STUDY

Dimensionless Number	Maximum	Minimum
Generalized Reynolds number	0.6	10.0
Generalized Prandtl number	7850	1000
Generalized Taylor number	201.1	13.1

*Calculated using $k_f = 0.637$ W/m°K, and $C_{pf} = 4179.6$ J/kg°K; (Incropera and Dewitt 1990)

Statistical Analyses. Statistical analyses were performed with a statistical program (SAS 1989) using a General Linear Model Procedure. Student's t test (Mendenhall 1979) was used to test the effect of SSHE process parameters (carrier viscosity, flow rates, mutator rotational speed, and particle size) on h_{fp}.

RESULTS AND DISCUSSION

Data on mean relative velocity and h_{fp} as influenced by carrier viscosity, flow rate, mutator rotational speed, and particle dimension are presented in Table 5 for the different correlations and experimental conditions. In general the data suggest that h_{fp} increased with increasing flow rate and mutator rotation, and decreased with increasing carrier medium viscosity and particle size. The minimum and maximum calculated values of h_{fp} were 597 and 1975 W/m^2°K, respectively with corresponding relative velocities of 0.040 and 0.295 m/s. Maximum and minimum standard deviations of relative velocity are 0.031 m/s and 0.004 m/s. Statistical analysis results indicated that the effects of the parameters tested (carrier medium viscosity, flow rate, rotational speed, and particle size) were statistically significant ($p < 0.05$).

These data are generally lower than those measured by the liquid crystal method (Balasubramaniam and Sastry 1994b), where the range was from 500 to 2398 W/m^2°K, although the comparison is not truly valid because of the different temperatures of the two studies (60C in the other study, 45C in this one). However, an extensive comparison between methods has been conducted for holding tube flow by Balasubramaniam and Sastry (1994a), where it was found that the liquid crystal method yielded the highest values of h_{fp}, followed by the relative velocity method and the moving thermocouple method. The differences were, however, not marked enough to be considered serious and inexplicable differences. The principal reason for the differences between the liquid crystal and relative velocity methods is the influence of rotation. In the former method, the effect of the entire flow field, including rotation, is observed. In the latter method, the heat transfer coefficient is inferred from the relative velocity data, using translational velocity differences, while ignoring particle rotational velocities. Thus the differences are not surprising, and similar results would be expected under the present set of conditions. Detailed discussion of these results is included in the original paper.

Use of Nusselt Number Correlations

The experimentally observed relative velocity values were substituted into one of the available empirical Nusselt number correlations (Eq. 1 to 3) to back calculate h_{fp}. Among the correlations tested, that of Ranz and Marshall yielded the lowest estimates of h_{fp}, while the Whitaker relation yielded the highest values. The h_{fp} values referred to in this paper were based on the Ranz and Marshall correlation (chosen because of conservative prediction), unless otherwise specified.

TABLE 5.
MEAN VALUES OF h_{fp} FOR SPHERICAL PARTICLES UNDER VARIOUS EXPERIMENTAL CONDITIONS IN A HORIZONTAL SCRAPED SURFACE HEAT EXCHANGER

Conc	Flow Rate	Rotational Speed	Size	V_t*	h_{fp}(W/m²°K)		
%	m^3/s	RPM	m	m/s	R & M	Kramers	Whitaker
0.5	0.000221	50	0.01703	0.153	1376	1397	1803
			0.01603	0.146	1382	1411	1800
			0.01295	0.123	1408	1471	1795
		70	0.01703	0.160	1399	1421	1841
			0.01603	0.151	1409	1436	1838
			0.01295	0.128	1436	1500	1839
		120	0.01703	0.173	1487	1465	1911
			0.01603	0.165	1491	1506	1947
			0.01295	0.139	1521	1577	1957
	0.000315	50	0.01703	0.171	1413	1436	1853
			0.01603	0.167	1446	1469	1878
			0.01295	0.133	1465	1531	1876
		70	0.01703	0.189	1508	1520	1983
			0.01603	0.182	1520	1527	1969
			0.01295	0.155	1564	1609	1995
		120	0.01703	0.186	1479	1494	1943
			0.01603	0.184	1533	1542	1992
			0.01295	0.153	1536	1569	1934
	0.000505	50	0.01703	0.220	1567	1577	2056
			0.01603	0.205	1562	1579	2033
			0.01295	0.168	1572	1611	1983
		70	0.01703	0.235	1662	1674	2208
			0.01603	0.228	1641	1650	2142
			0.01295	0.193	1718	1744	2185
		120	0.01703	0.277	1822	1830	2453
			0.01603	0.258	1840	1834	2431
			0.01295	0.224	1855	1868	2374
0.8	0.000221	50	0.01703	0.120	1057	1119	1424
			0.01603	0.114	1032	1097	1364
			0.01295	0.099	1069	1216	1457
		70	0.01703	0.139	1101	1152	1478
			0.01603	0.128	1104	1157	1461
			0.01295	0.107	1072	1175	1491
		120	0.01703	0.178	1328	1345	1795
			0.01603	0.159	1340	1354	1783
			0.01295	0.131	1326	1382	1723

TABLE 5. (Continued)

Conc %	Flow Rate m^3/s	Rotational Speed RPM	Size m	V_f* m/s	$h_{fp}(W/m^2°K)$ R & M	Kramers	Whitaker
0.8	0.000315	50	0.01703	0.160	1200	1233	1603
			0.01603	0.148	1219	1252	1608
			0.01295	0.129	1259	1323	1619
		70	0.01703	0.176	1235	1271	1665
			0.01603	0.163	1246	1287	1664
			0.01295	0.135	1244	1388	1724
		120	0.01703	0.192	1315	1336	1772
			0.01603	0.180	1368	1393	1836
			0.01295	0.157	1329	1402	1745
	0.000505	50	0.01703	0.193	1230	1272	1653
			0.01603	0.180	1256	1299	1671
			0.01295	0.143	1258	1337	1631
		70	0.01703	0.200	1240	1286	1676
			0.01603	0.192	1299	1363	1774
			0.01295	0.168	1357	1369	1682
		120	0.01703	0.213	1433	1438	1842
			0.01603	0.202	1447	1455	1907
			0.01295	0.197	1478	1516	1914
1.0	0.000221	50	0.01703	0.061	624	763	866
			0.01603	0.058	635	777	864
			0.01295	0.048	686	851	889
		70	0.01703	0.089	740	888	1074
			0.01603	0.076	760	918	1099
			0.01295	0.062	819	973	1088
		120	0.01703	0.095	781	886	1071
			0.01603	0.079	796	909	1083
			0.01295	0.066	823	973	1087
	0.000315	50	0.01703	0.098	828	955	1182
			0.01603	0.092	825	964	1170
			0.01295	0.072	841	995	1119
		70	0.01703	0.103	865	959	1187
			0.01603	0.109	886	1024	1269
			0.01295	0.082	895	1057	1221
		120	0.01703	0.131	1002	1119	1456
			0.01603	0.122	1045	1108	1412
			0.01295	0.094	1090	1226	1498

*Means of three replications

Influence of Carrier Medium

As the carrier medium concentration decreased, the relative velocity and h_{fp} increased ($p < 0.001$) (Fig. 2). A 42.6% increase in the average relative velocity was observed as a result of decreasing carrier CMC concentration from 1.0% to 0.5%. The observation is similar to previous heat transfer studies using non-Newtonian carriers (Alhamdan and Sastry 1990; Zuritz *et al.* 1990; Balasubramaniam and Sastry 1994a; and Zitoun and Sastry 1994).

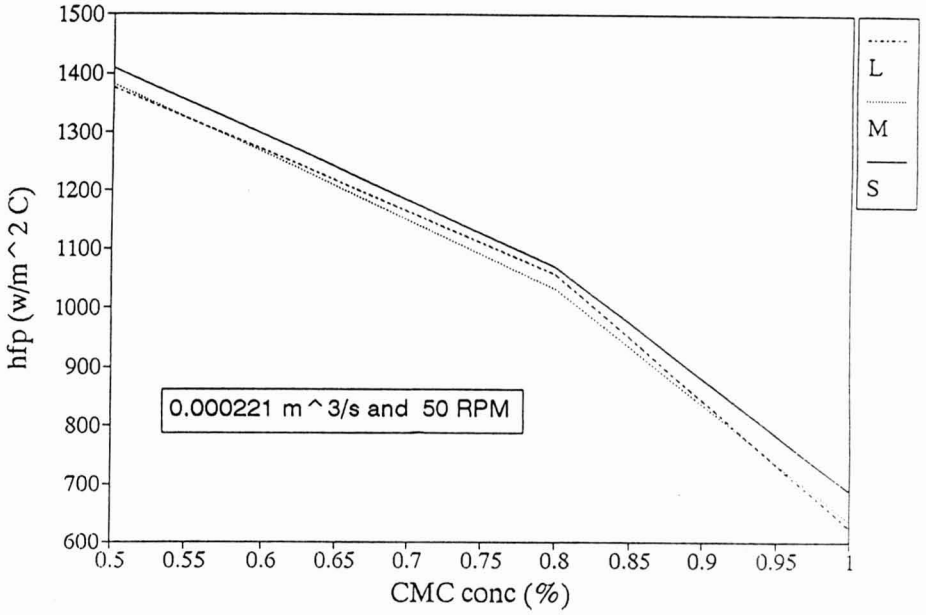

FIG. 2. EFFECT OF CARRIER MEDIUM VISCOSITY ON h_{fp} FOR DIFFERENT PARTICLE DIAMETERS
[L = 0.017 m, M = 0.016 m, and S = 0.0129 m]

Influence of Flow Rate

The relative velocity (and consequently h_{fp}) significantly increased with an increase in the axial flow rate ($p < 0.001$) (Fig. 3). The maximum and minimum values of the relative velocity ranged from 0.04 m/s to 0.295 m/s with corresponding Nusselt numbers of 12.2 to 49.7. The overall average value of Nusselt number for the study is 29.4, which is far higher than the limiting Nusselt number value of 2.0 characterized by zero relative velocity between the fluid and particle (Sastry *et al.* 1989), and preferred for regulatory purposes as

the worst case scenario (Pflug *et al.* 1990). The present estimated relative velocity was based on motion of a single particle in a fluid stream. Studies of Mwangi *et al.* (1993) indicated an 80-200% increase in heat transfer coefficient, when the solid fraction was increased to 3.22% from a single particle suspension. Further studies are necessary to visualize flow interactions and estimate relative velocity (and consequently h_{fp}) for a multiple particle scenario.

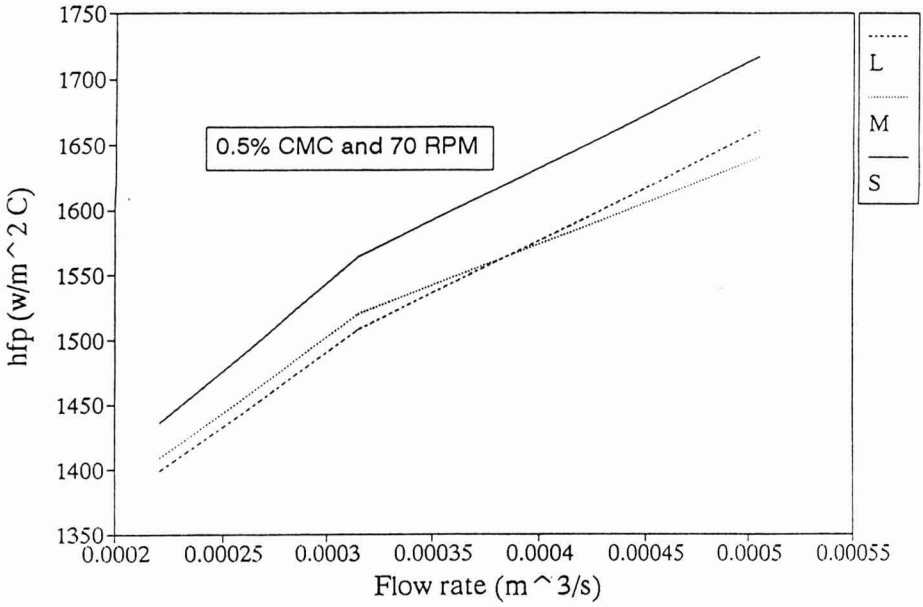

FIG. 3. EFFECT OF FLOW RATE ON h_{fp} FOR DIFFERENT PARTICLE DIAMETERS [L = 0.017 m, M = 0.016 m, and S = 0.0129 m]

Influence of Particle-to-Tube Diameter Ratio (d/D_c)

From Table 5 and Fig. 2 to 4, it can be observed that h_{fp} decreased with increasing particle dimension. Observations were in agreement with Zitoun and Sastry (1994). A radial variation in relative velocity (and h_{fp}) was documented in the earlier flow visualization studies for tube flow (Balasubramaniam and Sastry 1994a; and Zitoun and Sastry 1994). Due to the difficulties in controlling and visualizing radial location in the present studies, we did not attempt to investigate this variable.

Influence of Rotational Speed

In general, the relative velocity and h_{fp} increased with increasing rotational speed ($p < 0.05$) (Fig. 4) as rotation is expected to provide fluid agitation and enhanced heat transfer between fluid and particle. However, contrary to expectations, in some cases the effects levelled off at higher rotational speeds (Table 5). A plot of overall maximum, minimum, and average values of relative velocities for different rotational speeds (Fig. 5) indicates an increase of 0.018 m/s of minimum measured relative velocity (from 0.041 m/s at 50 RPM to 0.059 m/s at 120 RPM) with increasing rotational speed.

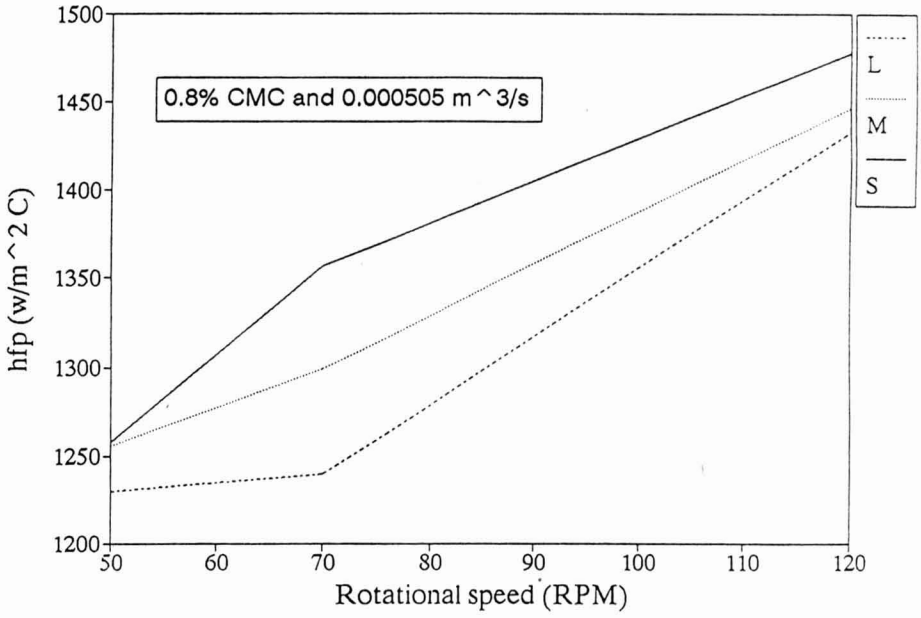

FIG. 4. EFFECT OF ROTATIONAL SPEED ON h_{fp} FOR DIFFERENT PARTICLE DIAMETERS
[L = 0.017 m, M = 0.016 m, and S = 0.0129 m]

Fluid Flow Field and Particle Trajectories in the SSHE

The relative velocity is a localized phenomenon which requires knowledge of the local fluid flow field and particle trajectory within the SSHE annulus. When the motion of the fluid is only created by mutator rotation (and in the absence of axial flow), a linear fluid velocity gradient could be expected in the

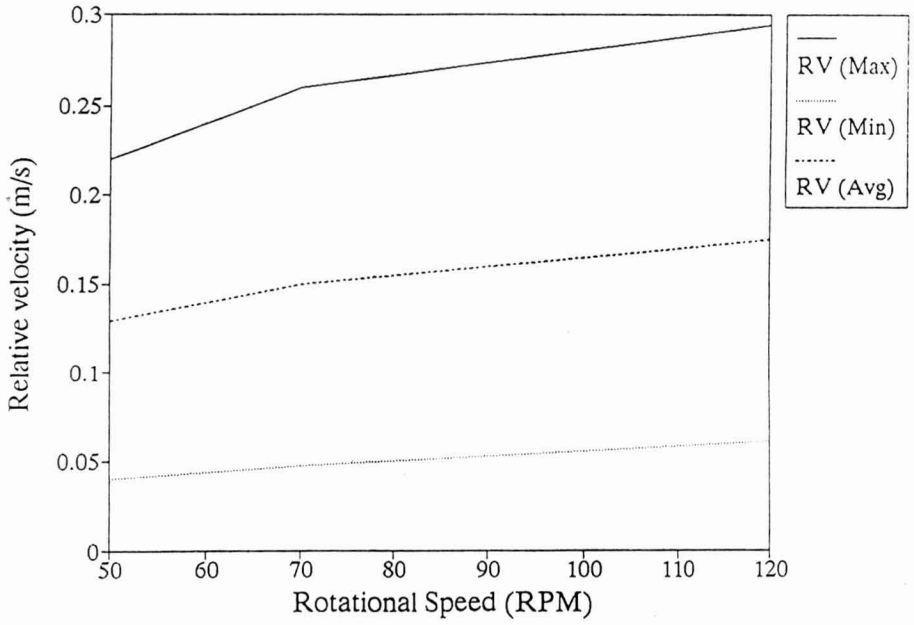

FIG. 5. MAXIMUM, MINIMUM, AND AVERAGE RELATIVE VELOCITY AS INFLUENCED BY MUTATOR ROTATIONAL SPEED

annulus (maximum at the mutator shaft and minimum at the cylinder wall with no slip conditions). On the contrary, in the absence of mutator rotation, and if only axial flow exists in the annulus, a parabolic (or flatter) velocity profile may exist, depending on the fluid rheological characteristics. Combining the above two cases, a complex skewed profile could be expected for the fluid in the annulus. The presence of periodic motion of the scraper blades and fluid-particle interactions could further significantly influence the velocity profile. Currently no mathematical models exist to describe fluid profiles in these situations.

Important forces that act on a moving body through a scraped surface heat exchanger are: (1) axially directed drag force caused by axial flow, (2) tangential drag due to mutator rotation; (3) centrifugal force, and (4) gravity. While the centrifugal and tangential drag forces may try to keep the body moving in a circular path, the axial component may cause the particle to move along a helical path. Gravitational forces may produce a tendency for particles to settle, and may be very important for a vertical SSHE. No apparent settling of the particles was observed during this study, indicating that the influence of gravitational force on the particle may be negligible in horizontal SSHEs.

Experimentally measured average particle revolution speed (Eq. 4) increased with increasing mutator rotational speed (Fig. 6) ($p < 0.05$). It was also observed that within each experimental run, a variation in the particle revolution speed occurred (Fig. 7 and Table 6). A plot of mutator rotational speed vs particle slip revolution speed (defined by Eq. 5) indicates that particle slip increased with increasing mutator rotational speed and particle size (Fig. 8). The smaller the particle inertia, the greater the tendency to readily follow the mutator rotational speed. A particle with higher mass, possibly due to its inertia might have responded slowly to the changes. The relative velocity increased with increasing particle revolution speed (Fig. 9).

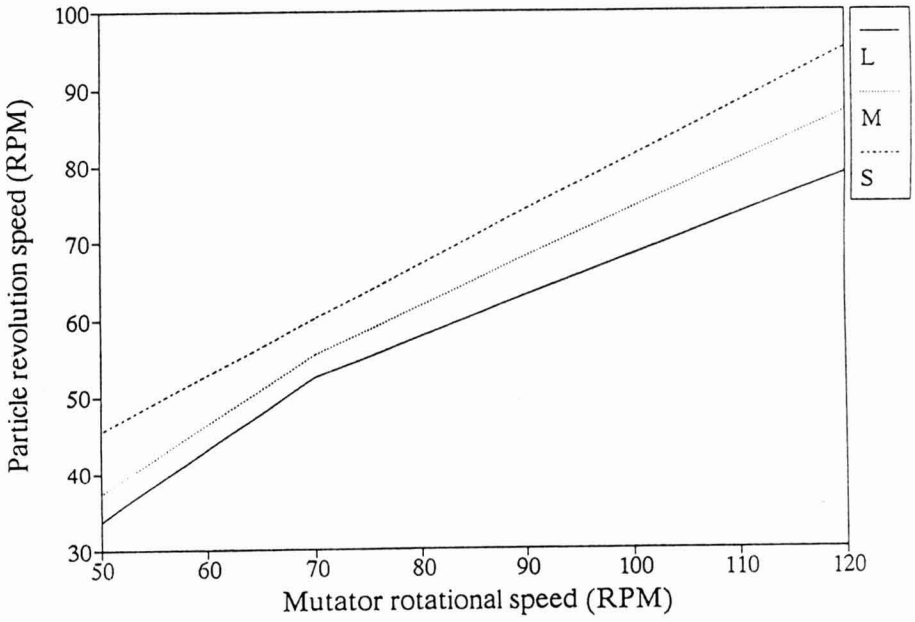

FIG. 6. INFLUENCE OF MUTATOR ROTATIONAL SPEED ON PARTICLE REVOLUTION SPEED FOR DIFFERENT PARTICLE SIZES
[CMC 1.0% and Q = 0.00315 m^3/s]

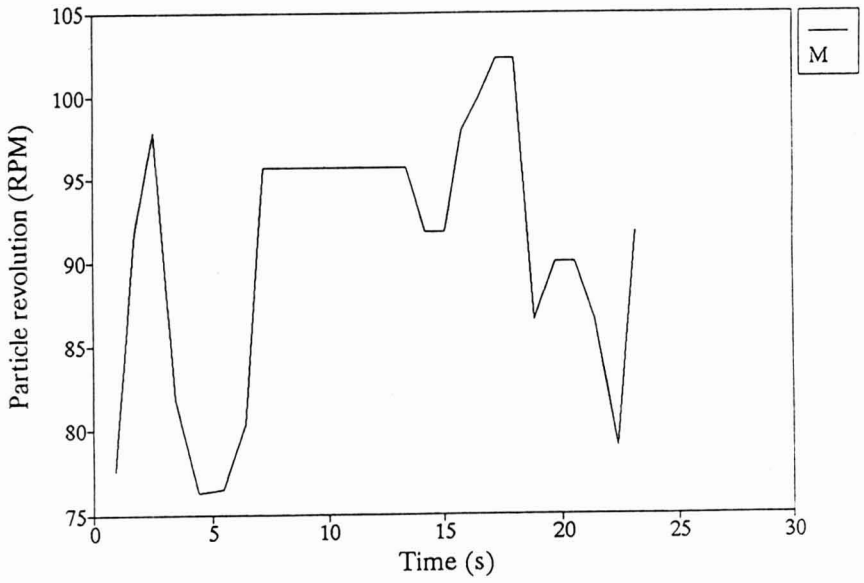

FIG. 7. SAMPLE PLOT OF VARIATION OF PARTICLE REVOLUTION SPEED DURING AN EXPERIMENTAL RUN
[Conc: 1%, Q = 0.000315 m^3/s, Mutator rotation = 120 RPM, and Particle size: 0.01603 m]

TABLE 6.
RANGE OF PARTICLE REVOLUTION SPEED FOR DIFFERENT MUTATOR ROTATIONAL SPEEDS
[CONC 1.0% AND Q = 0.000315 M^3/S]

Mutator Rotational Speed (RPM)	Particle Size (m)	Mean Rev. Speed (m/s)*	Std. Dev. m/s	Maximum m/s	Minimum m/s
50	0.01703	33.7	6.1	44.1	25.8
	0.01603	37.4	5.9	46.5	32.6
	0.01295	45.5	2.1	48.8	43.5
70	0.01703	53.6	4.2	56.0	46.8
	0.01603	58.6	3.8	57.7	48.2
	0.01295	60.2	5.3	64.0	51.0
120	0.01703	78.9	8.3	90.2	71.0
	0.01603	87.2	10.2	103.5	76.5
	0.01295	95.2	7.3	106.0	84.5

*Mean value of six replications.

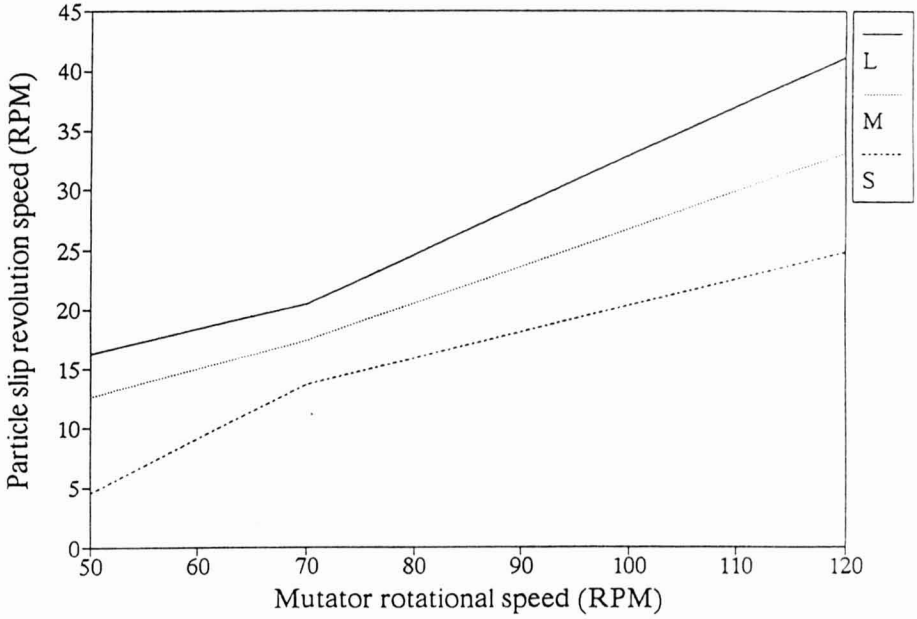

FIG. 8. INFLUENCE OF MUTATOR ROTATIONAL SPEED ON SLIP REVOLUTION SPEED
[Conc: 1% and Q=0.000315 m^3/s, and Particle size: L=0.017 m, M=0.016 m, and S=0.0129 m]

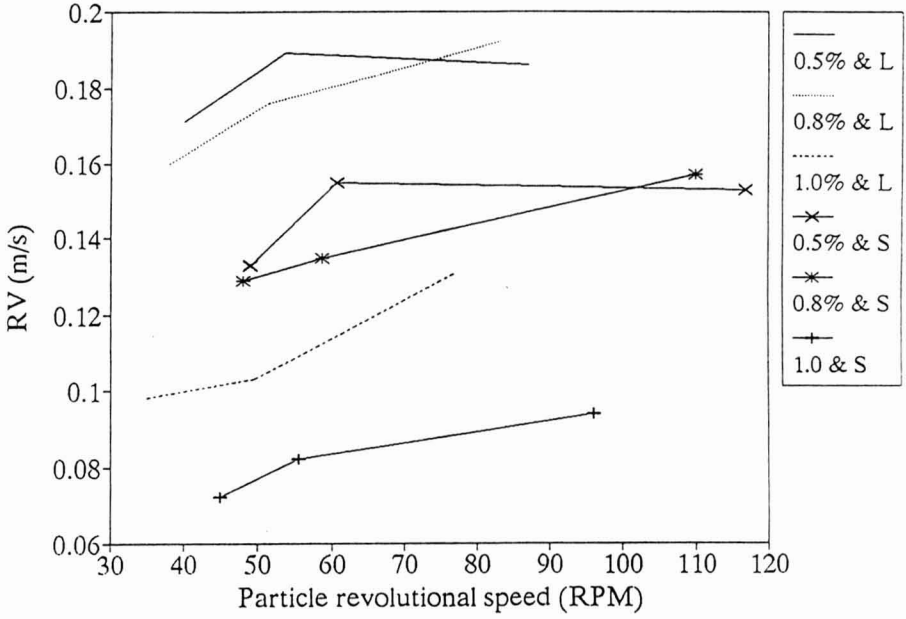

FIG. 9. INFLUENCE OF PARTICLE REVOLUTION SPEED ON RELATIVE VELOCITY
[Q=0.000315 m^3/s and mutator rotational speed = 120 RPM, and Particle size: L = 0.017 m, M = 0.016 m, and S = 0.0129 m]

Influence of Dimensionless Numbers

Nusselt number was mainly influenced by an increase in axial Reynolds number and less significantly by Taylor number (Fig. 10) ($p < 0.05$). The scatter in the data may be partially attributed to particle induced turbulence or variations in the particle radial location within the annulus. The complex fluid-particle trajectories (as explained above) and the periodic motion of scraper blades created a periodic disturbance of the flow field which may have further contributed to the scatter.

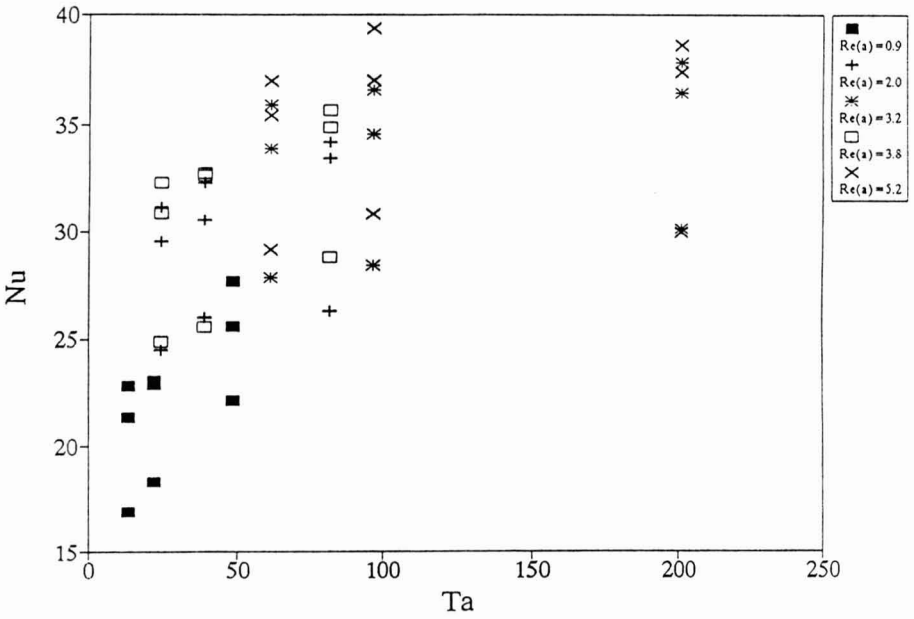

FIG. 10. INFLUENCE OF AXIAL REYNOLDS NUMBER AND TAYLOR NUMBER ON NUSSELT NUMBER

Particle Flow Visualization Studies

The flow field in a SSHE is a complex function of axial and rotational component velocities, resulting in a helical flow pattern. Accordingly, at low rotational speeds, elongated spiral trajectories of the particle around the mutator shaft was observed. As the rotational speed increased, the trajectories were increasingly shorter, depending upon the carrier medium viscosity, and the flow rate. Larger particles, on rare occasions, positioned themselves in between the blade and inner mutator shaft. This resulted in longer residence time for the

particles within the SSHE. No particle settling or rotation was observed. The major motions were axial with the flow, and rotational with the blades. Wake formation in the vicinity of the particle was not observed, since this study was conducted at a low Reynolds number range.

These studies were conducted using hollow aluminum spheres which approximated the density of real food particles. Thus, the flow of these particles would be expected to resemble those of real particles to the extent that density effects would affect flow behavior. The elasticity of the test particles would have been considerably different from real food particles; accordingly the trajectory following collisions may have been different.

The current design of scraped surface heat exchangers was originally used in the ice cream industry, and later adopted for heating heat sensitive liquid-particulate mixtures under aseptic conditions, which cannot otherwise be handled by tubular or plate type systems. As the present study suggests, processing liquid-solid mixtures at very high mutator rotational speeds may not increase the heat transfer between the fluid and particle. On the other hand, from the quality standpoint, operating at very high speed may increase the probability of particle entrapment and breakage within the SSHE leading to quality degradation. Further studies are necessary to improve SSHE design to enhance heat transfer between fluid and particle without sacrificing the quality of the product by optimizing various operating parameters and heat exchanger geometry.

Experimental Difficulties

The flow visualization technique is a detailed and yet time consuming study of the local flow field around the particle. The data were obtained from approximately 270 experimental runs and subsequent analyses of about 850 still frames for the measurement of relative velocity. Not all of the selected frames for measurement of relative velocity were successful since the movement of tracers over the particle was not predictable. For instance, on some occasions, the tracers or the particle were accelerated after being hit by the mutator blade and these situations were carefully excluded from the calculations. The high viscosity fluid (1% CMC) at times formed aggregates at the outlet. Hence, the experiment had to be suspended to clean the system. At higher rotational speeds, higher camera shutter speeds had to be used (1H250 or 1H500) to obtain sharp pictures of the particles and the tracers.

CONCLUSIONS

The relative velocity and h_{fp} increase with an increase in flow rate and rotational speed, and decrease with an increase in carrier medium viscosity. With an increase in particle dimension, a decrease in h_{fp} was observed. The

relative velocity ranged from 0.04 to 0.29 m/s with corresponding h_{fp} of 597 to 1975 W/m^2°K. With the most conservative Ranz and Marshall correlation, Nusselt numbers ranged from 12.1 to 49.7. The data suggest that the heat transfer coefficients increased with increasing mutator rotational speed up to a certain point, beyond which heat transfer did not necessarily increase. As determined in previous studies, the relative velocity method provides slightly lower h_{fp} in comparison to the liquid crystal method; however the differences are neither marked nor inexplicable; hence the approach does provide a degree of verification. The principal practical importance of these results is that h_{fp}, seems to be considerably higher than expected from a Nusselt number of 2.0 commonly associated for a sphere in a stagnant fluid.

LIST OF SYMBOLS

C_p Specific heat (J/kg°K)
C_{pf} Specific heat of fluid (J/kg°K)
d Particle diameter (m)
D_c Width of the clearance in SSHE ($D_c = D_o - D_i$)
D_i Mutator diameter (m)
D_o Inside diameter of the outer stationary cylinder of SSHE (m)
h_{fp} Liquid-to-particle convective heat transfer coefficient (W/m^2°K)
k_f Thermal conductivity of fluid (W/m°K)
K Consistency coefficient (Pas^n)
n Flow behavior index
N Mutator rotational speed (s^{-1})
Nu Nusselt number ($Nu = h_{fp}d/k_f$)
$Pr_{G,A}$ Generalized Prandtl number
($Pr_{G,A} = [C_p\ K\ (3n+1)/n)^n 2^{(n-1)}]\ /\ [4\ k_f V_f^{(1-n)} D_c^{\ (n-1)}]$)
$Re_{G,A}$ Generalized axial fluid Reynolds number
($Re_{G,A} = [8\ V_f^{(2-n)} D_c^{\ n} \rho]/[2^n\ K\ (3n+1)/n)^n]$)
$Re_{G,S}$ Generalized slip Reynolds number
($Re_{G,S} = [8\ V_r^{(2-n)} d^n \rho]/[2^n\ K\ (3n+1)/n)^n]$)
Ta_G Generalized Taylor number
($Ta_G = [8\ V_R^{(2-n)} D_c^{\ n} \rho (d/D_c)^{0.5}]/[2^n\ K\ (3n+1)/n)^n]$)
V_f Velocity of fluid (m/s)
V_r Relative velocity between fluid and particle (m/s)
$V_{m,r}$ Mutator rotational speed (s^{-1})
$V_{p,r}$ Particle revolution speed (s^{-1})
$V_{p,s,r}$ Particle slip revolution speed (s^{-1})

Greek Letters

$\dot{\gamma}$ Shear rate (s^{-1})
ρ Density (kg/m^3)
τ Shear stress (Pa)
μ Viscosity of bulk fluid (Pa.s)
μ_p Viscosity of fluid at particle surface (Pa.s)

REFERENCES

ALHAMDAN, A. and SASTRY, S.K. 1990. Natural convection heat transfer between non-Newtonian fluids and an irregular shaped particle. J. Food Process Engineering *13* 113–124.

BALASUBRAMANIAM, V.M. and SASTRY, S.K. 1994a. Liquid-to-particle convective heat transfer in non-Newtonian carrier medium during continuous tube flow. J. Food Engr. *23*, 169–187.

BALASUBRAMANIAM, V.M. and SASTRY, S.K 1994b. Liquid-to-particle heat transfer in continuous flow through a horizontal scraped surface heat exchanger. Trans. IChemE. Part C. *72* 189–196.

BOTT, T.R., AZOORY, S. and PORTER, K.E. 1968. Scraped surface heat exchanger. Part 2. Effects of axial dispersion on heat transfer. Trans IChemE. *46*, T37–T43.

CUEVAS, R. and CHERYAN, M. 1982. Heat transfer in a vertical liquid-film scraped-surface heat exchanger. Application of the penetration theory and wilson plots models. J. Food Process Engineering *5*, 1–21.

HÄRRÖD, M. 1990. Modeling the media-side heat transfer in scraped-surface heat exchangers. J. Food Engr. *13*, 1–21.

HEPPELL, N.J. 1985. Measurement of the liquid-solid heat transfer coefficient during continuous sterilization of liquids containing solids. Presented at the 4th Intl. Cong. on Engineering and Food, July 7-10. Edmonton, Alberta, Canada.

INCROPERA, F.P. and DEWITT, D.P. 1990. *Introduction to Heat Transfer*, 2nd. Ed. Addison-Wesley, Reading, MA.

KRAMERS, H. 1946. Heat transfer from spheres to flowing media. Physica *12* (2), 61–80.

MENDENHALL, K.M. 1979. *Introduction to Probability and Statistics*. 5th Ed. Duxbury Press. Belmont, CA.

MWANGI, J.M., RIZVI, S.S.H. and DATTA, A. 1993. Heat transfer to a particle in shear flow: application in aseptic processing. J. Food Engr. *19*, 55–74.

PFLUG, I.J., BERRY, M.R. and DIGNAN, D.M. 1990. Establishing the heat-preservation process for aseptically-packaged low-acid food containing large particulates, sterilized in a continuous heat-hold-cool system. J. Food Sci. *53*(4), 312–321.

RANZ, W.E. and MARSHALL, W.R., Jr. 1952. Evaporation from drop. Chem. Eng. Progress *48*, 141.

SAS. 1989. SAS User's Guide: Statistics, Version 6. SAS Institute, Cary, NC.

SASTRY, S.K., HESKITT, B.F. and BLAISDELL, J.L. 1989. Experimental and modeling studies on convective heat transfer at the particle-liquid interface in aseptic processing systems. Food Technol. *41*(3) 132–136, 143.

SASTRY, S.K., LIMA, M.A., BRIM, J., BRUNN, T. and HESKITT, B.F. 1990. Liquid-to-particle heat transfer during continuous tube flow: Influence of flow rate and particle to tube diameter ratio. J. Food Process Engineering *13*, 239–253.

TROMMELEN, A.M. 1967. Heat transfer in a scraped-surface heat exchanger. Trans. IChemE. *45*(19), T176–T178.

WEISSER, H. 1972. Untersuchungen zum Warrneubergang im Kratzkuhler. Ph.D. thesis, Karlsruhe Univ., Germany.

WHITAKER, S. 1972. Forced convection heat transfer correlations for flow in pipes, past flat plates, single cylinders, single spheres, and for flow in packed beds and tube bundles. AIChE J. *18*(2), 361–370.

ZITOUN, K.B. and SASTRY, S.K. 1994. Determination of convective heat transfer coefficient between fluid and cubic particle in continuous tube flow using noninvasive experimental techniques. J. Food Process Engineering *17*, 209–228.

ZURITZ, C.A., MCCOY, S.C. and SASTRY, S.K. 1990. Convective heat transfer coefficients for irregular particles immersed in non-Newtonian fluids during tube flow. J. Food Engr. *11* 159–174.

MODELING MICROWAVE COOKING OF COCKTAIL SHRIMP

P. MALLIKARJUNAN[1], Y.-C. HUNG and S.GUNDAVARAPU

Center for Food Safety & Quality Enhancement
Department of Food Science & Technology
University of Georgia, Georgia Experiment Station
Griffin, Georgia 30223-1797, USA

Received for Publication May 25, 1995

ABSTRACT

A mathematical model for microwave cooking of cocktail shrimp was developed. The model included heat and mass transfer and microbial inactivation kinetics. A simple 2 dimensional cylindrical slab geometry was used and model equations were solved using the finite difference method. The model predictions on temperature and mass loss were in good agreement with the observed data. Temperature predictions were within ±6C and mass predictions were within ±2 g of the observed data.

INTRODUCTION

The per capita seafood consumption in the U.S. grew by 18.7% between 1978 and 1989, expanding from 13 to 16 lbs. Increased seafood consumption has been attributed to rising personal incomes, changing lifestyles, and increasing awareness of health benefits attributed to seafood. Shrimp in all forms represent a major component of the nation's seafood industry. Shrimp consumption in the U.S. increased from 1.3 lbs. per capita (or 11% of total seafood consumption) in 1979 to 2.4 lbs. per capita (or 16% of total seafood consumption) in 1991 (National Marine Fisheries Service 1990). United States shrimp consumption increased by 22% between 1985 and 1988, compared to a 12% increase in total seafood consumption during the previous decade (Burtle 1990). Increased public awareness of health and nutritional concerns associated with seafood consumption has led consumers, industry officials, regulators and academic researchers to propose innovative products and processes for the seafood industry.

Microwave cooking is becoming popular as it is very quick, simple and fat free. Despite the versatility, microwaves are used more to reheat food than to cook it, probably because microwaved food does have a different taste than

[1]To whom correspondence should be addressed.

Journal of Food Process Engineering **19** (1996) 97–111.

conventionally cooked foods (Ruello 1987). Gast *et al.* (1980) showed that an initial reluctance to microwave cooked meat can be overcome if consumers are adequately informed on how to cook meat by microwaves. Successful results cannot be easily achieved by simply adapting conventional cooking to the microwave oven. Microwave heating of food is more "food dependent" than conventional heating, because of the mechanism of generation of heat by microwaves. Therefore, emphasis has to be given on understanding the heating profiles of each class of food during microwave treatment (Fung and Cunningham 1980).

Advantages of cooking food using microwaves are better nutrient and moisture retention and enhanced microbiological safety (Ruello 1987; Datta and Hu 1992). The reasons for better nutrient retention in microwave heated food are faster and shorter duration of heating. This rapid heating also provides a target bacterial reduction of 4D for microwave heating after 10 min compared to 65 min for conventional heating. On the other hand, an increase in heating rate increases the potential of nonuniform heating. Thus, the advantages of faster heating can be nullified by the increased nonuniformity (Datta and Hu 1992).

To avoid non-uniformity and overcooking of the food, the food should be cooked using a cooking pattern having heating and holding periods. The holding period can provide the time required for equilibrating the hot and cold spots and also provide the time for accumulation of lethality. It is best for seafood to microwave at medium power setting to avoid overcooking which results in a tough texture (Ruello 1987).

Successful microwaving of seafood depends on an understanding of how the particular seafood will behave when cooked by microwaves. Such knowledge can be used by food technologists to produce recipes and cooking instructions that are microwave specific and thus give consistent, satisfying results for the seafood products (Ruello 1987). To gain a better understanding of the process, a valid mathematical model to describe the microwave cooking processes is required. Thus, the objectives of this study were to:

(1) develop mathematical models to describe heat and mass transfer during microwave cooking of shrimp,
(2) validate the model using experimental data, and
(3) incorporate the microbial inactivation kinetics into the heat and mass transfer model to predict the safety of microwave cooked shrimp.

MODELING

Microwave heating of foods were modeled as slabs (Datta 1991; Zhou *et al.* 1992; Tong and Lund 1993), cylinders (Zhou *et al.* 1992; Chen *et al.* 1993) and spheres (Ohlsson and Risman 1978). The finite difference (Ohlsson and

Bengtsson 1971; Swami 1982; Tong and Lund 1993) and finite element methods (Zhou *et al.* 1992; Chen *et al.* 1993) were frequently used to solve the fundamental equations. Many of the models reported only considered heat transfer (Ohlsson and Risman 1978; Datta 1991; Chen *et al.* 1993). Few models (Zhou *et al.* 1992; Tong and Lund 1993) also considered mass transfer, however the loss of moisture due to steam escape was not considered.

Unlike simple cylindrical shape (e.g., water in a container or a potato), multinumber of shrimp in a container is heterogenous due to voids between shrimp and also the heterogeneity of each shrimp. Also, due to shrinkage during cooking, a considerable amount of change in shape also occurs. The complexities increase further by the temperature dependence of the thermal and physical properties of shrimp. During microwave cooking, shrimp releases its moisture as steam in addition to evaporation (due to vapor pressure difference). Because of the additional steam to the head space of the container, the ambient temperature above the head space in a closed container increases resulting in increased cooking efficiency.

To simplify the above complexities, the following assumptions were considered:

(1) Shrimp in the container were modeled as a cylindrical slab based on the mass and the density of the sample.
(2) Initial temperature and moisture distribution was assumed to be uniform.
(3) Shrinkage of shrimps during microwaving was neglected.
(4) Surface cooling was considered due to evaporation and natural convection, and
(5) The increase in head space temperature was also considered.

The heat transfer was considered due to conduction within the shrimp, convection at the product surface and heat generation due to microwaves:

$$\frac{\partial T}{\partial t} = \alpha\left[\frac{1}{r}\frac{\partial T}{\partial r}+\frac{\partial^2 T}{\partial r^2}+\frac{\partial^2 T}{\partial z^2}\right] + \frac{Q}{\rho C_p} \qquad (1)$$

Evaporation at the surface due to vapor pressure difference and steam release from the product during heating were considered for mass loss during microwaving.

$$-\frac{\partial m}{\partial t} = h_m A(P_s - P_a) + \frac{\rho V C_p}{\lambda_v}\left[\frac{\partial T}{\partial t}\right] \qquad (2)$$

The Lambert's law has been used very frequently to estimate microwave power absorption by food with reasonable accuracy (Decareau 1985). The heat generation during microwave heating is given as:

$$Q = Q_o \left[\exp\left[\frac{-(R-r)}{\delta_p} \right] + \exp\left[\frac{-(Z-z)}{\delta_p} \right] \right] \quad (3)$$

The boundary conditions for heat transfer in radial and axial directions are:

$$kA\frac{\partial T}{\partial r} = h_t A(T_s - T_a) + \lambda_v \dot{m} \quad (4)$$

$$kA\frac{\partial T}{\partial z} = h_t A(T_s - T_a) + \lambda_v \dot{m} \quad (5)$$

The increase in temperature in the head space was calculated using the heat balance between the air and the product surface:

$$V_h \rho_a C_{p,a} \frac{\partial T_a}{\partial t} = h_t A(T_s - T_a) \quad (6)$$

Temperature distributions obtained from the heat transfer model were then used to calculate the microbial inactivation. To model the microbial inactivation kinetics, a first order reaction kinetics was assumed:

$$-\frac{dN}{dt} = A_o \cdot e^{-\frac{E_a}{RT}} \cdot N \quad (7)$$

For a 100 g of shrimp sample (10 counts of jumbo sized shrimp), a simplified two dimensional axisymmetric (R-Z) circular slab shape was considered (Fig. 1). Considering the density of shrimp (1061 kg/m^3) and the container radius (55 mm), the shrimp samples were considered as a homogeneous patty with 55 mm radius and 10 mm in height. The finite difference method was used to obtain the difference equations in R-Z plane. Central difference method was used to obtain the difference equations. The difference equations were solved over time using a dynamic simulation software (DESIRE Ver 9.02, GA Korn Associates, Tucson, AZ).

EXPERIMENTAL PROCEDURE

Ten jumbo size shrimp were placed in a microwavable plastic container (Servin' Saver™, 435 ml (14 oz), Rubbermaid® Inc., El Paso, TX) and cooked using both a household type microwave oven (Model No. 56-9833-10/03, Tappan White Consolidated Industries Inc., Dublin, OH) and a laboratory type microwave oven (Model LBM 1.2 A, Cober Electronics Inc., Stamford, CT). Temperatures at four locations (Fig. 1) were measured using fluoroptic temperature probes (Model SFW-2, Luxtron Corp., Santa Clara, CA)

connected to a fluoroptic thermometer (Model 790, Luxtron Corp., Santa Clara, CA). For the geometric center of the domain (location 1) and middle point between the center and the surface locations (location 2), the probes were placed in the center of a shrimp in that preferred location. For surface location (location 3), the probe was placed on the surface of the shrimp placed on the top of the batch. The other probe was placed in the head space. Mass change during microwaving was measured using an electronic balance (Model 610D, Sartorius-Instruments Ltd., Surrey, U.K.). The bottom plate and turntable motor assembly from the Tappan microwave oven were removed to accommodate the weight change measurement. A placing table with a central rod connecting two plates was fabricated to place the sample over the balance (Fig. 2). The top plate of the placing table was placed inside the microwave oven and connected to the bottom plate of the placing table using a rod. The rod went through the hole created by the removal of turntable motor assembly. The bottom plate was then placed on the balance. The fluoroptic thermometer and the balance were

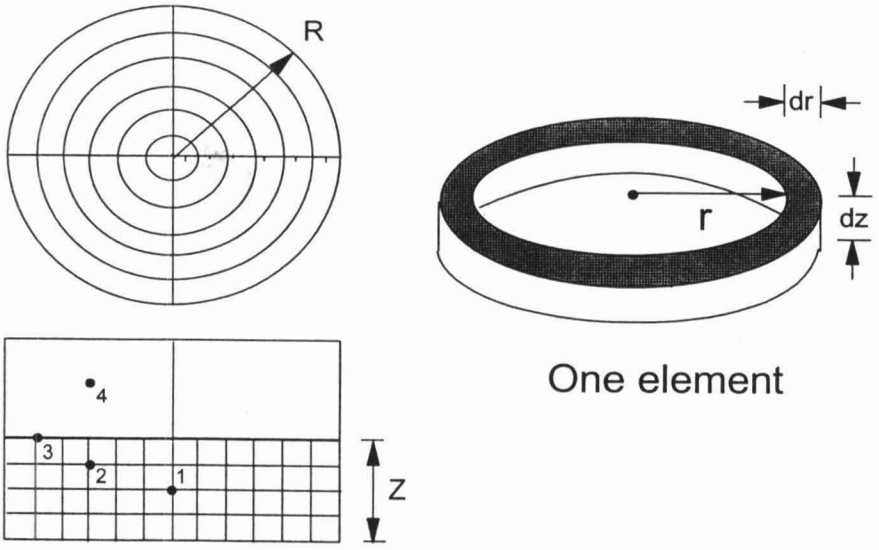

FIG. 1. SHRIMP IN THE CONTAINER AS A CYLINDRICAL SLAB WITH FINITE DIFFERENCE DISCRETIZATION AND THERMOCOUPLE LOCATIONS [(1) CENTER, (2) MIDPOINT BETWEEN THE CENTER AND SURFACE, (3) SURFACE AND (4) HEADSPACE ABOVE THE SHRIMP IN THE CONTAINER].

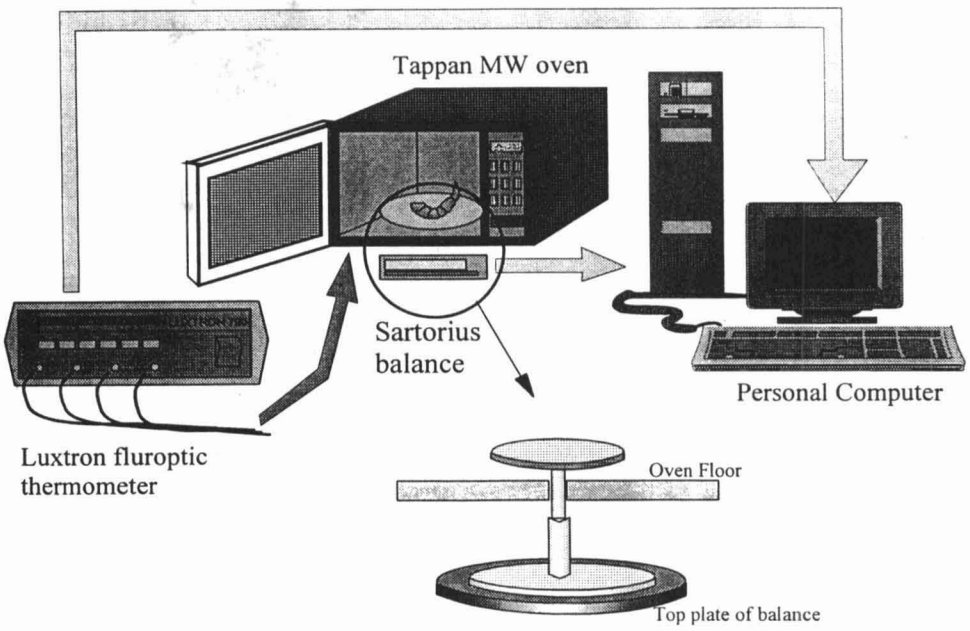

FIG. 2. SCHEMATIC DIAGRAM OF THE EXPERIMENTAL SET-UP

connected to a personal computer using RS232C serial interface for data acquisition. The power output from the microwave ovens were determined using the IMPI standard (IMPI 1989). Two beakers each having one liter of water at 20C was heated for 2 min and the actual power outputs were 800, 560, 400 and 240 W at 100, 70, 50, and 30% power levels, respectively. Shrimp were then cooked at different power levels (Table 1). Shrimp were also cooked using 700 W and 400 W power levels using the Cober laboratory type microwave oven. Holding time for each cooking pattern was provided to allow thermal equilibrium between hot and cold spots.

RESULTS AND DISCUSSION

Model Parameters

The thermal properties of shrimp reported by Chau and Snyder (1988) were used in this study. The values of the thermal conductivity, specific heat and density were 0.3211 W/(m.K), 3480 J/(kg K), and 1061 kg/m^3, respectively. The latent heat of vaporization was distributed into the specific heat term between 100 and 106C with a boiling point of 105C. This effect of latent heat of vaporization was considered only during heating and not during cooling.

TABLE 1.
HEATING PATTERNS AT DIFFERENT POWER LEVELS FOR MICROWAVE COOKING OF SHRIMP

Heating Pattern	Power Setting, %	Power Level, W	Time, s		
			Heating 1	Holding	Heating 2
Tappan Microwave Oven					
T1	30	240	75	45	50
T2	50	400	40	50	30
T3	70	560	30	90	20
T4	100	800	30	120	10
Cober LBM 1.2A Oven					
C1	50	400	100	120	--
C2	100	700	50	120	--

Above 106C the specific heat of steam (1880 J/(kg K)) was used as the specific heat of shrimp. To calculate the amount of heat transferred during natural convection, the surface heat transfer coefficient was calculated using the equation for a horizontal cylinder (Toledo 1991):

$$h_t = 1.3196 \left[\frac{\Delta T}{D}\right]^{0.25} \tag{8}$$

The surface mass transfer coefficient was calculated using the relationship (Sereno and Medeiros 1990):

$$\frac{h_t}{h_m \lambda_v} = 64.7 \text{ Pa/K} \tag{9}$$

Penetration depth of microwaves was calculated using the equation (Nelson *et al.* 1994):

$$\partial_p = \frac{\lambda_0}{2\pi(2\epsilon')^{0.5}} \left\{\left[1 + \left(\frac{\epsilon''}{\epsilon'}\right)^2\right]^{0.5} - 1\right\}^{-0.5} \tag{10}$$

where $\lambda 0 = 12.237$ cm at 2450 MHz. Dielectric properties of shrimp were determined using an open ended, semirigid, Teflon insulated coaxial line with copper conductors connected to a Network analyzer (Model 8510B, Hewlett Packard, Santa Clara, CA). The dielectric constant varied from 20 to 80 and the dielectric loss factor varied from 10 to 70 between 0.1 and 25 GHz for all the experiments. The data on dielectric constant and dielectric loss factor were

collected for 2450 MHz and the relationships for dielectric loss factor and dielectric constant with respect to temperature were obtained as:

$$\epsilon' = 60.9 + 0.047T - 0.0054T^2 \quad (11)$$

$$\epsilon'' = 16.5 - 0.27T - 0.0048T^2 \quad (12)$$

To calculate the inactivation kinetics of *Listeria monocytogenes* during microwaving, D values reported by Gundavarapu *et al.* (1995) were used. Arrhenius relationship was used to calculate the relationship between the rate constant and temperature between 55 and 70C (Fig. 3). The activation energy and the frequency factor were calculated as 347.3 kJ/(kg.mole. K), 1.623×10^{54} s^{-1}, respectively.

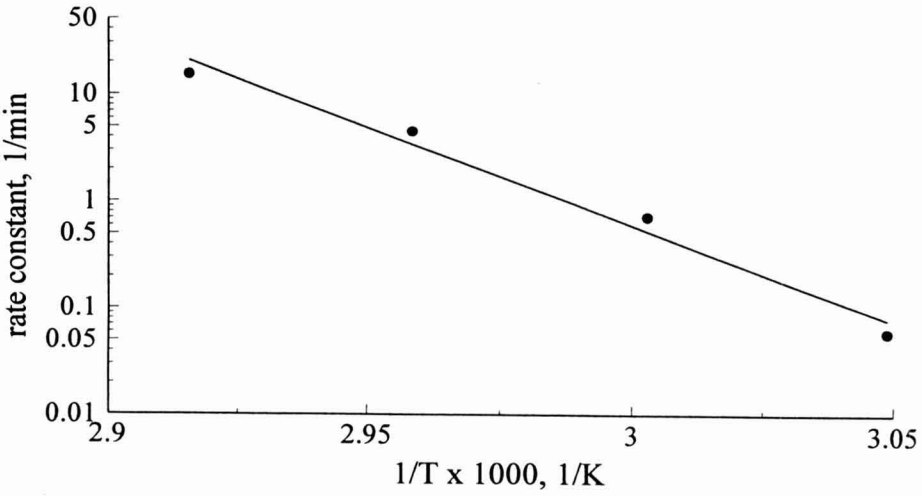

FIG. 3. RATE CONSTANT FOR THE INACTIVATION OF *LISTERIA MONOCYTOGENES* AS A FUNCTION OF TEMPERATURE USING FIRST ORDER REACTION KINETICS

The partial vapor pressure was calculated by multiplying the saturated vapor pressure by water activity or relative humidity. To obtain the saturated vapor pressure of air at any given temperature, the empirical equation proposed by Weiss (1977) was used:

$$P_s = 614.97 \cdot \exp\left[17.2694 * \frac{(T - 273)}{(T - 35.7)}\right] \quad (13)$$

Model Validation

The predicted and observed temperature at the surface and the center of a batch of shrimp cooked at 800 W power level using Tappan Microwave oven and heating pattern T4 are shown in Fig. 4. The predicted temperature agreed well with observed data during heating. The deviations between the observed and predicted temperature profiles and mass history were calculated using:

$$\sigma = \sqrt{\frac{\sum_{i=1}^{N} (Y_p - Y_o)^2}{n}} \quad (14)$$

The temperature predictions were within 6C (Table 2).

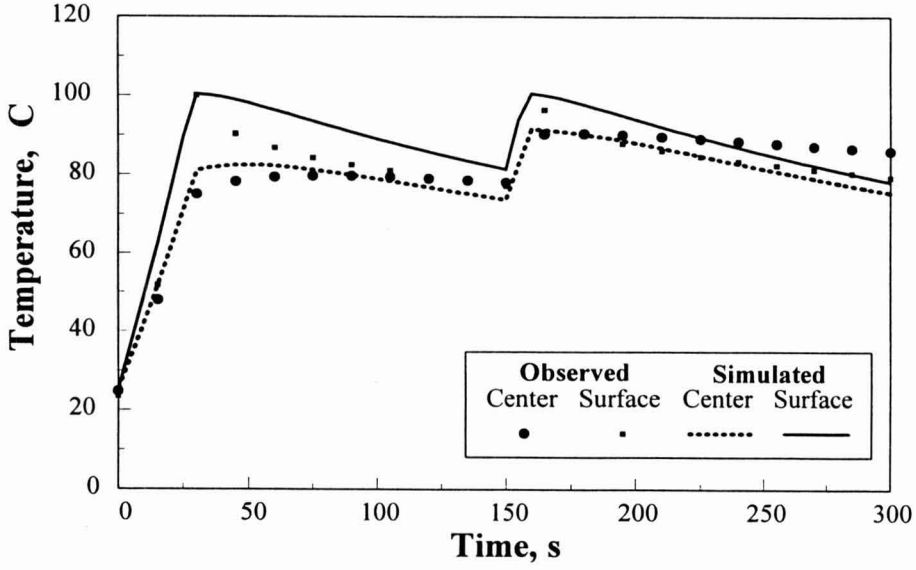

FIG. 4. PREDICTED AND OBSERVED TEMPERATURE HISTORY DURING MICROWAVE COOKING OF SHRIMP USING HEATING PATTERN T4

TABLE 2.
DEVIATION BETWEEN PREDICTED AND OBSERVED TEMPERATURES AND MASS OF SHRIMP FOR DIFFERENT HEATING PATTERNS

Heating Pattern	Deviation (σ)		Observed Mass Loss, %	Predicted Mass Loss %
	Temperature, C	Mass, g		
T1	5.83	1.82	16.8	17.5
T2	3.62	1.76	15.3	15.8
T3	2.78	1.98	16.5	16.3
T4	1.92	1.87	17.3	16.5
C1	2.15	*	16.3	17.1
C2	2.86	*	14.1	14.8

*mass history was not collected for Cober LBM 1.2A laboratory type microwave oven.

Minor differences between predicted and measured temperatures occurred during the holding (cooling) period for both locations (Fig. 4). The reasons for the differences are due to the model assumptions in neglecting the voids between shrimp, and shrinkage. The model assumed a continuous shrimp (as a patty). On the other hand, the air pockets in the voids and volume change in shrimp due to shrinkage allowed the observed center temperature to be higher than the predicted temperature. Due to the same phenomenon, the observed surface temperature was lower compared to the predicted surface temperature. This effect was well demonstrated for the heating pattern T1. This was mainly due to frequent intermittent holding time periods provided by the duty cycle (20 s) of the Tappan microwave oven during heating. For cooking at a 30% power setting, the microwave oven worked at 100% power level for 6 s and worked at 0% power level for 14 s to provide a net 30% power per duty cycle.

The predicted and observed mass for heating pattern T4 are shown in Fig. 5. In the initial attempts in modeling the mass transfer, without a steam generation term in Eq. 2, the predicted mass loss at the end of cooking was (2%). After the inclusion of moisture loss due to steam escape during heating, the mass loss predictions (12%) agreed very well with the observed data (Fig. 5). The mass loss in the observed and predicted data followed the heating pattern with rapid moisture loss during heating due to steam release compared to slow moisture loss during holding (evaporative cooling) period. The difference in mass loss predictions was highly attributed to the amount of noise recorded due to the operation of the fan in the microwave oven. It was also difficult to separate noises with on and off cycling of the magnetron for lower power settings compared to pattern T4. However, the recorded total mass loss agreed well with the measured results (Table 2) and the deviation between the observed and predicted data were within 2 g.

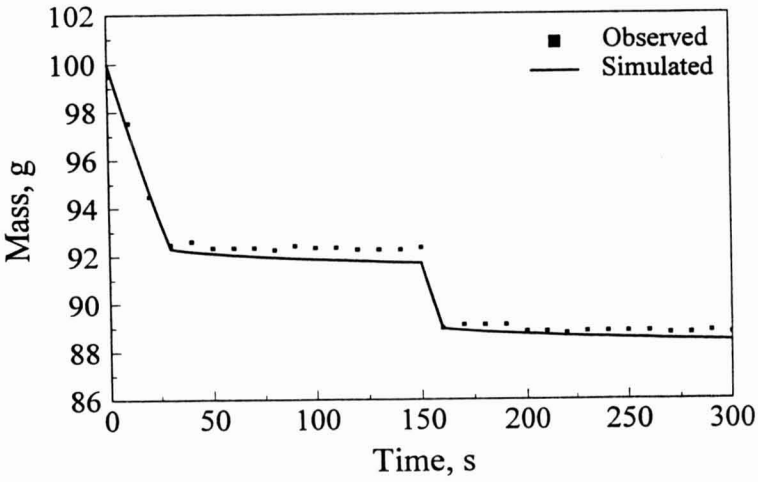

FIG. 5. PREDICTED AND OBSERVED MASS HISTORY DURING MICROWAVE COOKING OF SHRIMP USING HEATING PATTERN T4

Microbial Inactivation Kinetics

The calculated inactivation kinetics curves for *Listeria monocytogenes* during heating were plotted against time for different power levels (Fig. 6). As expected, the higher the power level, the shorter the time to reach a 10 D microbial reduction.

With the consumer at home in mind, a new cooking pattern (one heating and holding pattern instead of a heating/holding/heating) was developed and the cooking time required for a 10 D reduction of *Listeria monocytogenes* was calculated and the results are shown in Table 3. The heating time is the time duration for the microwave oven to heat the product. The total cooking time included heating and holding times and is calculated from the beginning of cooking (heating period) to until temperature at the coldest point inside the sample to fall below 70C during holding. The cooking patterns were computed so that every pattern provided the temperature at or above 70C at the coldest point for 2 min. This criterion was considered based on the suggestion from Coote *et al.* (1991) and Gaze *et al.* (1989). Thus, holding time is the difference between heating time and total cooking time.

Validation results were conducted to verify the model predictions using a 5 strain mixture of *Listeria monocytogenes* (Gundavarapu *et al.* 1995). The shrimp samples were inoculated with approximately 5×10^5 CFU/g by injecting a 10 μl portion into the geometric center of the second segment of each shrimp. No viable microorganisms were detected in uninoculated shrimps after microwave

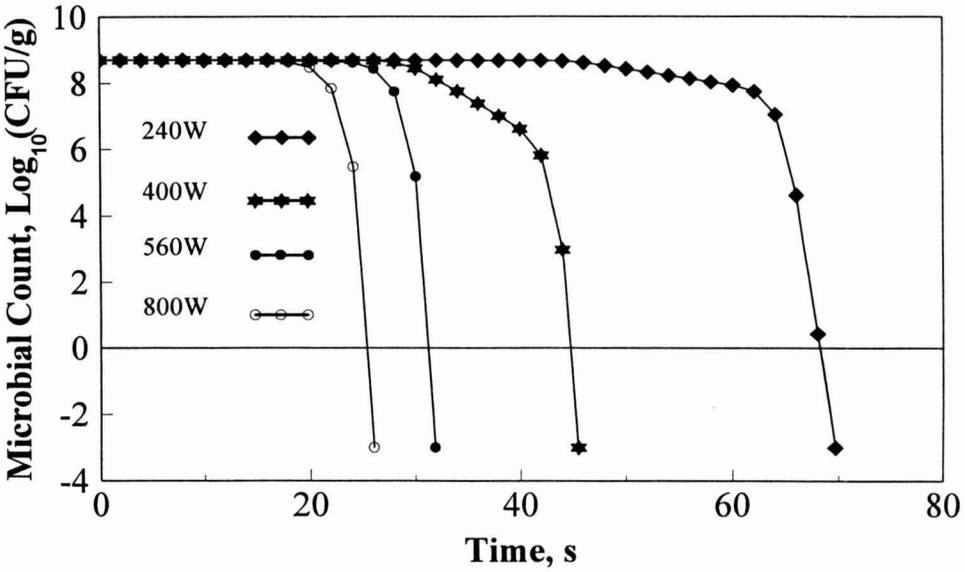

FIG. 6. INACTIVATION CURVES FOR *LISTERIA MONOCYTOGENES* DURING CONTINUOUS HEATING FOR DIFFERENT MICROWAVE POWER LEVELS USING TAPPAN MICROWAVE OVEN

TABLE 3.
THE TIMINGS FOR MICROWAVE COOKING OF SHRIMP WITH ONE HEATING / HOLDING TO ACHIEVE A 10 D REDUCTION IN *LISTERIA MONOCYTOGENES* WITH AT LEAST 2 MIN ABOVE 70C

Power Level, W	Time to Reach 70C	Time, s		
		Heating Time	Holding Time	Total Cooking Time
240	85	140	65	205
400	48	70	95	165
560	33	52	98	150
800	27	40	102	142

cooking. For the inoculated samples, they found at least one replication in each of the four treatments tested positive for the presence of *Listeria* after microwave cooking. This could be due to the void spaces between the shrimp and the assuming the microorganisms to be homogeneously distributed instead of a localized contamination. With a 20% increase in the cooking times, no evidence of *L. monocytogenes* was found in cooked shrimp.

In order to study the effect of microwave cooking on consumer acceptance, a separate study was conducted (Gundavarapu 1995). All the microwave cooking treatments were found acceptable (like moderately to like very much) by the consumers for all the attributes evaluated (color, flavor, texture, juiciness, and overall acceptability). Nearly 80% of the consumers were willing to buy microwave cooked shrimp.

CONCLUSIONS

(1) The models for describing the heat and mass transfer during microwave cooking of shrimp were in good agreement with the experimental data for temperature and the mass loss predictions.
(2) Temperature predictions were within $\pm$6C.
(3) The mass loss predictions were within $\pm$2 g.
(4) Cooking patterns at different power levels were established to assure a 10 D reduction of *Listeria monocytogenes*.

ACKNOWLEDGMENTS

This work was supported by State and Hatch Funds allocated to the Georgia Agricultural Experiment Station and by a grant from the National Oceanic and Atmospheric Administration Office of Sea Grant under Grant number NA26RG-0373-01. The views expressed herein are those of the authors and do not necessarily reflect the views of NOAA or any of its sub-agencies.

NOTATION

α Thermal diffusivity of shrimp, m^2/s
ϵ' Dielectric constant
ϵ'' Dielectric loss factor
δ_p Penetration depth, m
λ_v Latent heat of vaporization, J/kg
ρ Density of shrimp, kg/m^3
ρ_a Density of air, kg/m^3
A Cross sectional area, m^2
A_0 Frequency factor for inactivation of *Listeria monocytogenes*, s^{-1}
C_p Specific heat of shrimp, J/(kg.K)
$C_{p,a}$ Specific heat of air, J/(kg.K)
D Characteristic dimension to calculate heat transfer coefficient, m
E_a Activation energy for inactivation of *Listeria monocytogenes*, J/(kg.mol.K)
h_m Surface mass transfer coefficient, kg of Water / (m^2.Pa.s)
h_t Surface heat transfer coefficient, $W/(m^2.K)$
k Thermal conductivity of shrimp, W/(m.K)

m Moisture content, kg of Water / kg of Solids
N Microbial population, CFU/g
n Number of data points in Eq. 14
P_a Partial vapor pressure of the air, Pa
P_s Partial vapor pressure at the product surface, Pa
P_{sat} Saturated vapor pressure, Pa
Q Heat generation, W/m^3
Q_0 Heat generation at the surface of the material, W/m^3
r Radial position, m
R Radius of the product, m
R_G Universal gas constant, J/kg.mol
t Time, s
T Temperature, K
T_a Ambient temperature, K
T_s Surface temperature, K
V Product volume, m^3
V_h Head space volume, m^3
y_0 Observed data (temperature or mass)
y_p Predicted data (temperature or mass)
z Axial distance, m
Z Thickness of the product, m

REFERENCES

BURTLE, G.J. 1990. Aquaculture Development Plan, Working Draft Copy. University of Georgia Coastal Plain Experiment Station. Tifton, GA.

CHAU, K.V. and SNYDER, G.V. 1988. Mathematical model for temperature distribution of thermally processed shrimp. Trans. ASAE *31*(2), 608–612.

CHEN, D.D., SINGH, R.K., HAGHIGHI, K. and NELSON, P.E. 1993. Finite element analysis of temperature distribution in microwaved cylindrical potato tissue. J. Food Eng. *18*, 351–368.

COOTE, P.J., HOLYOAK, C.D. and COLE, M.B. 1991. Thermal inactivation of *Listeria monocytogenes* during a process simulating temperatures achieved during microwave heating. J. App. Bacteriol. *70*, 489–494.

DATTA, A.K. 1991. Mathematical modeling of microwave processing as a tool to study safety. Paper No. 91-6614. ASAE International Winter Meeting, American Society of Agricultural Engineers, St. Joseph, MI.

DATTA, A.K. and HU, W. 1992. Optimization of quality in microwave heating. Food Technol. *46*, (12) 53–56.

DECAREAU, R.V. 1985. *Microwaves in the Food Processing Industry*. Academic Press, Orlando, FL.

FUNG, D.Y.C. and CUNNINGHAM, F.E. 1980. Effect of microwaves on microorganisms in foods. J. of Food Prot. *43*(8), 641–650.

GAST, B., SEPERICH, G.J. and LYTLE, R. 1980. Beef preparation expectations as defined by microwave user survey-a marketing opportunity. Food Technol. *34*(10), 41–43.

GAZE, J.E., BROWN, G.D., GASKELL, D.E. and BANKS, J.G. 1989. Heat resistance of *Listeria monocytogenes* in homogenates of chicken, beef steak and carrot. Food Microbiol. *6*, 251–259.

GUNDAVARAPU, S. 1995. Quality and microbiological safety of microwave cooked shrimp. M.S. Thesis, University of Georgia, Athens, GA.

GUNDAVARAPU, S., HUNG, Y.-C., BRACKETT, R.E. and MALLIKARJUNAN, P. 1995. Evaluation of microbiological safety of shrimps cooked in the microwave oven. J. Food Prot. *58* (7), 742–747.

IMPI, 1989. Procedure for power output measurement of consumer microwave ovens. Microwave World *10*(5), 15-16.

National Marine Fisheries Service, 1990. Current Fishery Statistics No. 8900. Fisheries of the United States, 1989. National Marine Fisheries Service. Silver Springs, MD.

NELSON, S.O., FORBUS, W.R., JR. and LAWRENCE, K.C. 1994. Microwave permittivities of fresh fruits and vegetables from 0.2 to 20 GHz. Trans. ASAE *37*(1), 183–189.

OHLSSON, T. and BENGTSSON, N. 1971. Microwave heating profiles in foods. Microwave Ener. Applic. Newslet. *4*(6), 2.

OHLSSON, T. and RISMAN, P.O. 1978. Temperature distribution of microwave heating - spheres and cylinders. J. Microwave Pow. *13*(4), 303–310.

RUELLO, J.H. 1987. Seafood and microwaves: some preliminary observations. Food Technol. Australia *39*(11), 527–530.

SERENO, A.M. and MEDEIROS, G.L. 1990. A simplified model for the prediction of drying rates for foods. J. Food Eng. *12*, 1–11.

SWAMI, S. 1982. Microwave heating characteristics of simulated high moisture foods. M.S. Thesis, Univ. Mass., Amherst, MA.

TOLEDO, R.T. 1991. *Fundamentals of Food Process Engineering*. Van Nostrand Reinhold, New York.

TONG, C.H. and LUND, D.B. 1993. Microwave heating of baked dough products with simultaneous heat and moisture transfer. J. Food Eng. *19*, 319–339.

WEISS, A. 1977. Algorithms for the calculation of moist air properties on a hand calculator. Trans. ASAE. *20*, 1133–1136.

ZHOU, L., PURI, V.M. and ANATHESWARAN, R.C. 1992. Evaluation of food quality and safety during microwave heating using finite element model. Paper No. 92-6577. ASAE International Winter Meeting, American Society of Agricultural Engineers, St. Joseph, MI.

RESEARCH NOTE
ESTIMATING SHEETING ROLL CLOSING FORCES THROUGH MEASUREMENT OF ROLL POWER CONSUMPTION

LEON LEVINE

Leon Levine & Associates
2665 Jewel Lane
Plymouth, MN 55447

Accepted for Publication February 22, 1996

ABSTRACT

An important factor in the design of the sheeting operation used in the snack food and bakery industries are the forces exerted on the rolls as a result of the pressure developed between the rolls. These forces can cause significant mechanical deflections that result in nonuniform products being produced across the width of the rolls. Unfortunately, measurements of closing forces on operating sheeting systems can be difficult to obtain. This note illustrates a simple method for estimating the difficult to obtain sheeter closing forces from more easily obtained power measurements. A limited quantity of data confirms the accuracy of the procedure.

INTRODUCTION

The equations for the capacity, power consumption, pressure development, and closing forces encountered in the sheeting of doughs may be found in the literature. Levine and Drew (1990, 1994) summarize and extend the underlying mathematical theory described by Middleman (1977) for performing these calculations. Unfortunately, in commercial situations, complete and accurate rheological data is often not available for the material being sheeted. A major source of this problem is the fact that the doughs being processed are changing continuously, so that laboratory rheological measurements do not necessarily reflect the actual rheological condition of the material during processing. In addition, the actual rheology of the materials being sheeted are so complex, that the mathematical solutions for sheeting these materials do not exist. The literature only provides solutions for simple shear thinning materials described by the power law.

Journal of Food Process Engineering **19** (1996) 113–119.

As a result, the simplest approach to obtaining crucial engineering design information may be to use an existing sheeting system as a crude rheometer. This allows one to estimate an effective "in-process" rheological model. This is readily accomplished with easy to obtain power measurements. Once these power measurements are made, one can, as shall be illustrated, obtain an estimate of the forces exerted on the sheeting rolls as a result of the pressure developed between the rolls. These forces are an important factor in the design of sheeting equipment. They are needed to estimate the stiffness required of the sheeting rolls and shafts to prevent excessive deflections. These deflections result in poor product weight control and quality.

METHODS

Theoretical equations for power and force are provided by Levine and Drew (1990). The equations for power consumption and force are given as,

$$P = E(n) \cdot m \cdot U^2 \left[\frac{U}{H_0}\right]^{n-1} \cdot \sqrt{\frac{R}{H_0}} \cdot c_p(RR,n) \tag{1}$$

$$F = F(n) \cdot m \left[\frac{U}{H_0}\right]^{n} \cdot R \cdot C_f(RR,n) \tag{2}$$

The leading coefficients, E(n) and F(n), which are a function of the flow index are provided by Middleman (1977). The indicated functions of reduction ratio and flow index, $C_p(RR,n)$ and $C_f(RR,n)$ are presented graphically by Levine and Drew (1990, 1994). Figures 1, 2 and 3 provide the leading coefficients and the functions for various values of the flow index and reduction ratio. The power and force, if the dough may be approximated as a power law fluid, should be the same as that calculated through the use of Eq. 1 and 2. We can combine these equations to obtain force as function of power and other variables. One obtains,

$$F = \frac{P}{U} \cdot \frac{F(n)}{E(n)} \cdot \frac{C_f(RR,n)}{(RR,n)} \cdot \sqrt{\frac{R}{H_0}} \tag{3}$$

Equation 3 indicates that if the flow index of the material is known then one can obtain force estimates from power measurements. The problem is then to obtain some sort of meaningful estimate of the flow index. This is readily accomplished by measuring power consumption at several sheeter speeds.

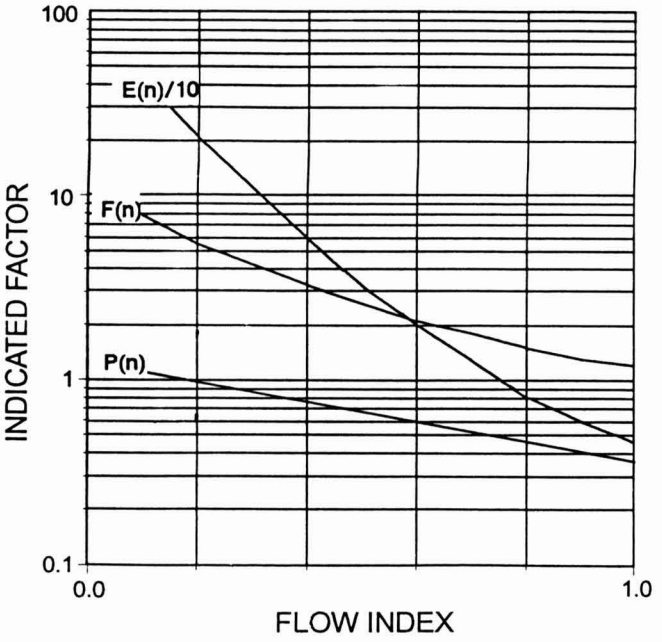

FIG. 1. PRESSURE, FORCE, AND POWER FACTORS VERSUS FLOW INDEX
Middleman (1977).

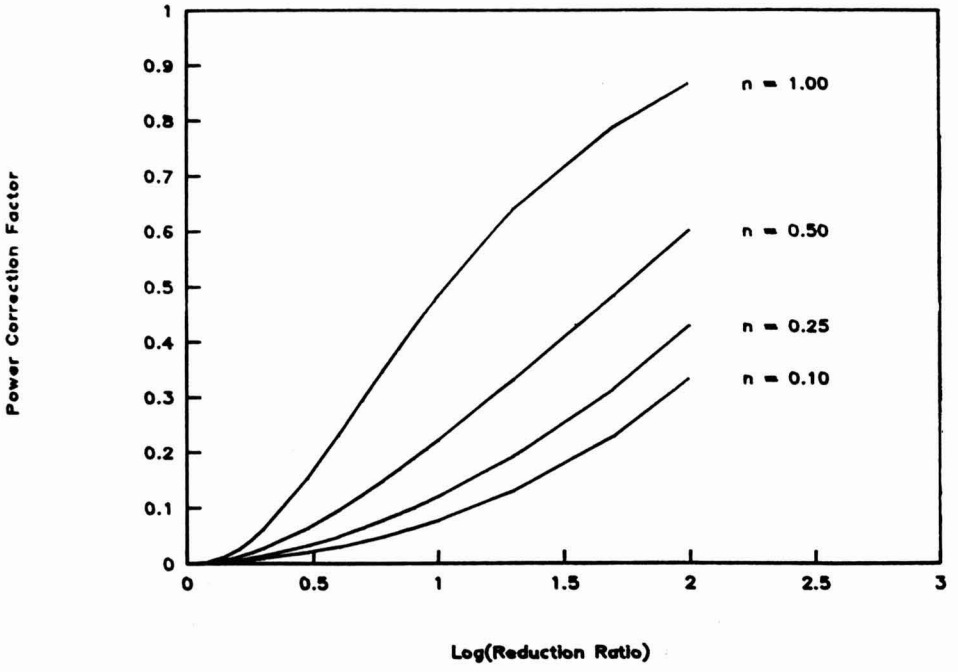

FIG. 2. POWER CORRECTION VERSUS REDUCTION RATIO
No Speed Differential

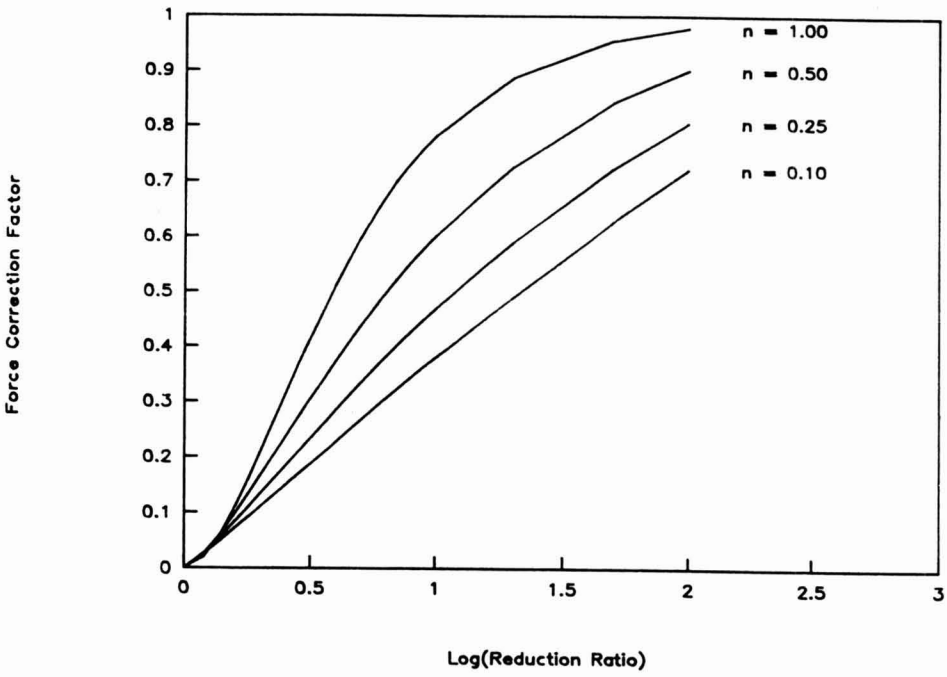

FIG. 3. FORCE CORRECTION VERSUS REDUCTION RATIO
No Speed Differential

Equation 1 can be reduced to,

$$P \alpha U^{1+n} \tag{4}$$

So measurement of power consumption at various speeds gives an estimate of the flow index. As shall be illustrated a very limited quantity of data is needed.

EXPERIMENTAL VERIFICATION

Power and force measurements were taken during the commercial production of a product. Power was determined by measuring the amperage and voltage of a DC motor. Bearing, gear train, etc. (no load) losses were obtained by measuring voltage and amperage when no dough was passing through the rolls. The power being consumed by the motor is given by,

$$P_{consumed} = V \cdot I \tag{5}$$

The actual power delivered to the shaft is given by,

$$P_{delivered} = e \cdot V \cdot I \tag{6}$$

Note that to obtain actual power estimates even when one uses a wattmeter, one must correct the power consumption by the motor efficiency. This correction is often overlooked. Failure to apply this correction can cause very large errors, particularly when dealing with small horsepower and/or lightly loaded motors. Motor efficiency curves can be obtained from the motor manufacturer.

The actual power delivered to the dough is now calculated as follows,

$$P_{net} = \left[P_{load} - P_{noload}\right]_{delivered} \tag{7}$$

Force measurements were obtained by measuring the strain on the frame supporting the rolls. The force on the rolls causes the frame to deflect. This deflection is proportional to the force being exerted by the dough on the rolls. The system was calibrated by applying known loads with a hydraulic jack.

Since these experiments were at a commercial facility, with limited available time, only limited data were obtained. The reduction ratio was approximately 50, the gap between the rolls was approximately 2.1 mm, and roll diameter was approximately 224 mm. Power and force were measured at two different roll speeds, 9 and 27 rpm. Table 1 summarizes the power measurements obtained.

TABLE 1.
POWER MEASUREMENTS

	Consumed by Motor		Delivered by Motor		
Speed (rpm)	Noload Power[1] (watts)	Loaded Power[1] (watts)	Noload Power (watts)	Loaded Power (watts)	Power Delivered (watts)
27	1424 (0.79)	2085 (0.81)	1132	1694	562
9	477 (0.79)	648 (0.81)	379	525	146

[1]The numbers in parentheses are the estimated motor efficiencies (electrical power input/shaft power output).

With the two power measurements, Eq. 4 allows us to estimate the flow index n. The calculation proceeds as follows:

$$(1+n)=\left[\frac{\ln(562)-\ln(146)}{\ln(27)-\ln(9)}\right]=1.23 \tag{8}$$

So the flow index is approximately 0.23. This value may now be used, along with the two power measurements and the appropriate factors from Fig. 1, 2, and 3 in Eq. 3. An estimate of force is obtained.

Table 2 is a comparison of the measured and calculated roll forces. The agreement is quite good. Undoubtedly, the estimates would be improved with more measurements of power consumption.

TABLE 2.
CALCULATED AND ACTUAL FORCE MEASUREMENTS

Speed (rpm)	Measured Force (newtons)	Calculated Force (newtons)
27	12,400	11,100
9	9,200	8,640

NOMENCLATURE

$C_f(RR,n)$	Force correction factor for finite feed sheet
$C_p(RR,n)$	Power correction factor for finite feed sheet
e	Motor efficiency
E(n)	Factor for calculation of power (infinite feed sheet)
F	Force/width on rolls
F(n)	Factor for calculation of force (infinite feed sheet)
H_0	Half of the gap between the rolls
I	Motor current
m	Power law fluid consistency
n	Power law flow index
Po	Power consumption/width
rpm	Roll rotational speed
R	Roll radius
RR	Reduction ratio (ratio of inlet thickness to gap)
U	Peripheral speed of rolls
V	Motor Voltage

REFERENCES

LEVINE, L. and DREW, B. 1990. Rheological and engineering aspects of the sheeting and laminating of dough. In *Dough Rheology and Baked Product Texture*, (H. Faridi and J.M. Faubion, eds.) Van Nostrand Reinhold, New York.

LEVINE, L. and DREW, B. 1994. Sheeting of cookie and cracker doughs. In *The Science of Cookie and Cracker Production*. (H. Faridi, ed.) Chapman and Hall, New York.

MIDDLEMAN, S. 1977. *Fundamentals of Polymer Processing*. p. 180, McGraw-Hill, New York.

FNP PUBLICATIONS IN FOOD SCIENCE AND NUTRITION

Journals

JOURNAL OF FOOD LIPIDS, F. Shahidi
JOURNAL OF RAPID METHODS AND AUTOMATION IN MICROBIOLOGY, D.Y.C. Fung and M.C. Goldschmidt
JOURNAL OF MUSCLE FOODS, N.G. Marriott, G.J. Flick, Jr. and J.R. Claus
JOURNAL OF SENSORY STUDIES, M.C. Gacula, Jr.
JOURNAL OF FOODSERVICE SYSTEMS, C.A. Sawyer
JOURNAL OF FOOD BIOCHEMISTRY, J.R. Whitaker, N.F. Haard and H. Swaisgood
JOURNAL OF FOOD PROCESS ENGINEERING, D.R. Heldman and R.P. Singh
JOURNAL OF FOOD PROCESSING AND PRESERVATION, D.B. Lund
JOURNAL OF FOOD QUALITY, J.J. Powers
JOURNAL OF FOOD SAFETY, T.J. Montville
JOURNAL OF TEXTURE STUDIES, M.C. Bourne and M.A. Rao

Books

OF MICROBES AND MOLECULES: FOOD TECHNOLOGY AT M.I.T., S.A. Goldblith
MEAT PRESERVATION: PREVENTING LOSSES AND ASSURING SAFETY, R.G. Cassens
S.C. PRESCOTT, M.I.T. DEAN AND PIONEER FOOD TECHNOLOGIST, S.A. Goldblith
FOOD CONCEPTS AND PRODUCTS: JUST-IN-TIME DEVELOPMENT, H.R. Moskowitz
MICROWAVE FOODS: NEW PRODUCT DEVELOPMENT, R.V. Decareau
DESIGN AND ANALYSIS OF SENSORY OPTIMIZATION, M.C. Gacula, Jr.
NUTRIENT ADDITIONS TO FOOD, J.C. Bauernfeind and P.A. Lachance
NITRITE-CURED MEAT, R.G. Cassens
POTENTIAL FOR NUTRITIONAL MODULATION OF AGING, D.K. Ingram *et al.*
CONTROLLED/MODIFIED ATMOSPHERE/VACUUM PACKAGING OF FOODS, A.L. Brody
NUTRITIONAL STATUS ASSESSMENT OF THE INDIVIDUAL, G.E. Livingston
QUALITY ASSURANCE OF FOODS, J.E. Stauffer
THE SCIENCE OF MEAT AND MEAT PRODUCTS, 3RD ED., J.F. Price and B.S. Schweigert
HANDBOOK OF FOOD COLORANT PATENTS, F.J. Francis
ROLE OF CHEMISTRY IN PROCESSED FOODS, O.R. Fennema, *et al.*
NEW DIRECTIONS FOR PRODUCT TESTING OF FOODS, H.R. Moskowitz
PRODUCT TESTING AND SENSORY EVALUATION OF FOODS, H.R. Moskowitz
ENVIRONMENTAL ASPECTS OF CANCER: ROLE OF FOODS, E.L. Wynder *et al.*
FOOD PRODUCT DEVELOPMENT AND DIETARY GUIDELINES, G.E. Livingston, R.J. Moshy, and C.M. Chang
SHELF-LIFE DATING OF FOODS, T.P. Labuza
ANTINUTRIENTS AND NATURAL TOXICANTS IN FOOD, R.L. Ory
UTILIZATION OF PROTEIN RESOURCES, D.W. Stanley *et al.*
VITAMIN B_6: METABOLISM AND ROLE IN GROWTH, G.P. Tryfiates
POSTHARVEST BIOLOGY AND BIOTECHNOLOGY, H.O. Hultin and M. Milner

Newsletters

MICROWAVES AND FOOD, R.V. Decareau
FOOD INDUSTRY REPORT, G.C. Melson
FOOD, NUTRITION AND HEALTH, P.A. Lachance and M.C. Fisher
FOOD PACKAGING AND LABELING, S. Sacharow

GUIDE FOR AUTHORS

Typewritten manuscripts in triplicate should be submitted to the editorial office. The typing should be double-spaced throughout with one-inch margins on all sides.

Page one should contain: the title, which should be concise and informative; the complete name(s) of the author(s); affiliation of the author(s); a running title of 40 characters or less; and the name and mail address to whom correspondence should be sent.

Page two should contain an abstract of not more than 150 words. This abstract should be intelligible by itself.

The main text should begin on page three and will ordinarily have the following arrangement:

Introduction: This should be brief and state the reason for the work in relation to the field. It should indicate what new contribution is made by the work described.

Materials and Methods: Enough information should be provided to allow other investigators to repeat the work. Avoid repeating the details of procedures that have already been published elsewhere.

Results: The results should be presented as concisely as possible. Do not use tables *and* figures for presentation of the same data.

Discussion: The discussion section should be used for the interpretation of results. The results should not be repeated.

In some cases it might be desirable to combine results and discussion sections.

References: References should be given in the text by the surname of the authors and the year. *Et al.* should be used in the text when there are more than two authors. All authors should be given in the Reference section. In the Reference section the references should be listed alphabetically. See below for style to be used.

RIZVI, S.S.H. 1986. Thermodynamic properties of foods in dehydration. In *Engineering Properties of Foods*, (M.A. Rao and S.S.H. Rizvi, eds.) pp. 133–214, Marcel Dekker, New York.

MICHAELS, S.L. 1989. Crossflow microfilters ins and outs. Chem. Eng. *96*, 84–91.

LABUZA, T.P. 1982. *Shelf-Life Dating of Foods*, pp. 66–120, Food & Nutrition Press, Trumbull, CT.

Journal abbreviations should follow those used in *Chemical Abstracts*. Responsibility for the accuracy of citations rests entirely with the author(s). References to papers in press should indicate the name of the journal and should only be used for papers that have been accepted for publication. Submitted papers should be referred to by such terms as "unpublished observations" or "private communication." However, these last should be used only when absolutely necessary.

Tables should be numbered consecutively with Arabic numerals. The title of the table should appear as below:

TABLE 1.
ACTIVITY OF POTATO ACYL-HYDROLASES ON NEUTRAL LIPIDS, GALACTOLIPIDS AND PHOSPHOLIPIDS

Description of experimental work or explanation of symbols should go below the table proper. Type tables neatly and correctly as tables are considered art and are not typeset. Single-space tables.

Figures should be listed in order in the text using Arabic numbers. Figure legends should be typed on a separate page. Figures and tables should be intelligible without reference to the text. Authors should indicate where the tables and figures should be placed in the text. Photographs must be supplied as glossy black and white prints. Line diagrams should be drawn with black waterproof ink on white paper or board. The lettering should be of such a size that it is easily legible after reduction. Each diagram and photograph should be clearly labeled on the reverse side with the name(s) of author(s), and title of paper. When not obvious, each photograph and diagram should be labeled on the back to show the top of the photograph or diagram.

Acknowledgments: Acknowledgments should be listed on a separate page.

Short notes will be published where the information is deemed sufficiently important to warrant rapid publication. The format for short papers may be similar to that for regular papers but more concisely written. Short notes may be of a less general nature and written principally for specialists in the particular area with which the manuscript is dealing. Manuscripts that do not meet the requirement of importance and necessity for rapid publication will, after notification of the author(s), be treated as regular papers. Regular papers my be very short.

Standard nomenclature as used in the engineering literature should be followed. Avoid laboratory jargon. If abbreviations or trade names are used, define the material or compound the first time that it is mentioned.

EDITORIAL OFFICE: DR. D.R. HELDMAN, COEDITOR, *Journal of Food Process Engineering*, Food Science/Engineering Unit, University of Missouri-Columbia, 235 Agricultural/Engineering Bldg., Columbia, MO 65211 USA; or DR. R.P. SINGH, COEDITOR, *Journal of Food Process Engineering*, University of California, Davis, Department of Agricultural Engineering, Davis, CA 95616 USA.

JOURNAL OF FOOD PROCESS ENGINEERING VOLUME 19, NUMBER 1

CONTENTS